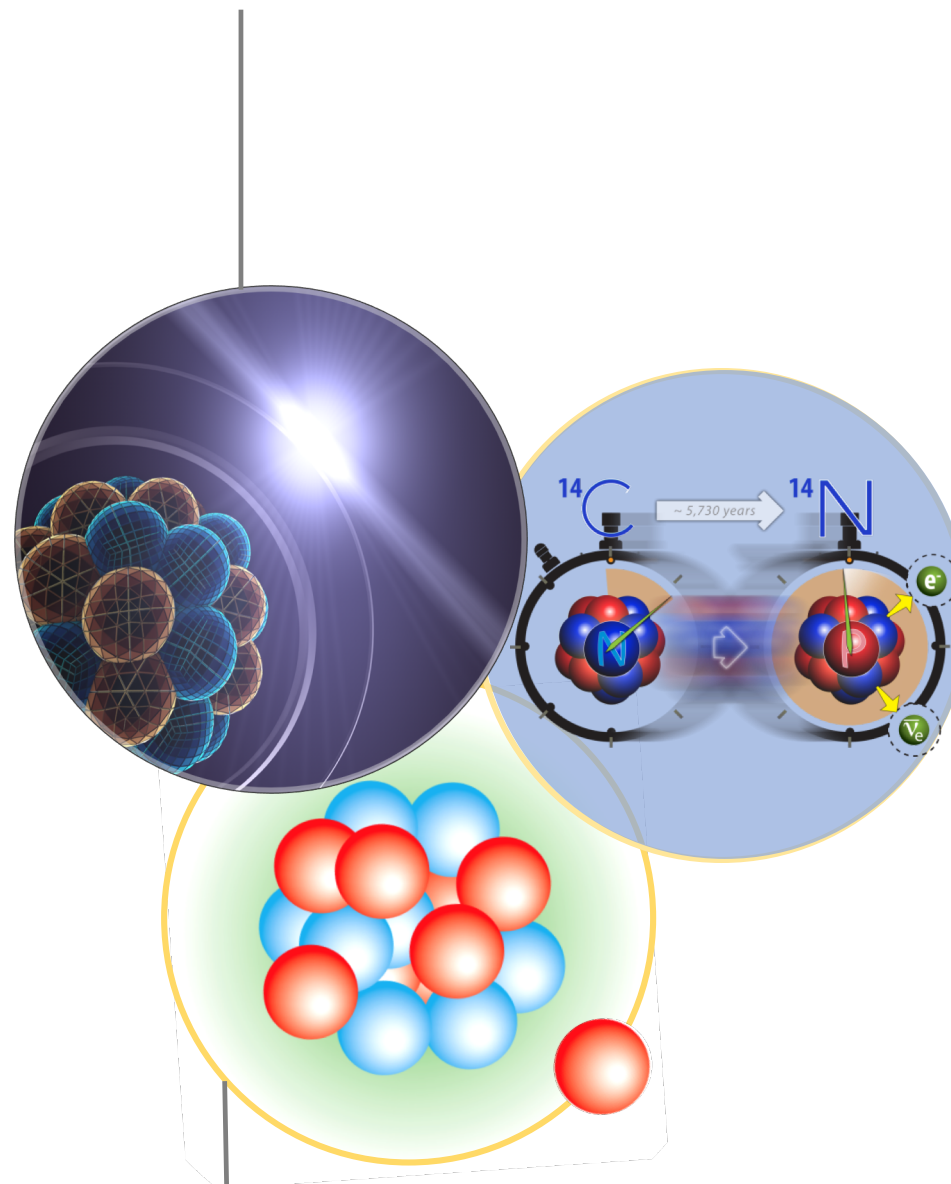


Collectivity in nuclei from ab-initio methods

Gaute Hagen
Oak Ridge National Laboratory

Fundamental Physics with
Radioactive Molecules

INT, March 13th, 2024



Collaborators

@ ORNL / UTK: **B. Acharya, Baishan Hu, G. R. Jansen, Z. H. Sun, T. Papenbrock**

@ CEA/Saclay: T. Duguet

@ Chalmers: A. Ekström, C. Forssén

@ Mainz: S. Bacca

@ WUSTL: **S. Novario**

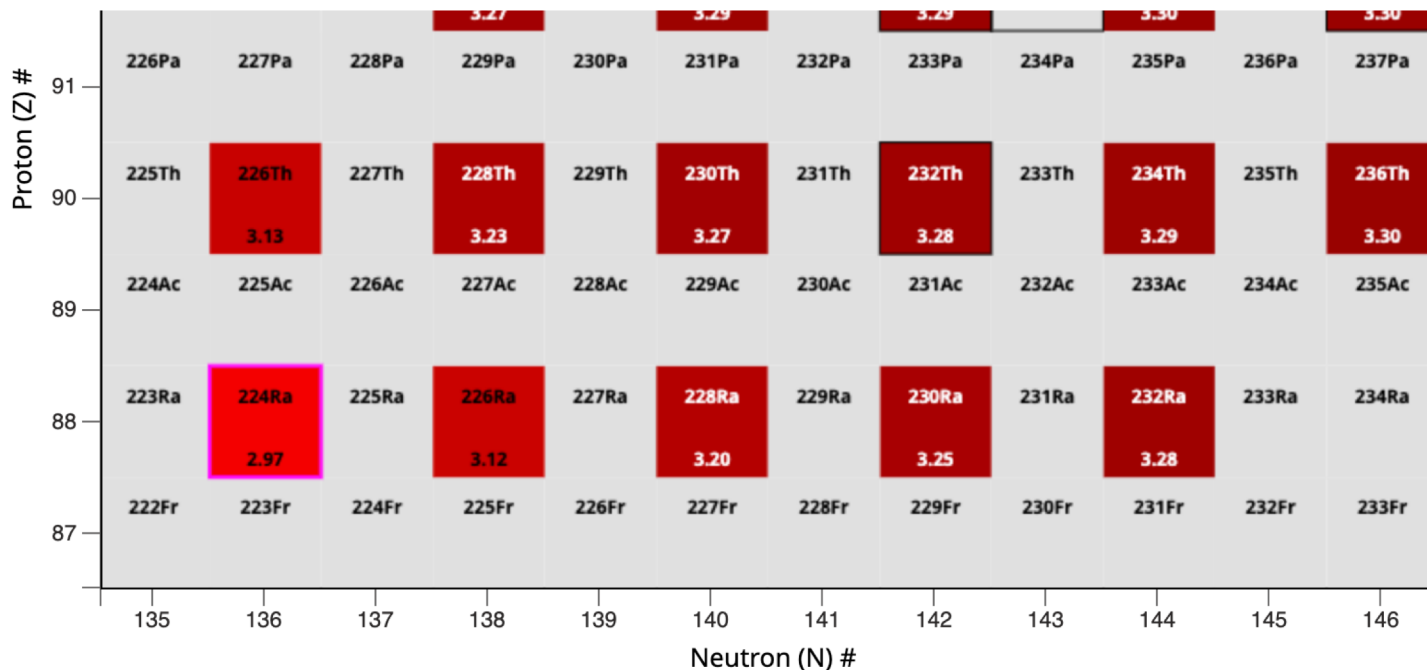
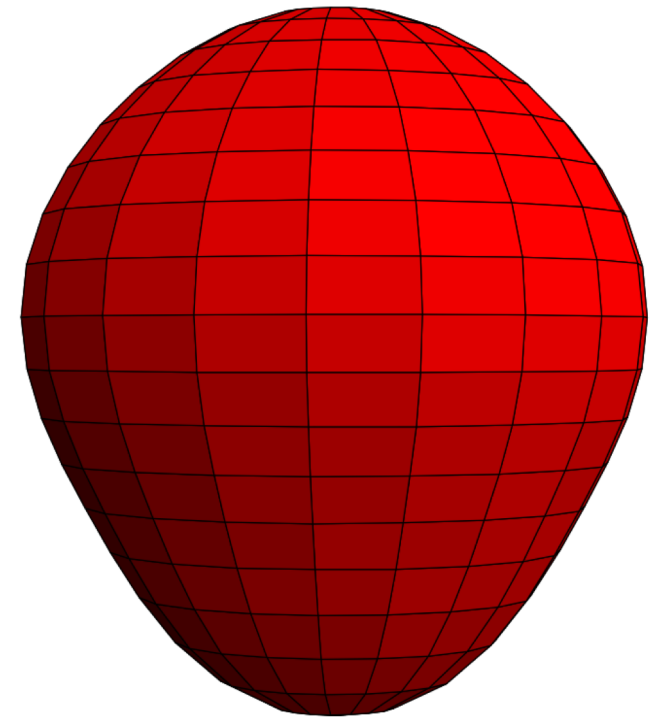
@ TRIUMF: P. Navratil

@ TU Darmstadt: **A. Tichai**

Ab-initio description of Schiff moments in heavy deformed nuclei?

Computation of Schiff moment in ^{225}Ra relevant for EDM searches in atoms and molecules. Schiff moment is particularly sensitive to octupole deformation

$$S \equiv \langle \Psi_0 | \hat{S}_0 | \Psi_0 \rangle \approx \sum_{i \neq 0} \frac{\langle \Psi_0 | \hat{S}_0 | \Psi_i \rangle \langle \Psi_i | \hat{V}_{PT} | \Psi_0 \rangle}{E_0 - E_i} + \text{c.c.},$$



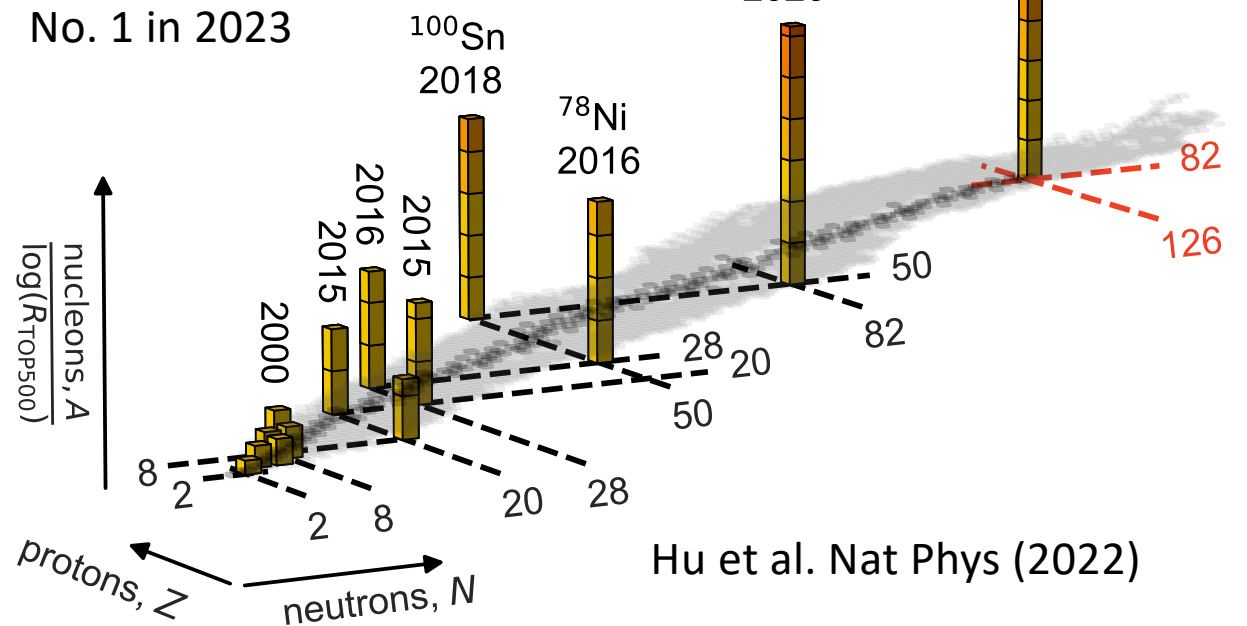
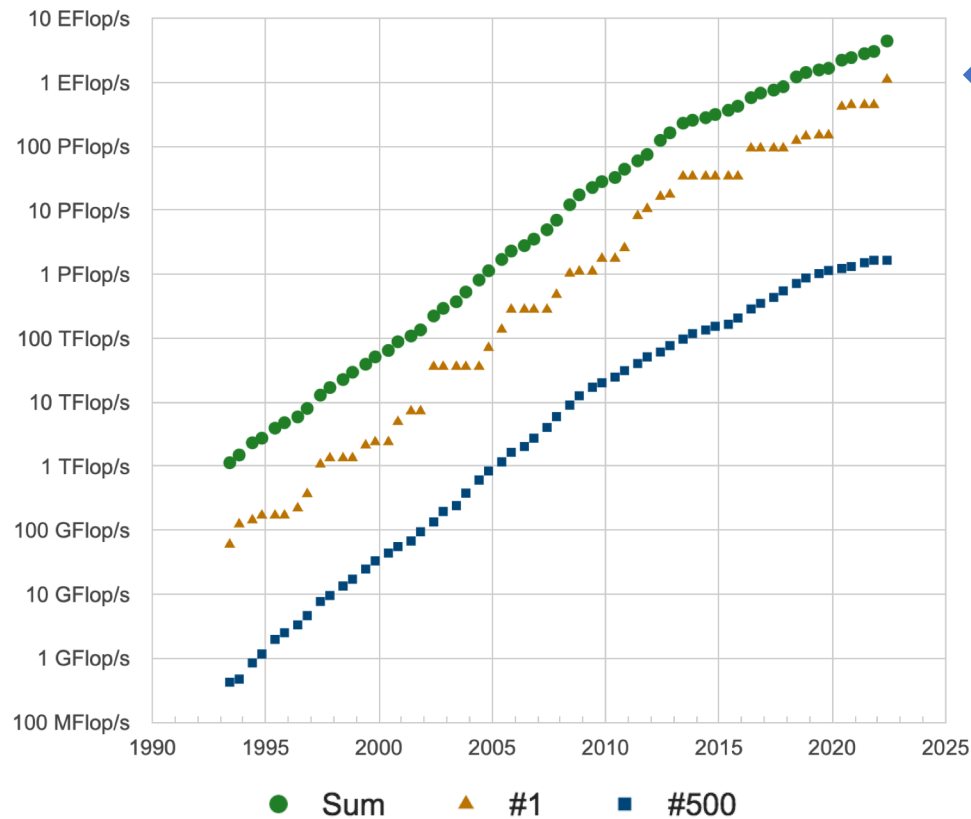
J. Dobaczewski and J. Engel, PRL 2005

$\frac{1}{2}^+$ and $\frac{1}{2}^-$ parity doublet in ^{225}Ra differ by only 50keV

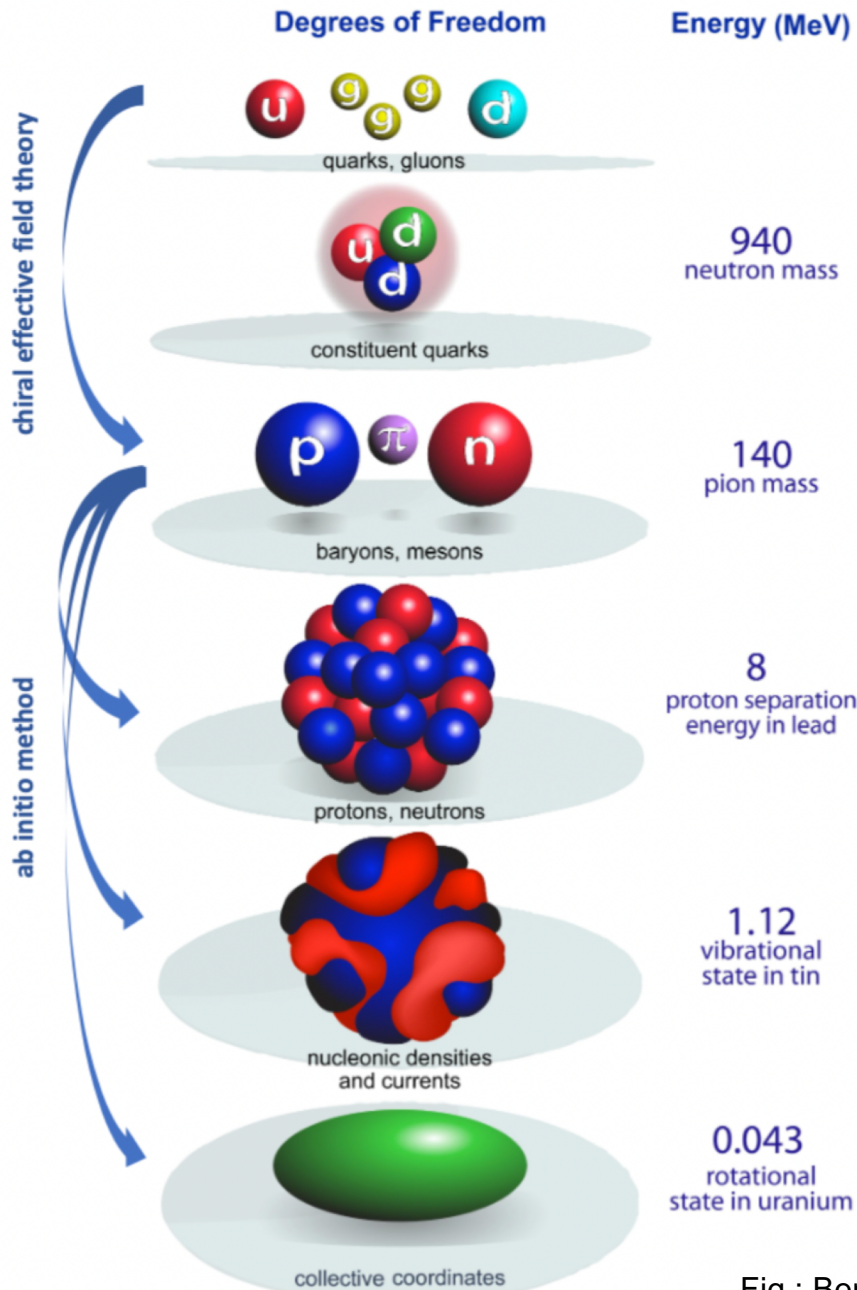
Trend in realistic ab-initio calculations

- Tremendous progress in recent years because of ideas from EFT and the renormalization group
- Computational methods with polynomial cost (coupled clusters 😊 quantum computing 🤔)
- Ever-increasing computer power?

Development with time (top500.org)



Multiscale physics of nuclei from ab-initio methods



What is ab initio in nuclear theory?

A. Ekström et al, Frontiers (2023)

“we interpret the ab initio method to be a systematically improvable approach for quantitatively describing nuclei using the finest resolution scale possible while maximizing its predictive capabilities”

- Nuclei exhibit multiple energy scales ranging from hundreds of MeV in binding energies to fractions of an MeV for low-lying collective excitations.
- Describing these different energy scales within a unified ab-initio framework from chiral interactions is a long-standing challenge

Fig.: Bertsch, Dean, Nazarewicz, SciDAC review (2007)

Solving the quantum many-nucleon problem

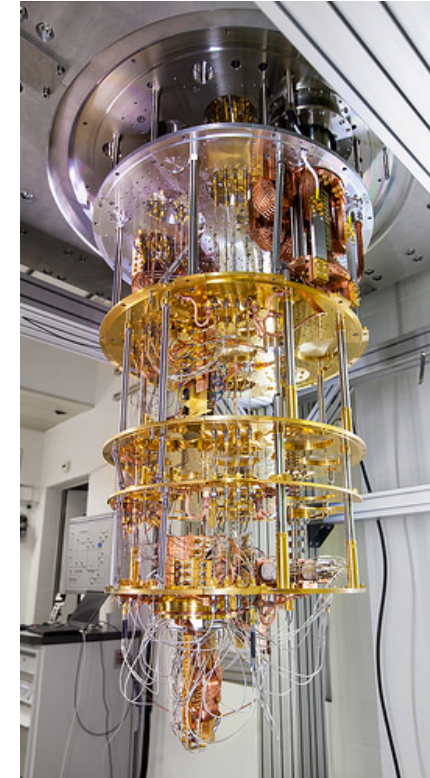
An exponentially hard problem to solve!

$$H|\Psi\rangle = E|\Psi\rangle$$

1.1 exaflops



IBM Q Experience



Polynomial scaling

Systematically improvable approaches
with controlled approximations:
Coupled-cluster, IMSRG, Gorkov, SCGF,...

↓
Emulators?

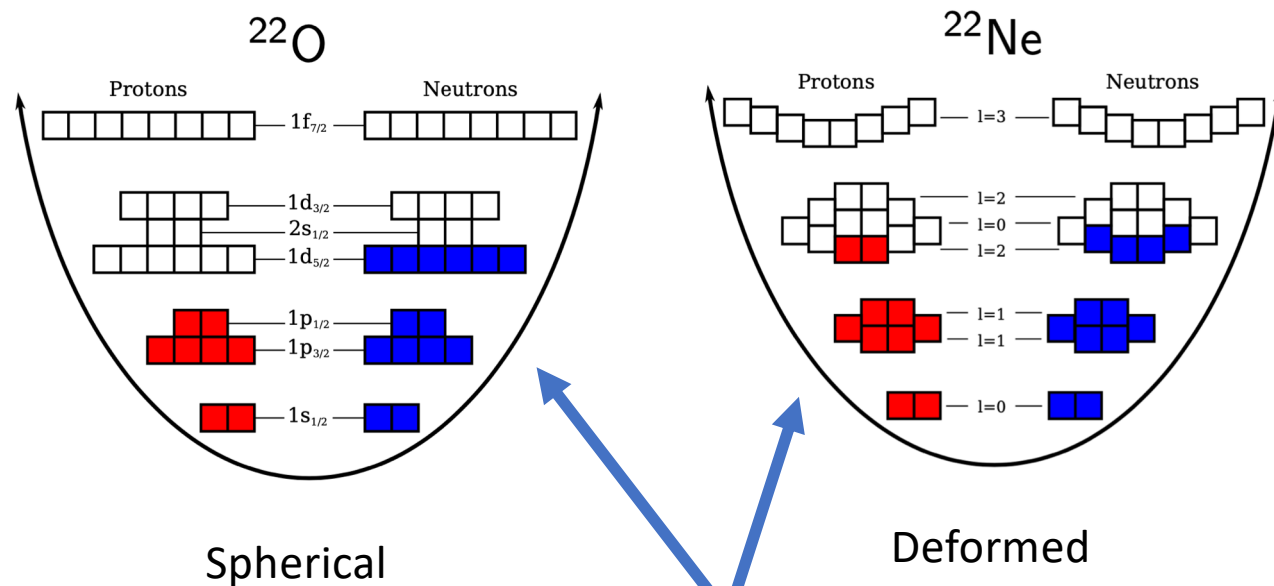


Fault tolerant quantum computing??

Coupled-cluster computations of deformed nuclei

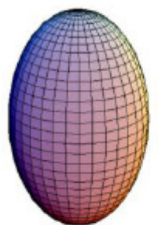
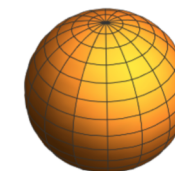
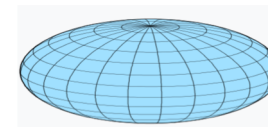
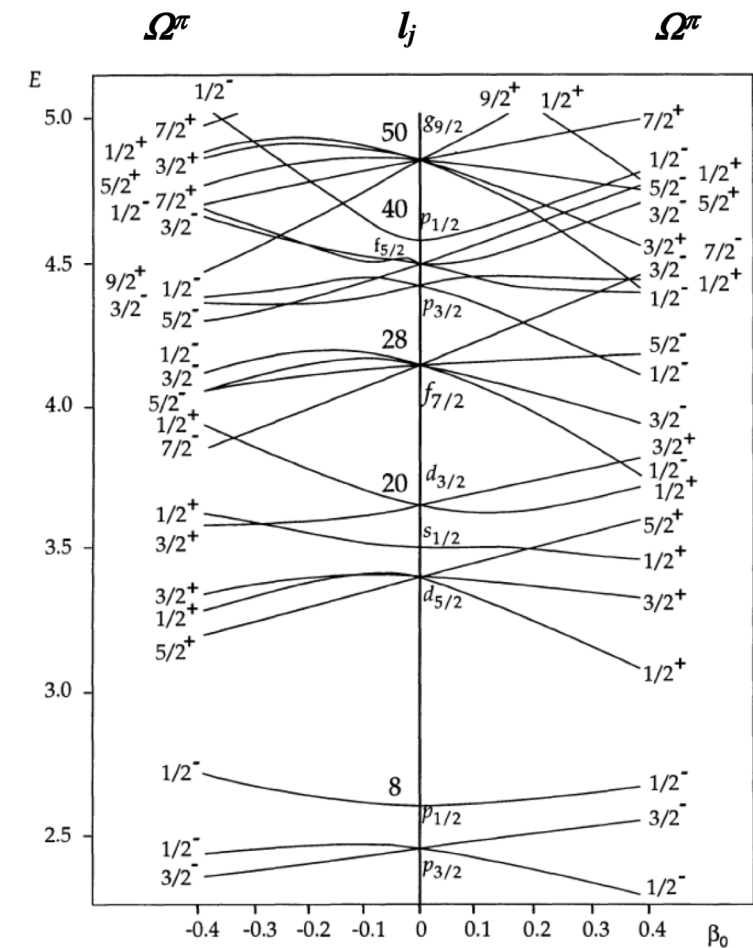
The key lies in choosing the correct starting point

Wave-function based methods starts from a mean-field reference state



$$|\Psi\rangle = \Omega |\Phi\rangle$$

Wave-operator (includes many-body correlations)



Coupled-cluster method

$$\Psi = e^T |\Phi\rangle$$

$$T = T_1 + T_2 + \dots$$

$$T_1 = \sum_{ia} t_i^a a_a^\dagger a_i \quad T_2 = \frac{1}{4} \sum_{ijab} t_{ij}^{ab} a_a^\dagger a_b^\dagger a_j a_i$$

$$\bar{H}_{\text{CCSD}} = \begin{pmatrix} 0\text{p}0\text{h} & 1\text{p}1\text{h} & 2\text{p}2\text{h} \\ E_{\text{CCSD}} & \bar{H}_{0S} & \bar{H}_{0D} \\ 0 & \bar{H}_{SS} & \bar{H}_{SD} \\ 0 & \bar{H}_{DS} & \bar{H}_{DD} \end{pmatrix} \begin{matrix} 0\text{p}0\text{h} \\ 1\text{p}1\text{h} \\ 2\text{p}2\text{h} \end{matrix}$$

$$E = \langle \Phi | \bar{H} | \Phi \rangle$$

$$0 = \langle \Phi_i^a | \bar{H} | \Phi \rangle$$

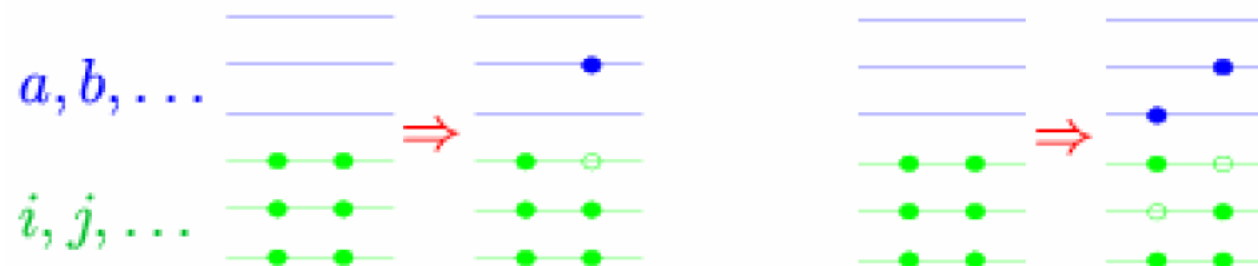
$$0 = \langle \Phi_{ij}^{ab} | \bar{H} | \Phi \rangle$$

$$\bar{H} \equiv e^{-T} H e^T = (H e^T)_c = \left(H + H T_1 + H T_2 + \frac{1}{2} H T_1^2 + \dots \right)_c$$

- ☺ Scales gently (polynomial) with increasing system size
- ☺ Truncation is only approximation
- ☺ Fulfills a bi-variational principle
- ☺ A lot of freedom in the choice of reference state (spherical, deformed, pairing,...)

CCSD generates similarity transformed Hamiltonian with no 1p-1h and no 2p-2h excitations

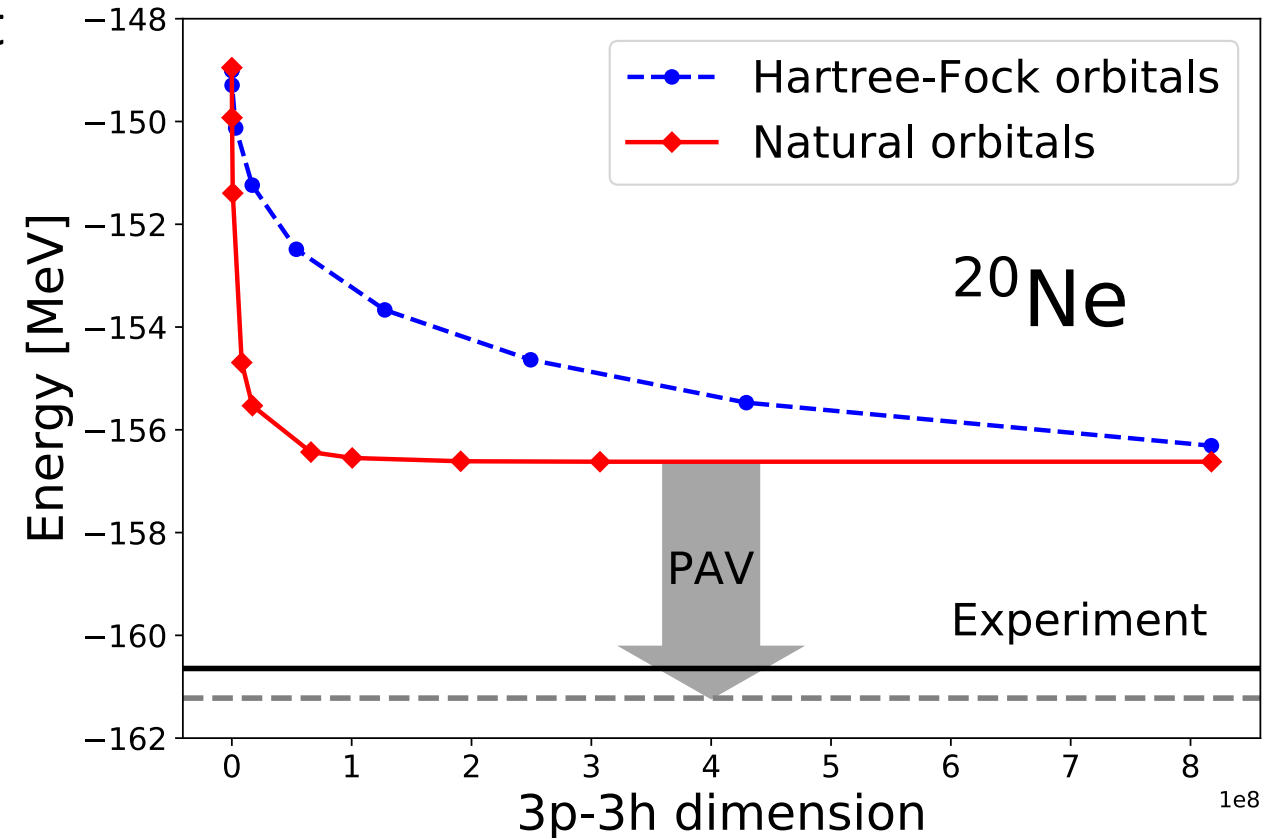
Correlations are *exponentiated* 1p-1h and 2p-2h excitations. Part of Ap-Ah excitations included!



Coupled-cluster computations of deformed nuclei

1. Compute Hartree-Fock reference state
 - Nontrivial vacuum state informs us about emergent breaking of symmetries
 - Yields normal-ordered two-body Hamiltonian
2. Include dynamical (extensive) correlations via coupled-cluster theory
 - (or via IMSRG, or Gorkov methods, or Green's functions)
 - Cost increases polynomial with mass number
3. Perform symmetry projections
 - Non-extensive contributions to the energy
 - Often relevant for transition matrix elements

S. J. Novario, et al PRC 102, 051303 (2020)



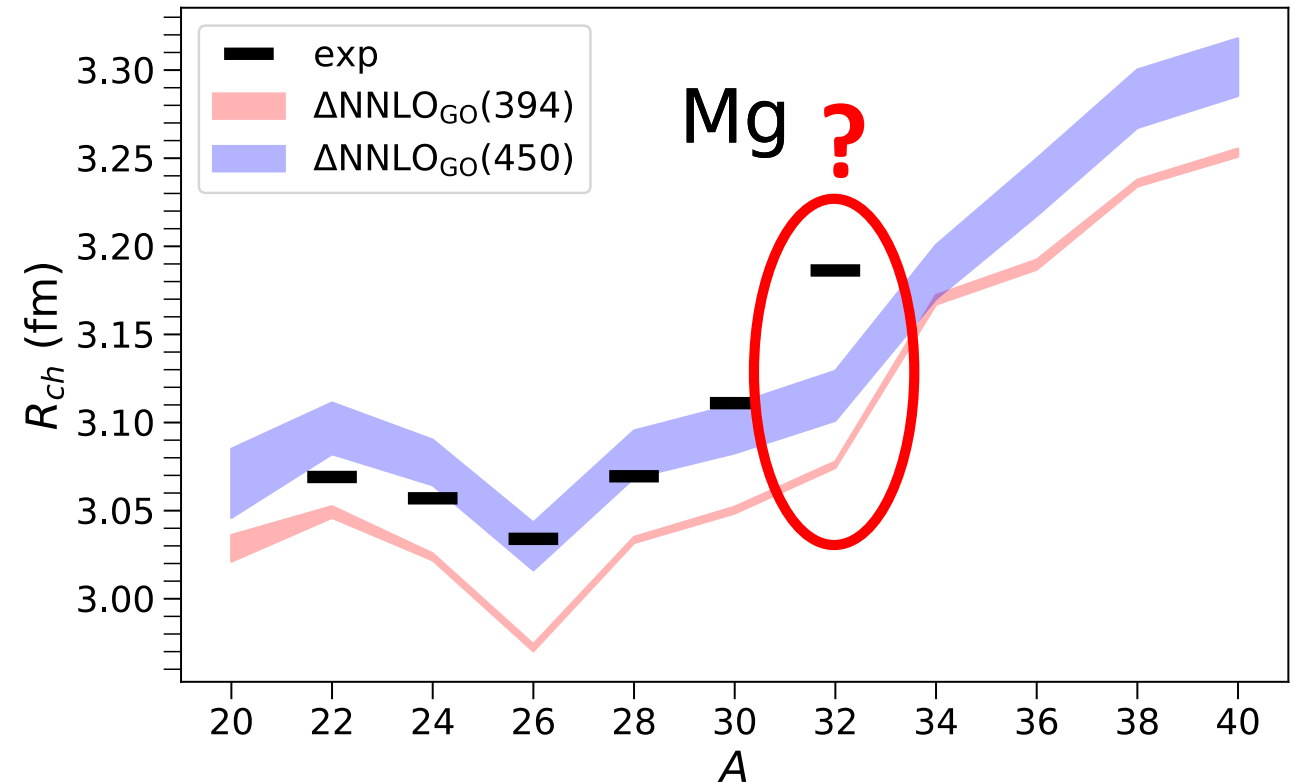
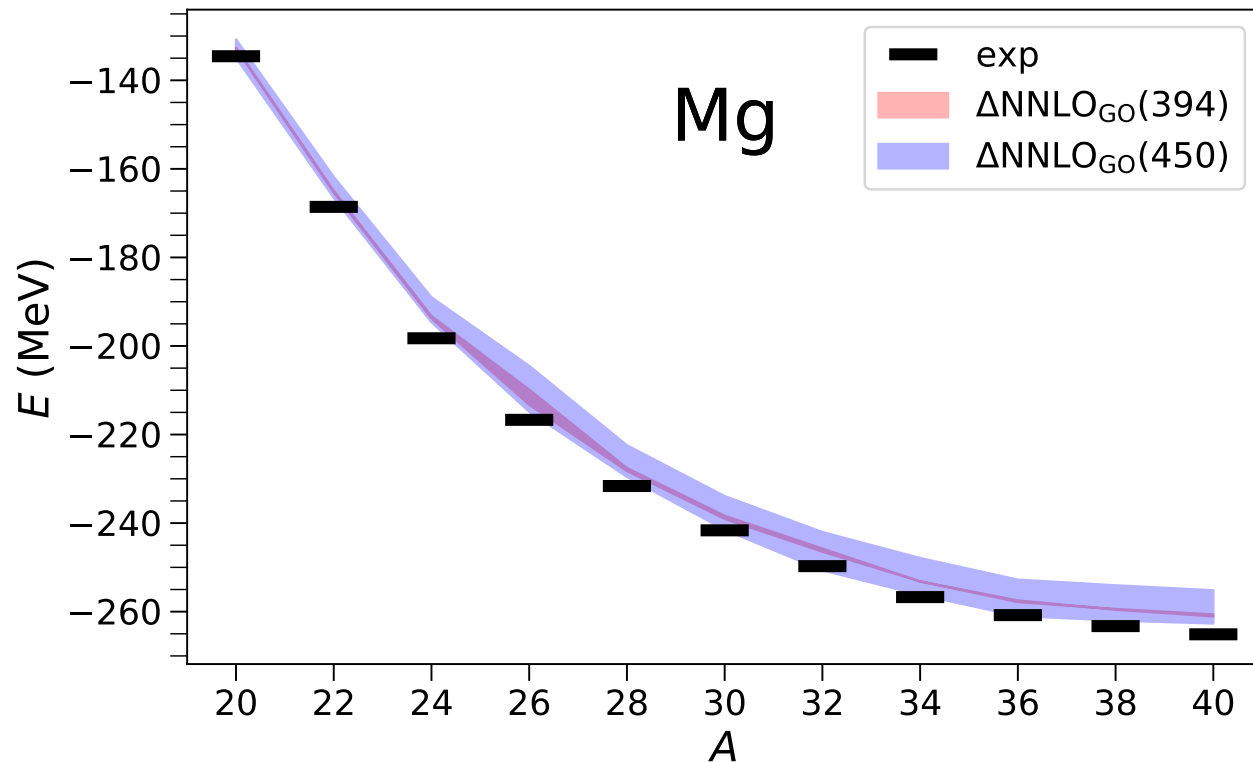
Total energy:

$$E = E_{\text{ref}} + \Delta E_{\text{CC}} + \delta E$$

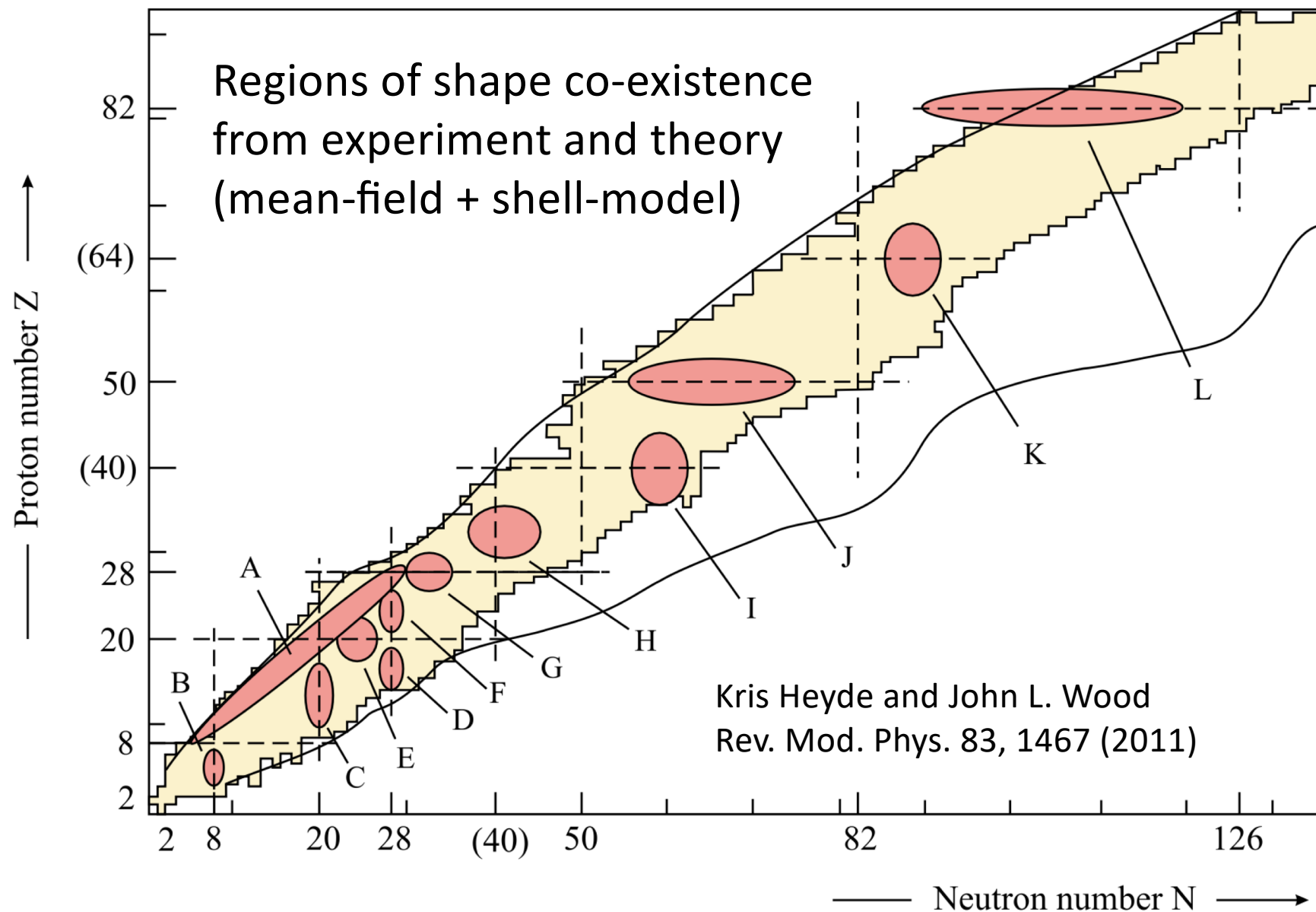
What's going with the charge radius at $N = 20$?



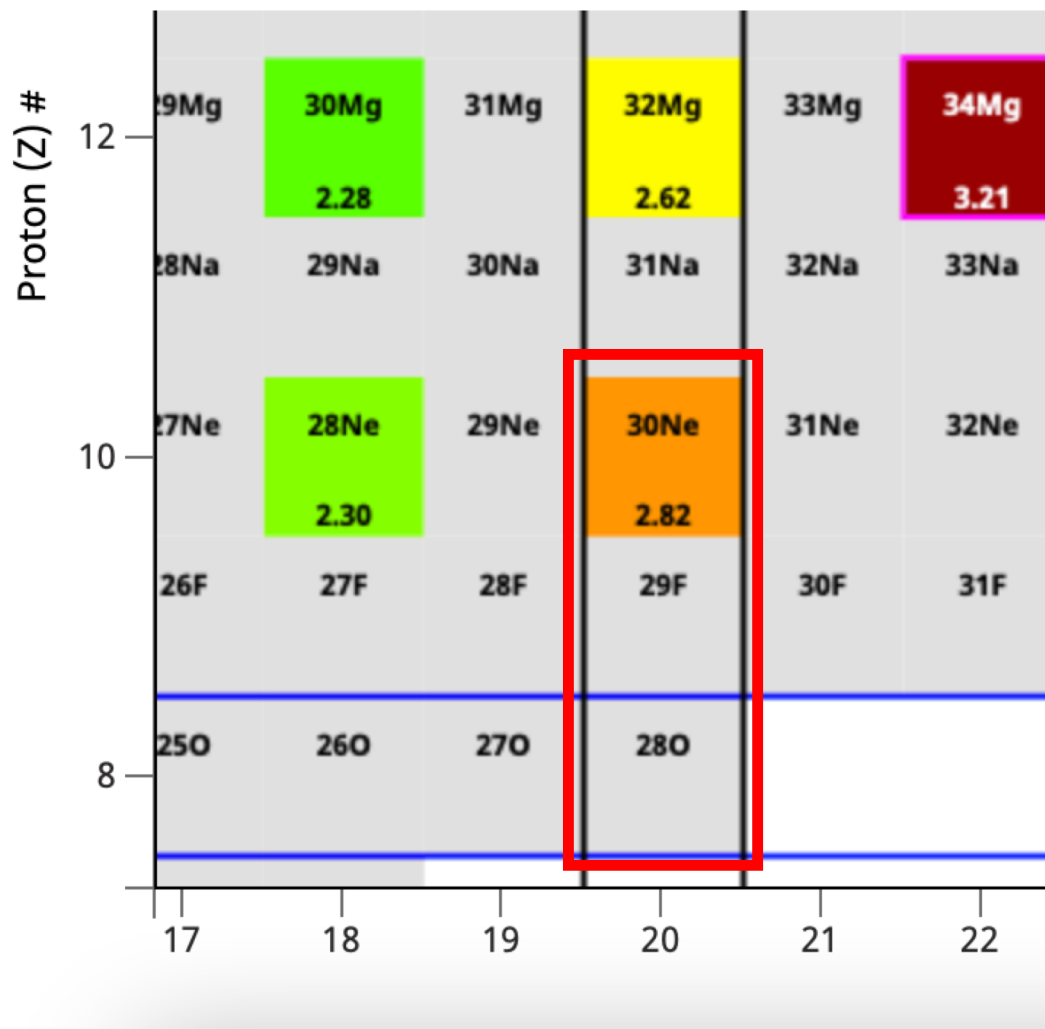
Interaction/method deficiency or something else?



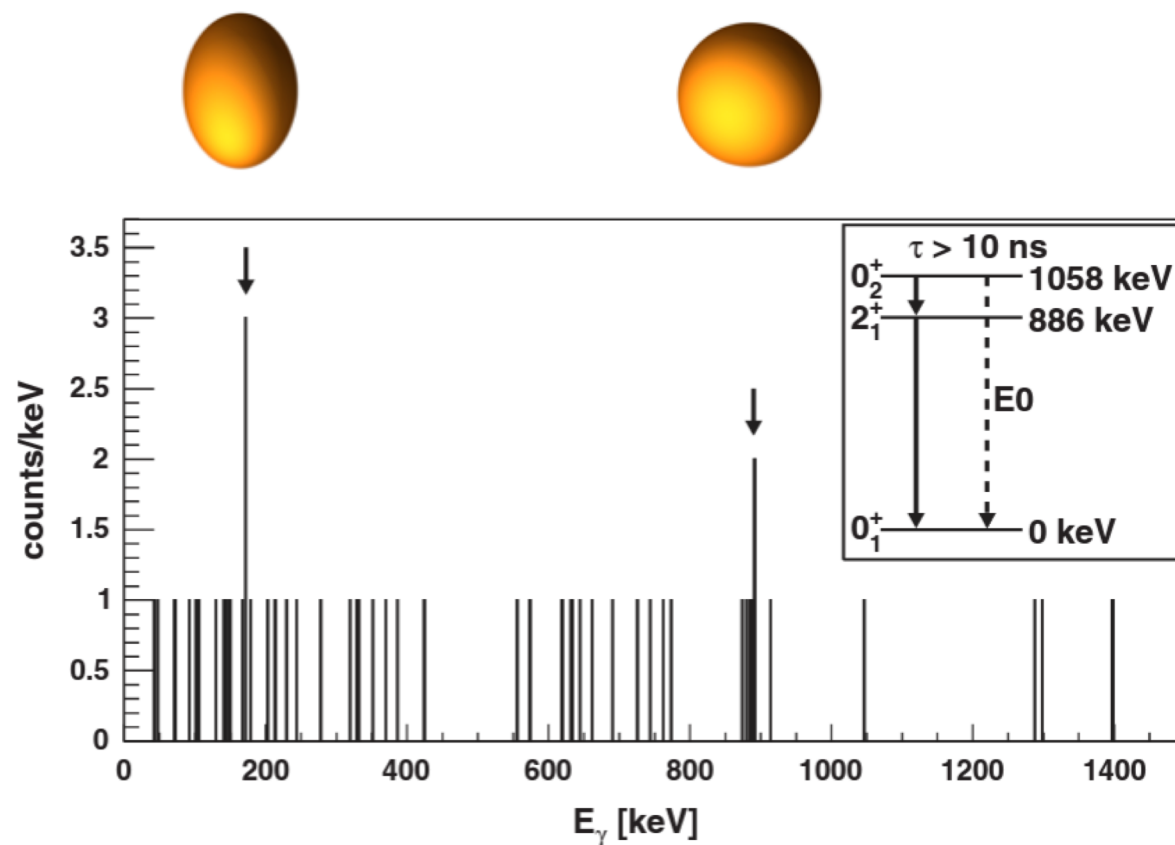
Onset of deformation and shape co-existence in nuclei



Onset of deformation and shape co-existence along N = 20

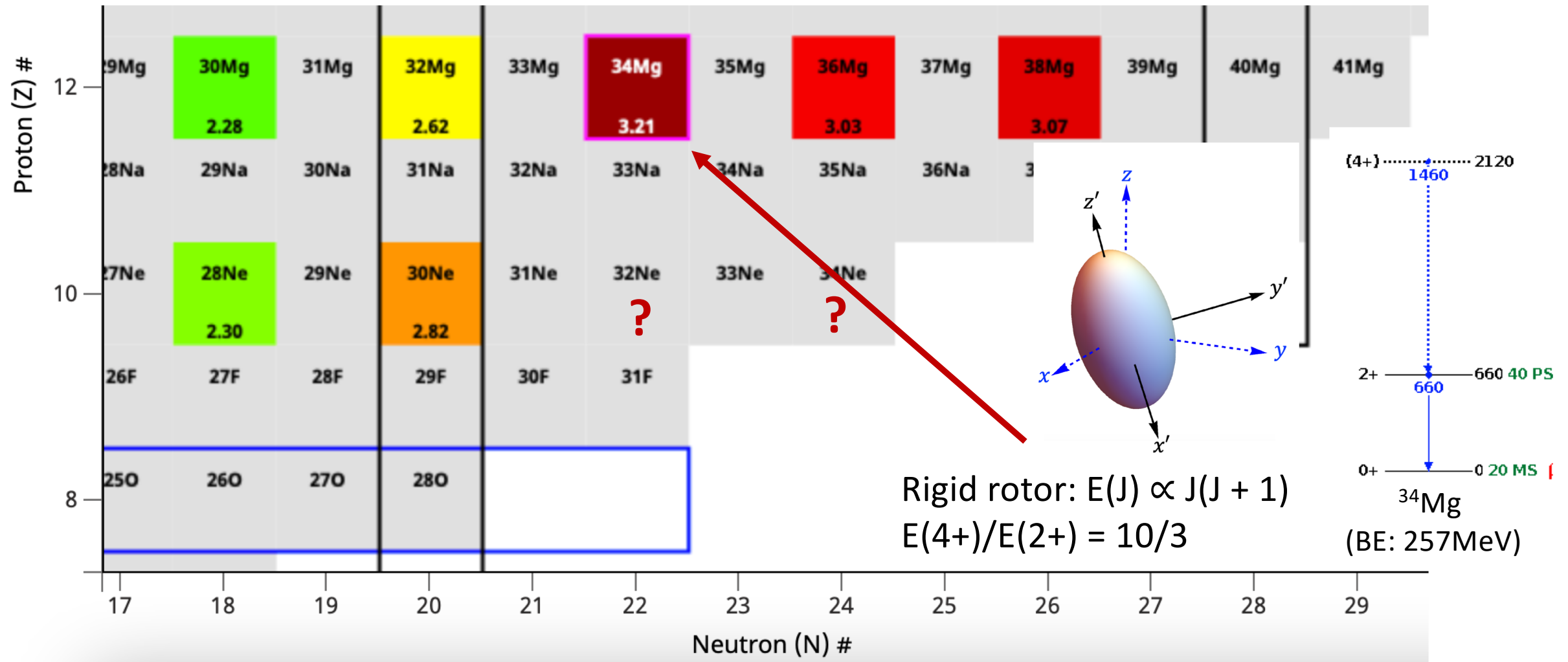


Shape co-existence in ^{32}Mg



K. Wimmer et al, PRL (2010)

Collectivity in neutron-rich neon and magnesium isotopes from coupled-cluster methods



G. Hagen, S. J. Novario, Z. H. Sun, T. Papenbrock, G. R. Jansen, J. G. Lietz, T. Duguet, A. Tichai Phys. Rev. C 105, 064311 (2022)

S. J. Novario, G. Hagen, G. R. Jansen, T. Papenbrock, Phys. Rev. C 102, 051303 (2020)

Symmetry restored coupled-cluster theory

Projection after variation (PAV): $E^{(J)} = \frac{\langle \tilde{\Psi} | P_J H | \Psi \rangle}{\langle \tilde{\Psi} | P_J | \Psi \rangle}$

Right coupled-cluster state: $|\Psi\rangle = e^T |\Phi_0\rangle$

Left state is parametrized differently:

$$\langle \tilde{\Psi} | = \langle \Phi_0 | (1 + \Lambda) e^{-T}$$

Bi-variational

$$P_J = \frac{1}{2} \int_0^\pi d\beta \sin(\beta) d_{00}^J(\beta) R(\beta)$$



Image credit: Wikimedia Commons

For axial symmetry around the z-axis the rotation operator is:

$$R(\beta) \equiv e^{i\beta J_y}$$

Symmetry restored coupled-cluster theory

The kernels can be evaluated by using Thouless theorem:

$$\langle \Phi_0 | R(\beta) = \langle \Phi_0 | R(\beta) | \Phi_0 \rangle \langle \Phi_0 | e^{V_1(\beta)}$$

$$\mathcal{H}(\beta) = \langle \Phi | \bar{R}(\beta) | \Phi \rangle \langle \Phi | Z(\beta) \tilde{H}(\beta) e^{V(\beta)} e^{T_2} | \Phi \rangle$$

$$\mathcal{N}(\beta) = \langle \Phi | \bar{R}(\beta) | \Phi \rangle \langle \Phi | Z(\beta) e^{V(\beta)} e^{T_2} | \Phi \rangle$$

Similarity transformed rotation operator and Hamiltonian:

$$\bar{R}(\beta) = e^{-T_1} R(\beta) e^{T_1}$$

$$\tilde{H}(\beta) = e^{V_1(\beta)} \bar{H} e^{-V_1(\beta)}$$


$$e^{V(\beta)} e^{T_2} | \Phi \rangle = e^{W_0(\beta) + W_1(\beta) + W_2(\beta) + \dots} | \Phi \rangle$$

- Does not truncate
- How to evaluate the disentangled amplitudes?

[Qiu et al, J. Chem. Phys. 147, 064111 (2017)]

Solving for the disentangled amplitudes [Qiu et al]

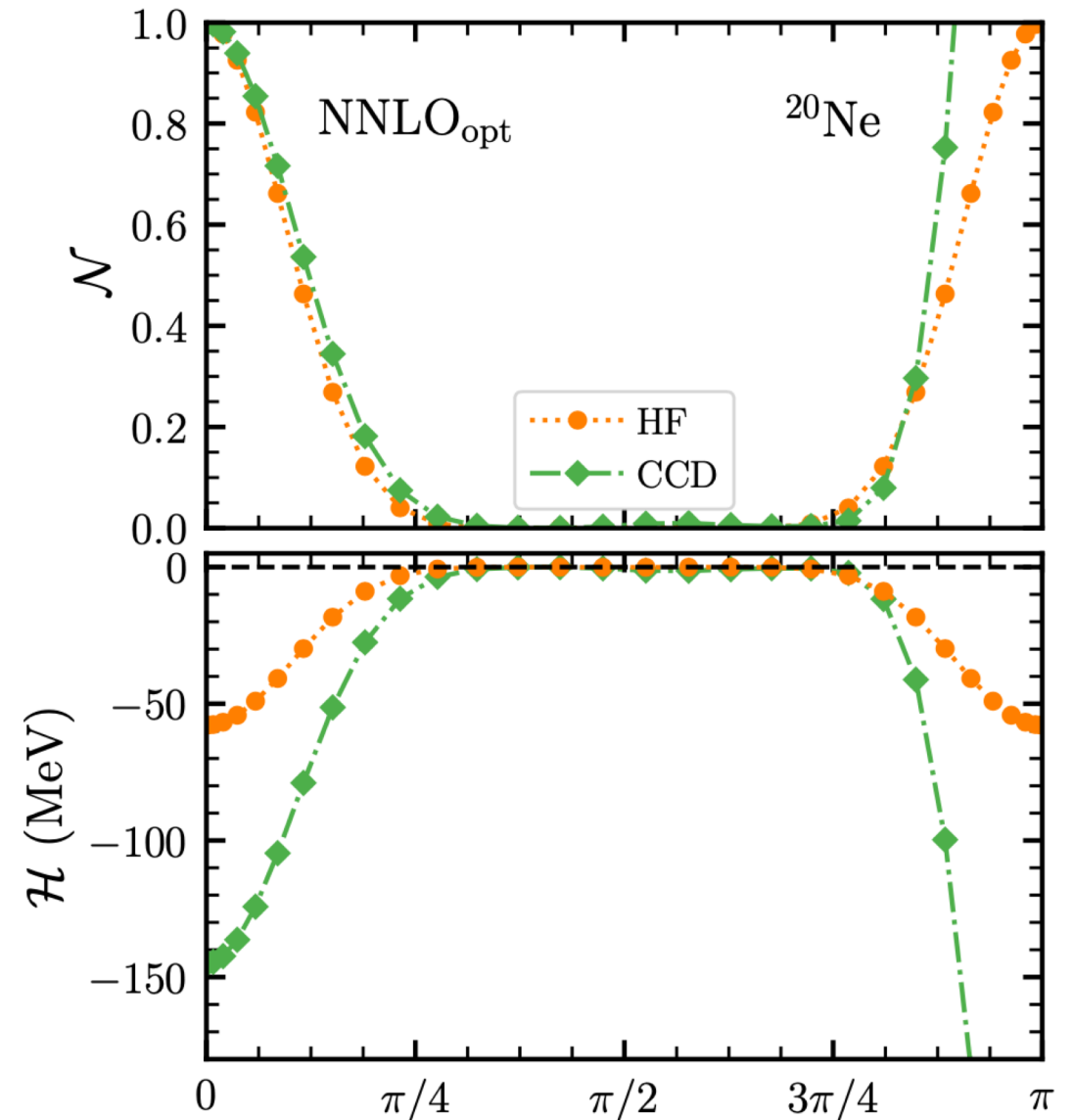
Approximate:
$$e^{V(\beta)} e^{T_2} |\Phi\rangle \approx e^{W_0(\beta) + W_1(\beta) + W_2(\beta)} |\Phi\rangle$$

Taking the derivative with respect to β leads to a set of ODEs with initial conditions:

$$W_0(\beta = 0) = W_1(\beta = 0) = 0, W_2(\beta = 0) = T_2$$

[Qiu et al, J. Chem. Phys. 147, 064111 (2017)]

- Approximate restoration of symmetries
- Can lead to stiffness as $dV(\beta)/d(\beta)$ might be large for $\langle \Phi | R(\beta) | \Phi \rangle \approx 0$.
- The truncation at W_2 might lead to loss of accuracy at larger angles
- Kernels are not symmetric around $\beta = \frac{\pi}{2}$



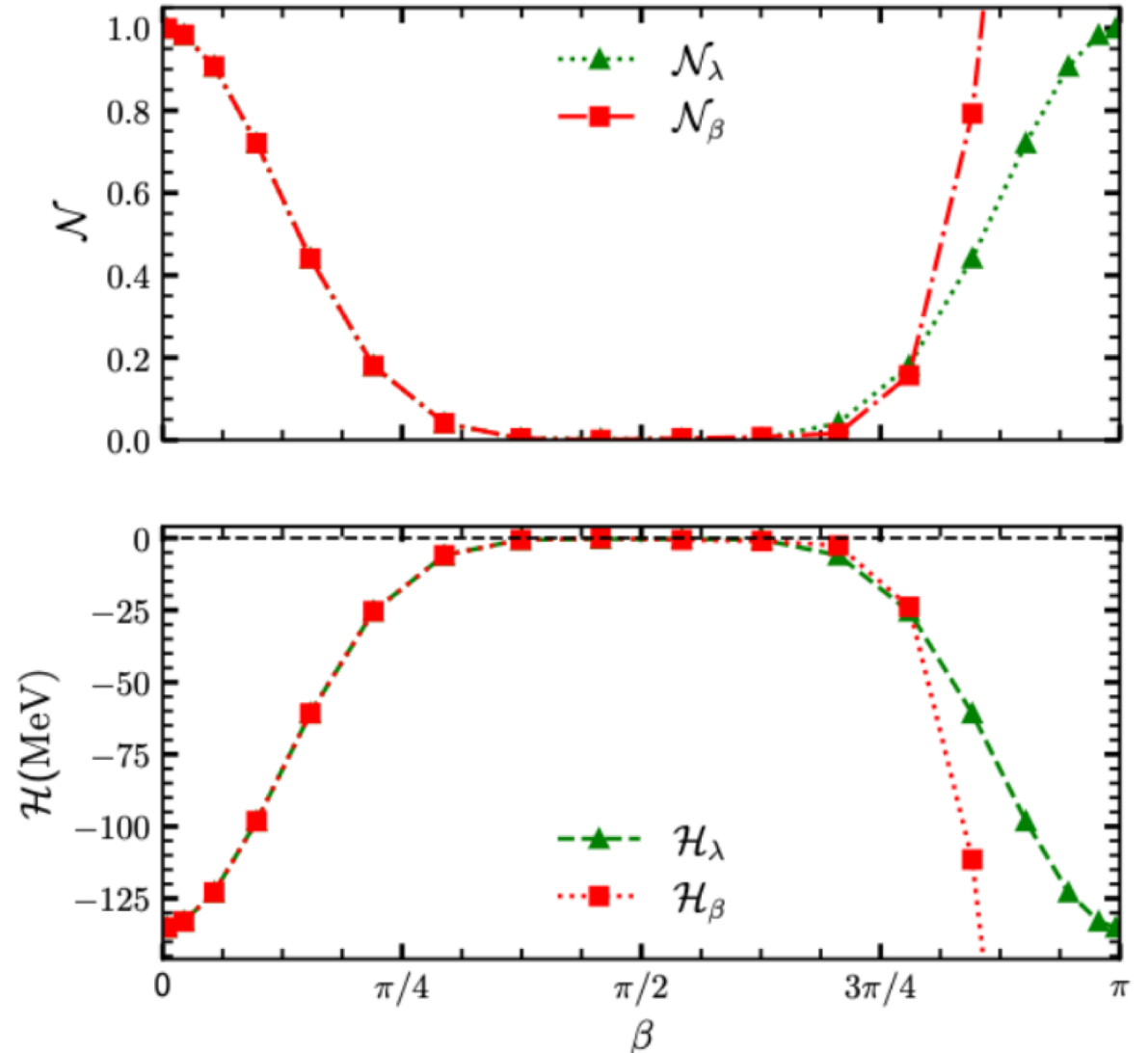
New approach to solve for disentangled amplitudes

We write: $e^{\lambda V} e^{T_2} |\Phi\rangle \approx e^{W_0(\lambda) + W_1(\lambda) + W_2(\lambda)} |\Phi\rangle$

Taking the derivative with respect to λ for fixed β leads to a new set of ODEs with initial conditions: $W_n(\lambda = 0) = T_n$

- Approximate restoration of symmetries
- Significantly improves stability of ODEs
- Kernels are fully symmetric around $\beta = \frac{\pi}{2}$

Zhonghao Sun, A. Ekstrom, C. Forssen,
G. Hagen, G. R. Jansen, T. Papenbrock (2024)



Electromagnetic transitions

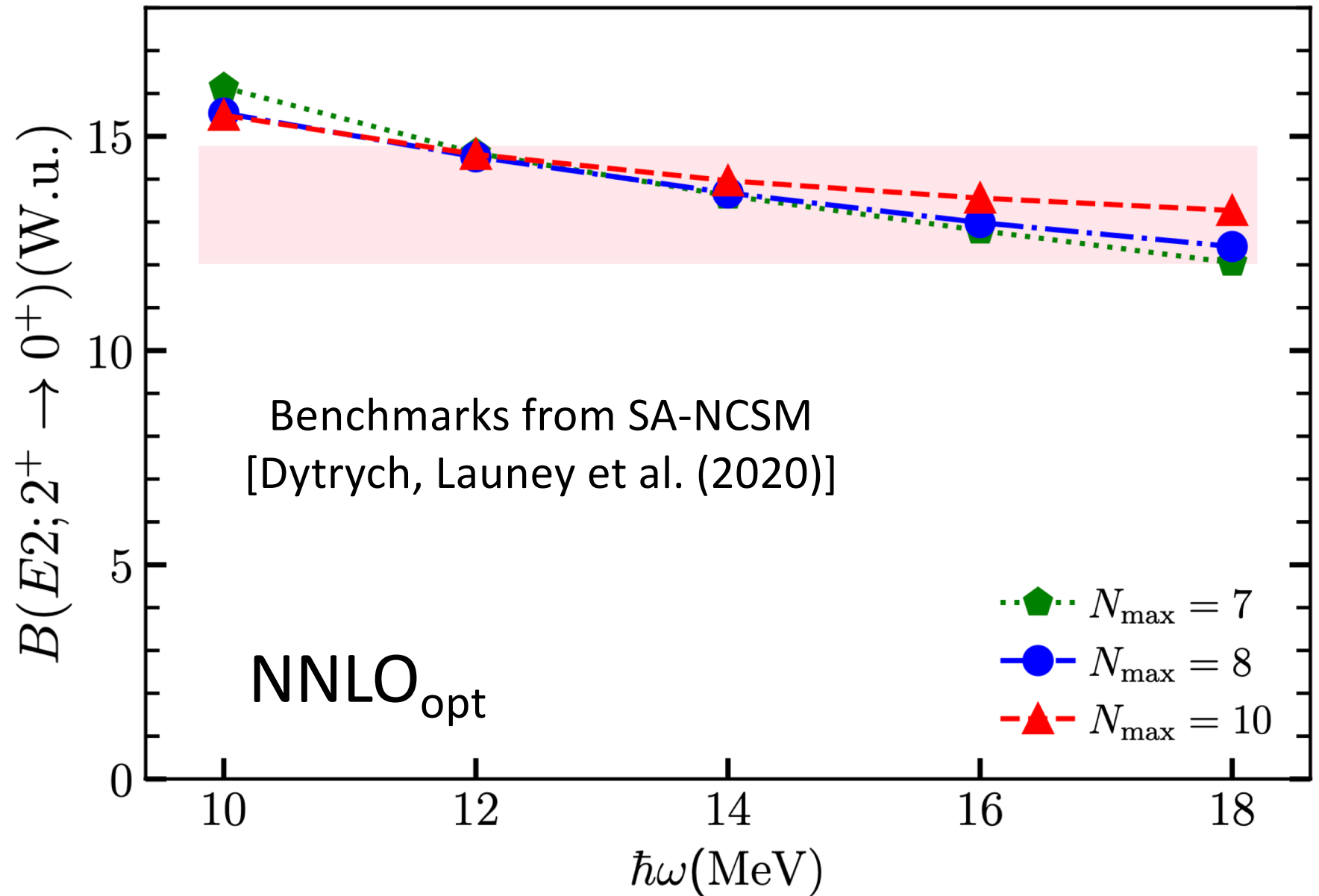
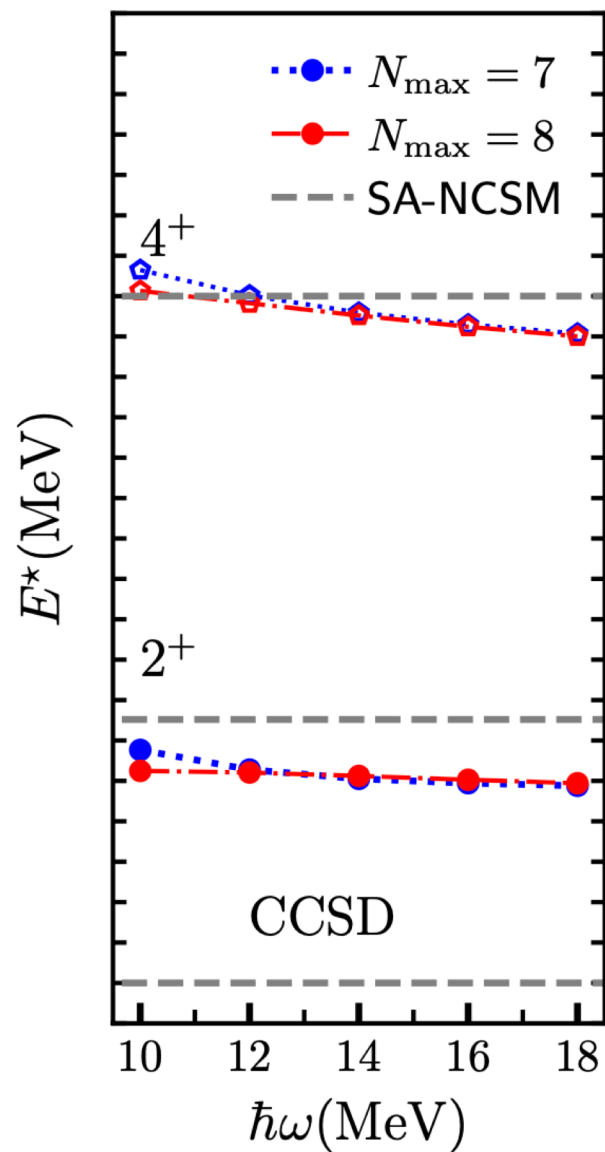
$$B(E2, \downarrow) \equiv |\langle 0^+ || Q_2 || 2^+ \rangle|^2$$

$$B(E2, \downarrow) = \frac{\langle \tilde{\Psi} | P_0 Q_{20} P_2 | \Psi \rangle \langle \tilde{\Psi} | P_2 Q_{20} P_0 | \Psi \rangle}{\langle \tilde{\Psi} | P_0 | \Psi \rangle \langle \tilde{\Psi} | P_2 | \Psi \rangle}$$

Recall the left and right coupled-cluster states:

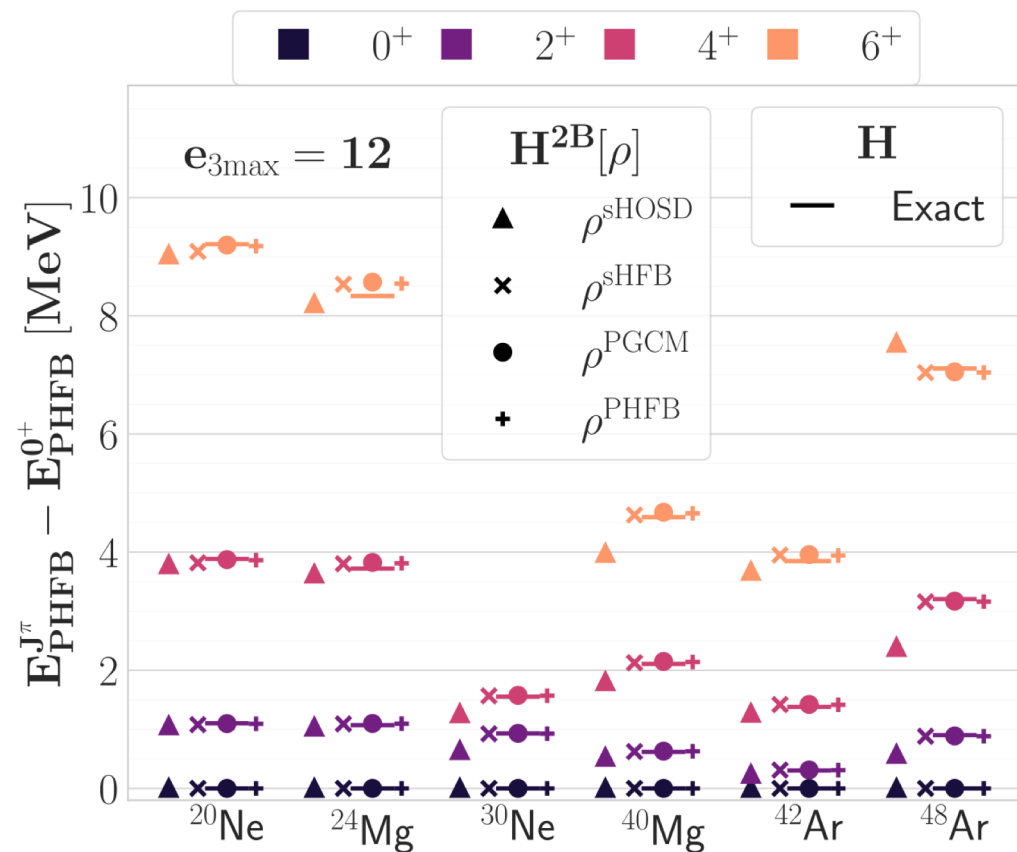
$$\langle \tilde{\Psi} | \equiv \langle \Phi_0 | (1 + \Lambda) e^{-T} \quad | \Psi \rangle \equiv e^T | \Phi_0 \rangle$$

Benchmarking projected coupled-cluster in ^{20}Ne

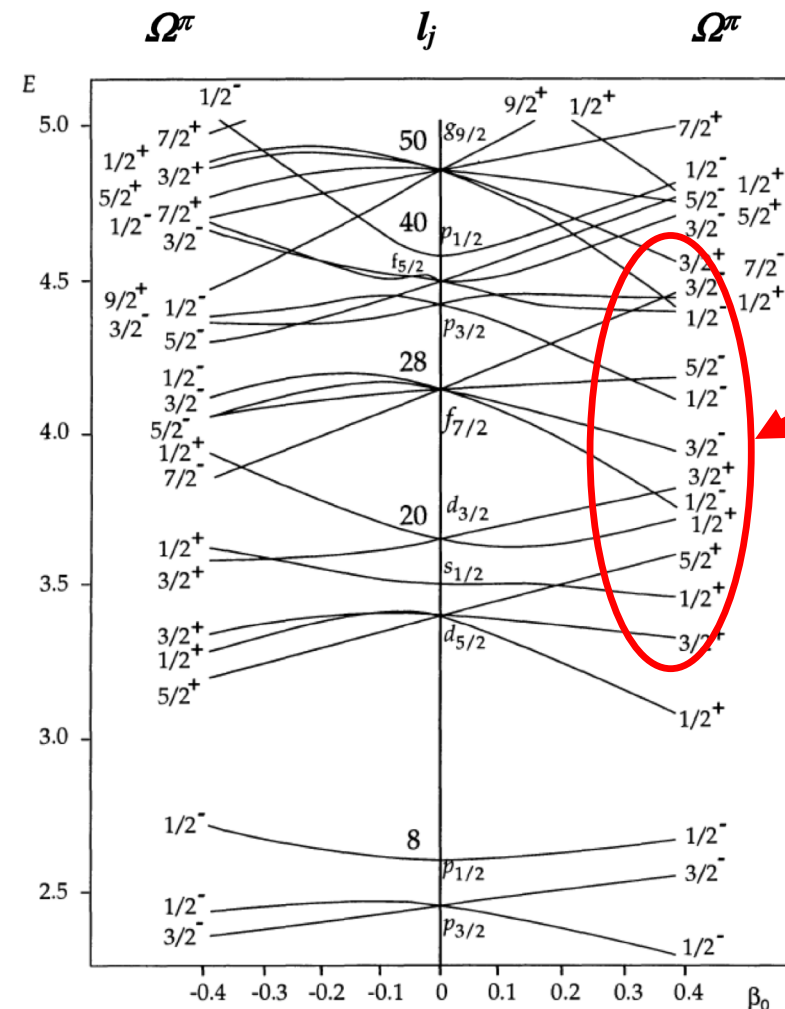


Inclusion of three-body forces

- The normal ordered 2-body approximation breaks rotational symmetry when normal-ordered with respect to a broken symmetry reference state
- Perform spherical HF with fractional filling to normal-order three-nucleon force
- Use normal-ordered Hamiltonian in the 2-body approximation in a second HF calculation of deformed nuclei

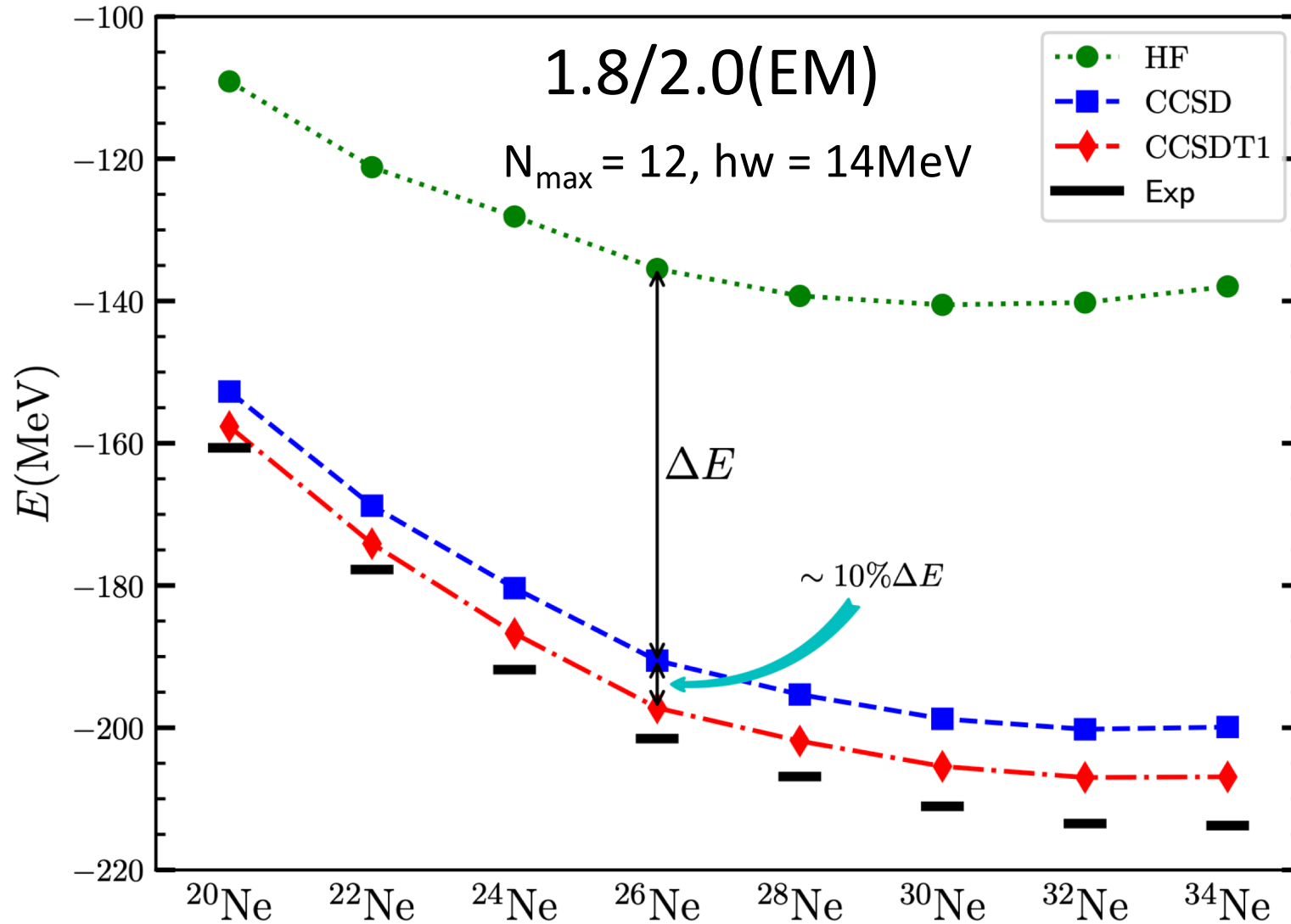


Mikael Frosini et al, Eur. Phys. J. A 57 (2021)



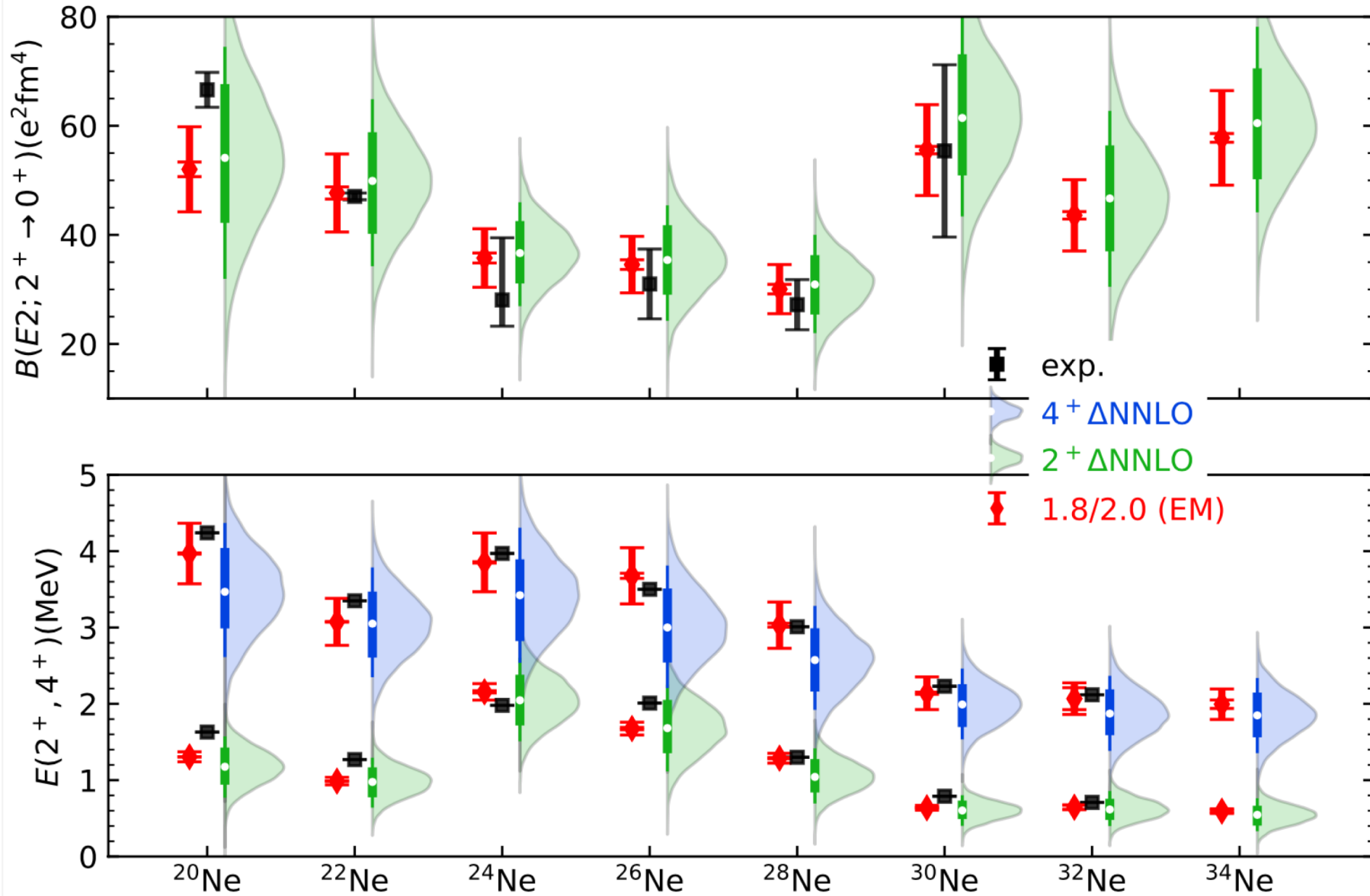
What is the correct spherical filling in very deformed nuclei?

Ground-state energies of neon isotopes



- Use natural orbitals for better convergence of triples excitations
- Computed binding energies overall in good agreement
- Triples excitations yield $\sim 10\%$ of CCSD correlation energy

Collectivity in neon isotopes

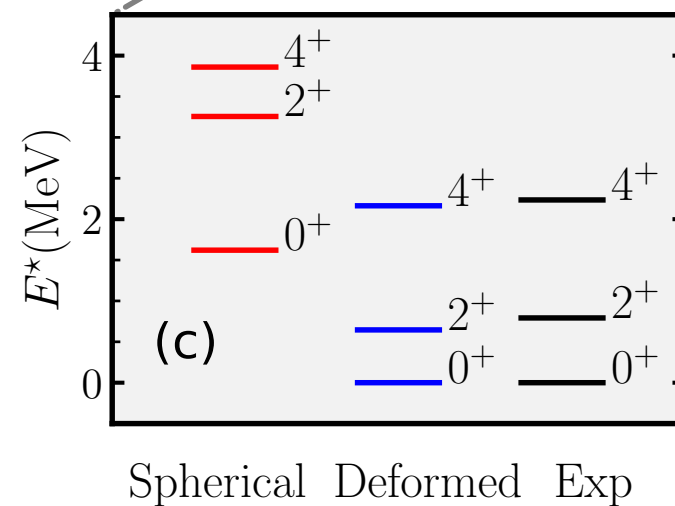
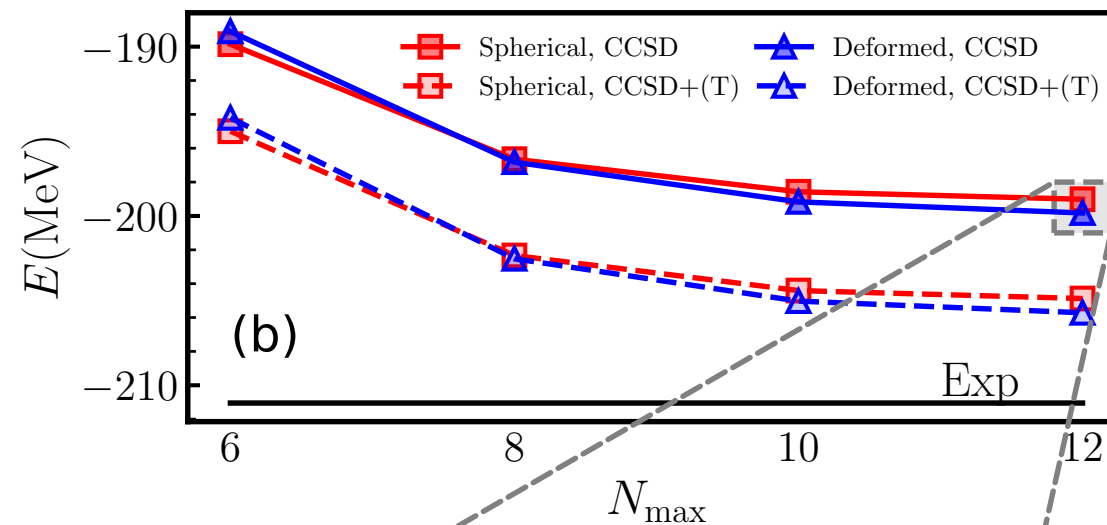
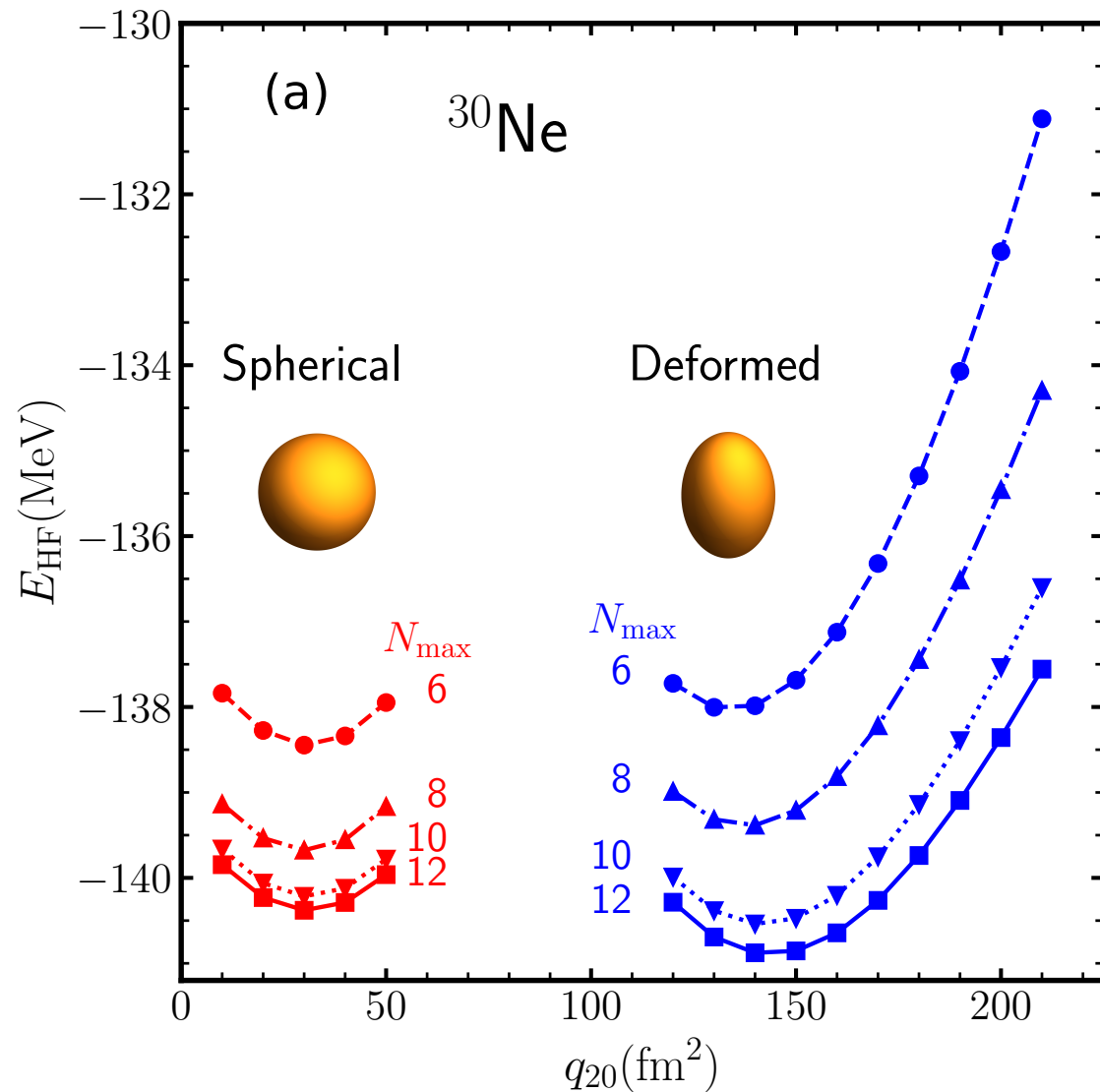


Rotational structure of neutron-rich neon isotopes in good agreement with data

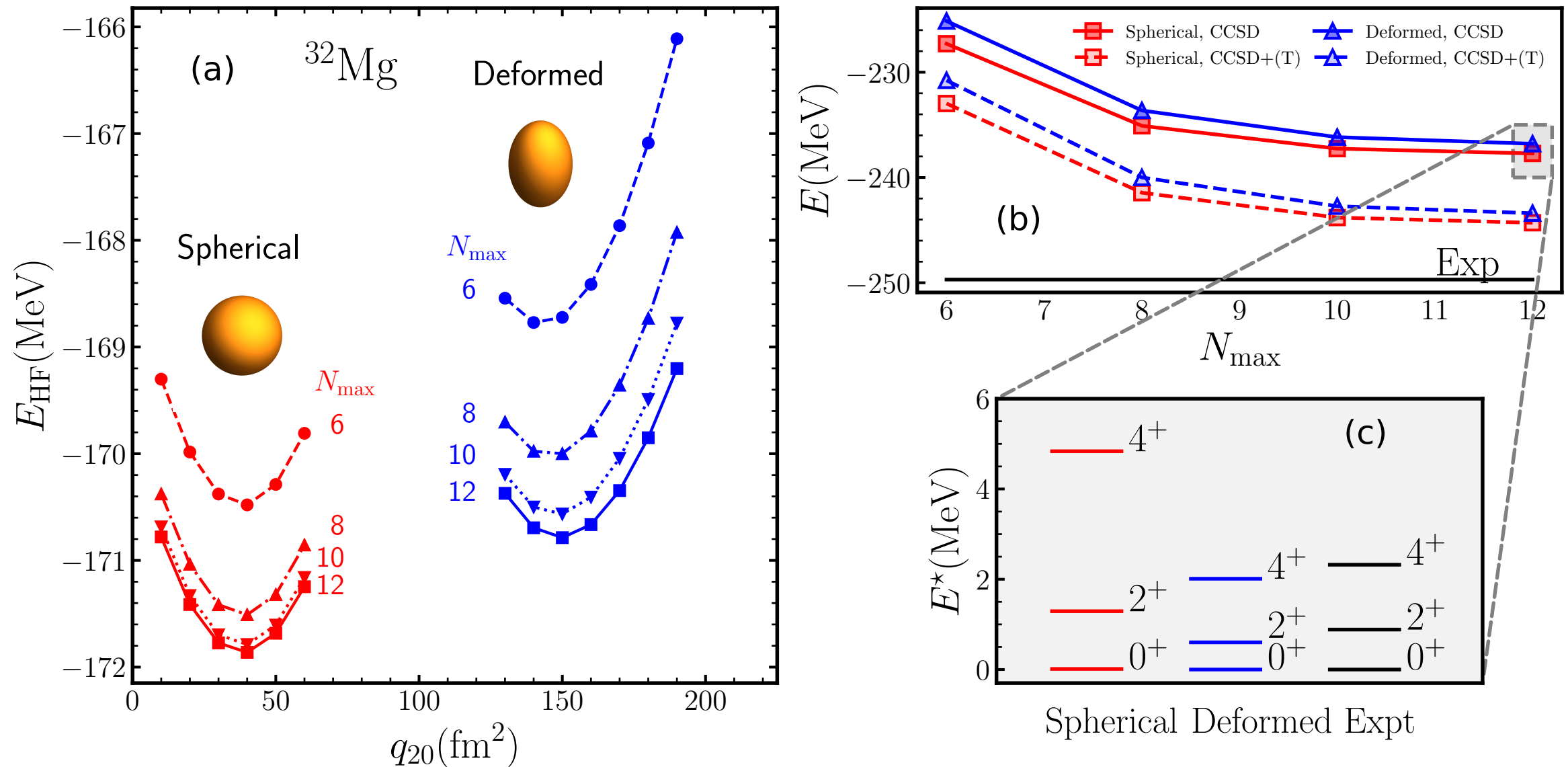
Spectra of $^{30-34}\text{Ne}$ follow that of a rigid rotor $E(J) \propto J(J + 1)$

Small energies reflect a large moment of inertia and a strong deformation

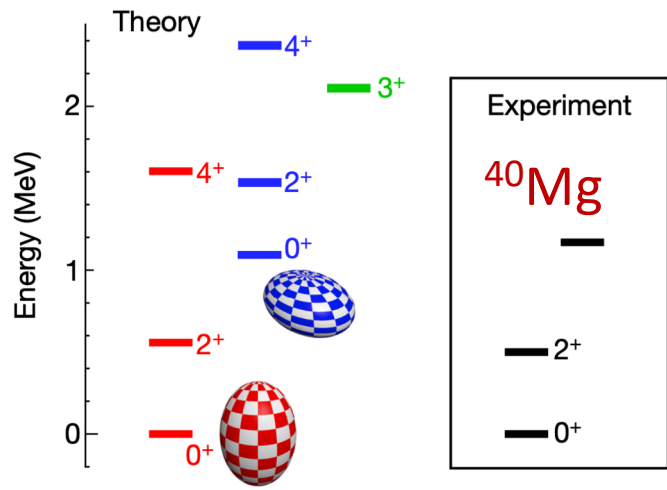
Shape co-existence in ^{30}Ne



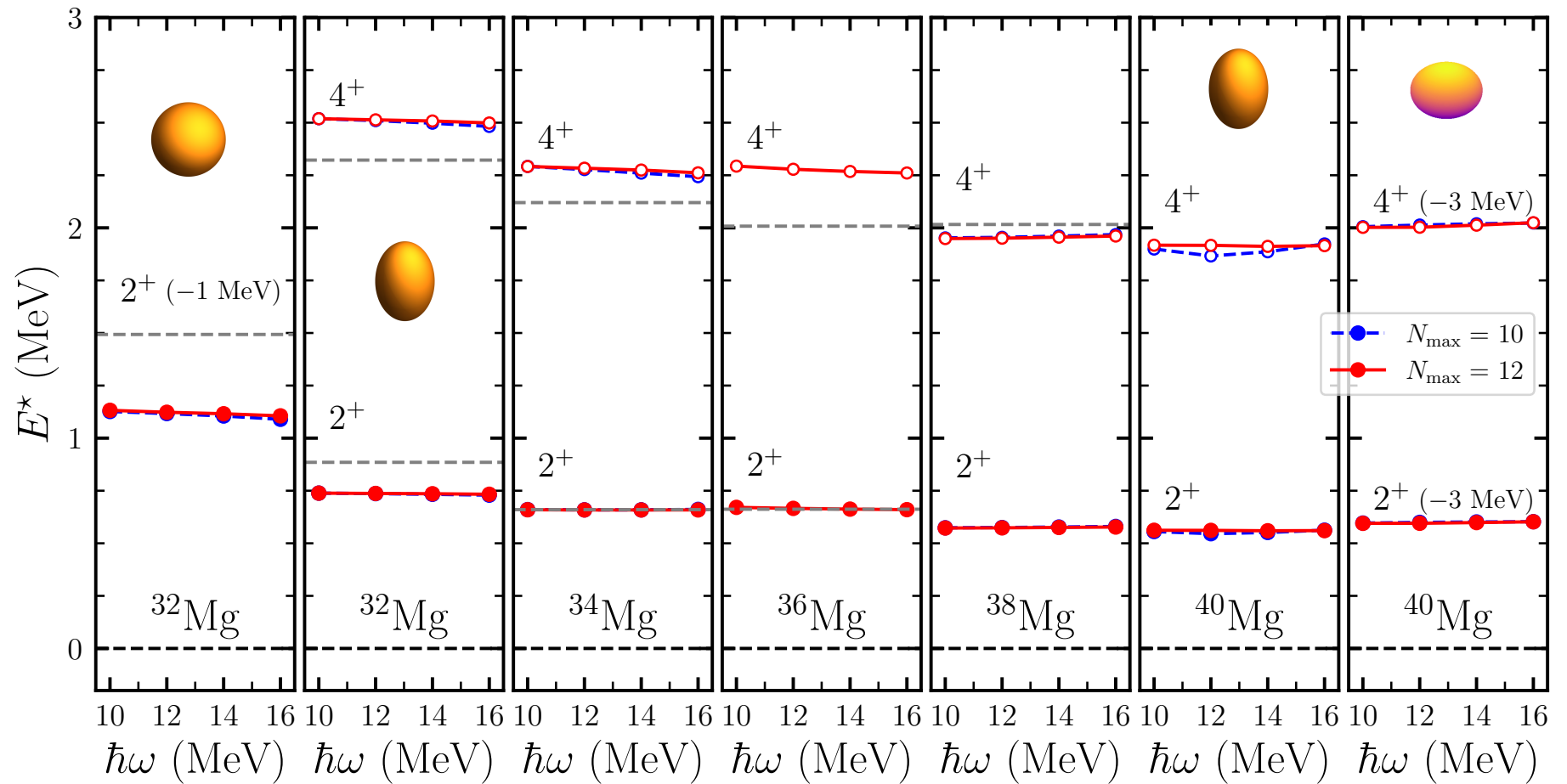
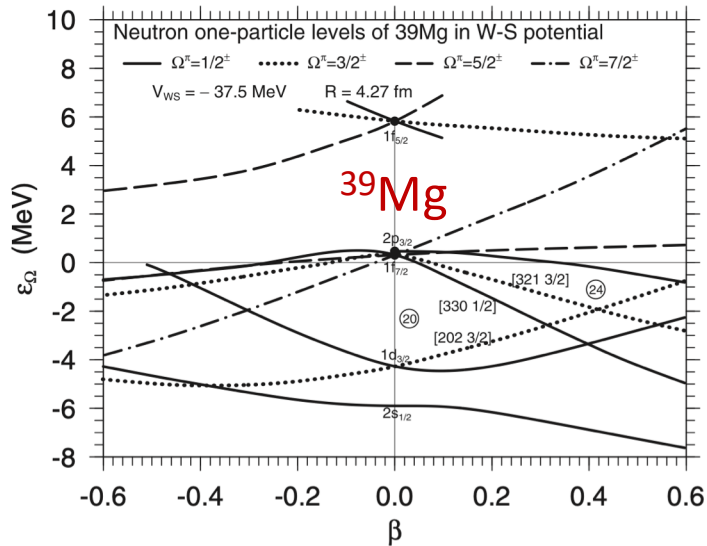
Shape co-existence in ^{32}Mg



Deformation in neutron-rich magnesium



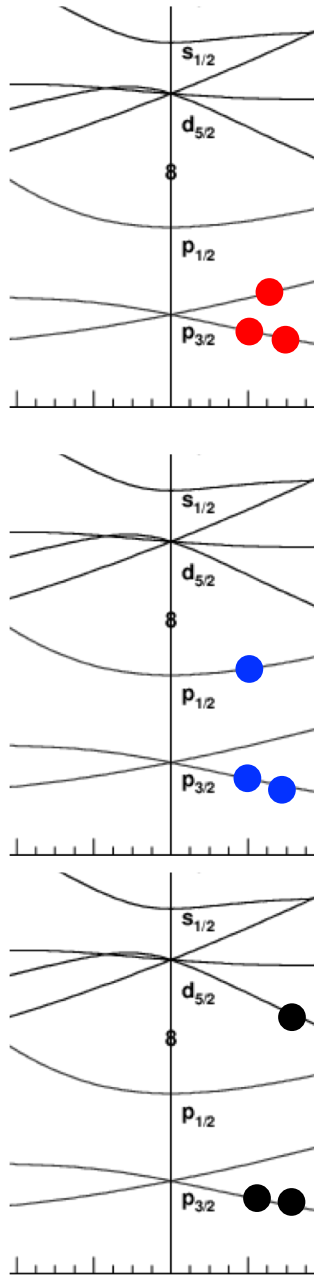
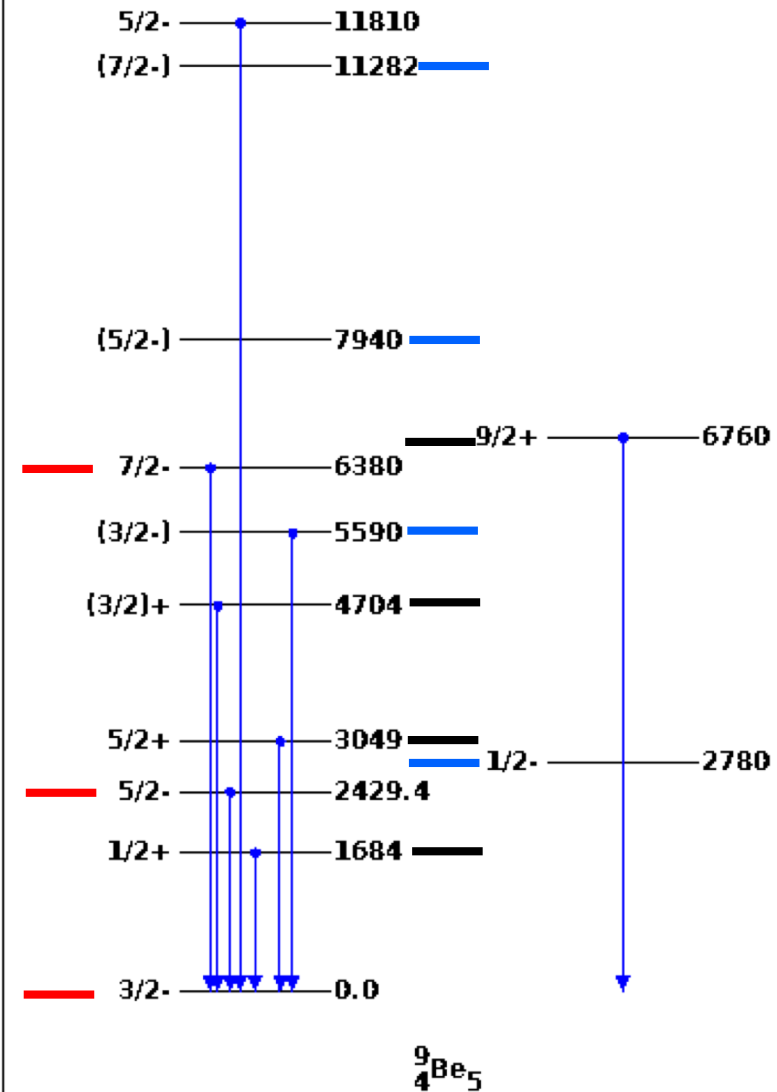
Crawford et al. PRL 122, 052501 (2019)
Tsunuda et al, Nature 587, 66 (2020)



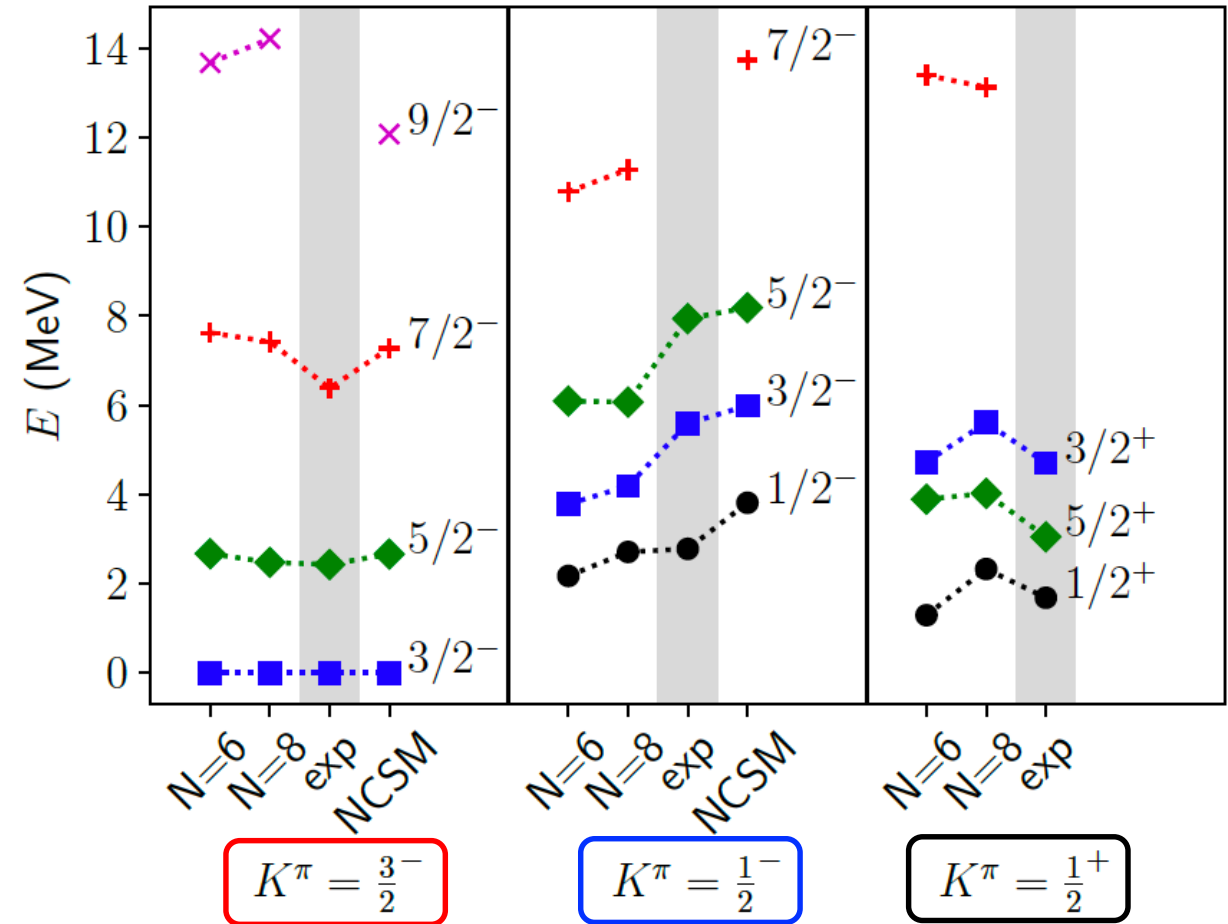
- Rotational structure in good agreement with experiment
- Indications of shape co-existence in ^{40}Mg
- Find oblate band in ^{40}Mg 2-3MeV above the prolate band

Making sense of spectra in odd-mass nuclei

Looks complicated;
shown data lacks understanding



Zhonghao Sun et al., in preparation
Hartree-Fock computations yield deformed reference
Coupled-cluster + projection yields bands

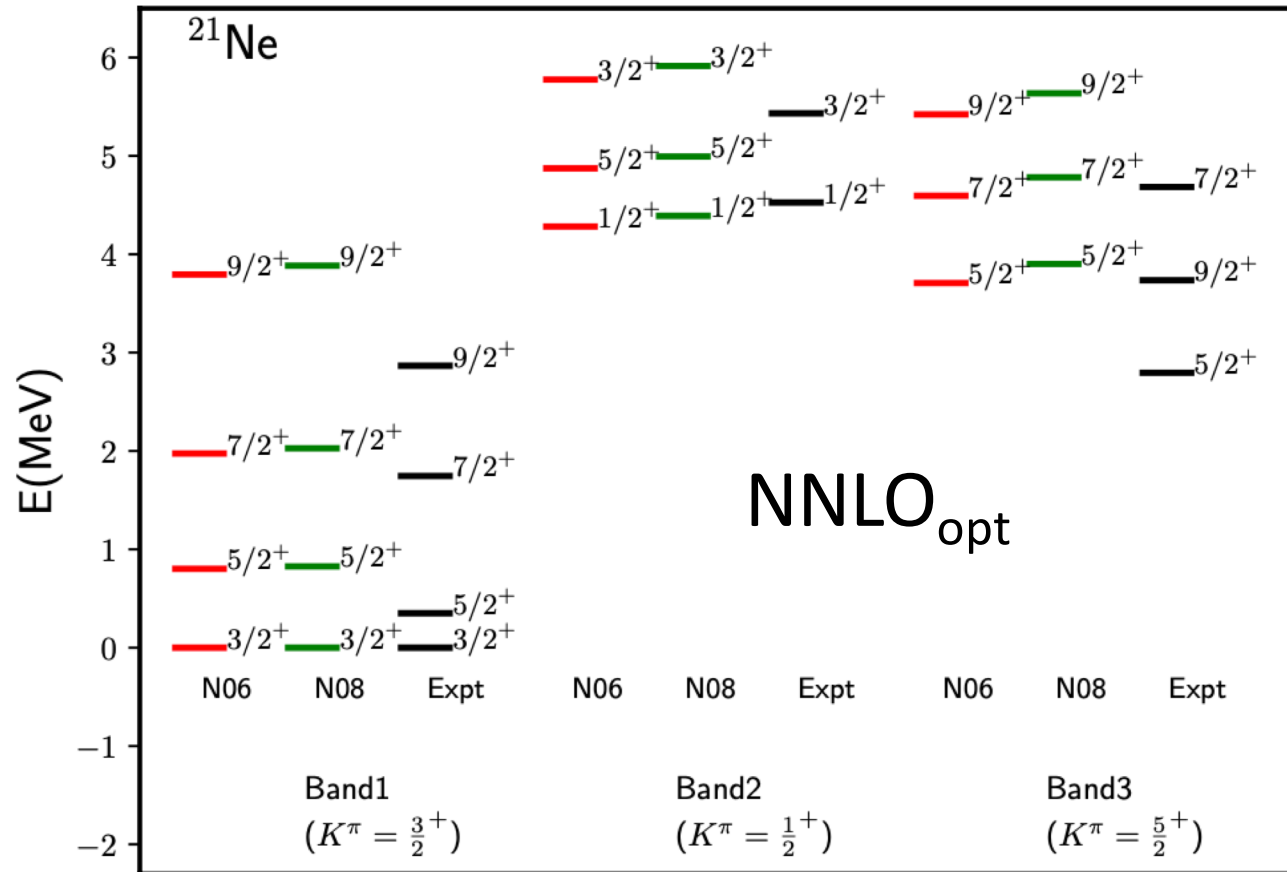


NCSM from Caprio, Maris, Vary & Smith,
Int. J. Mod. Phys. E 24, 1541002 (2015)

Rotational bands in odd-mass nuclei

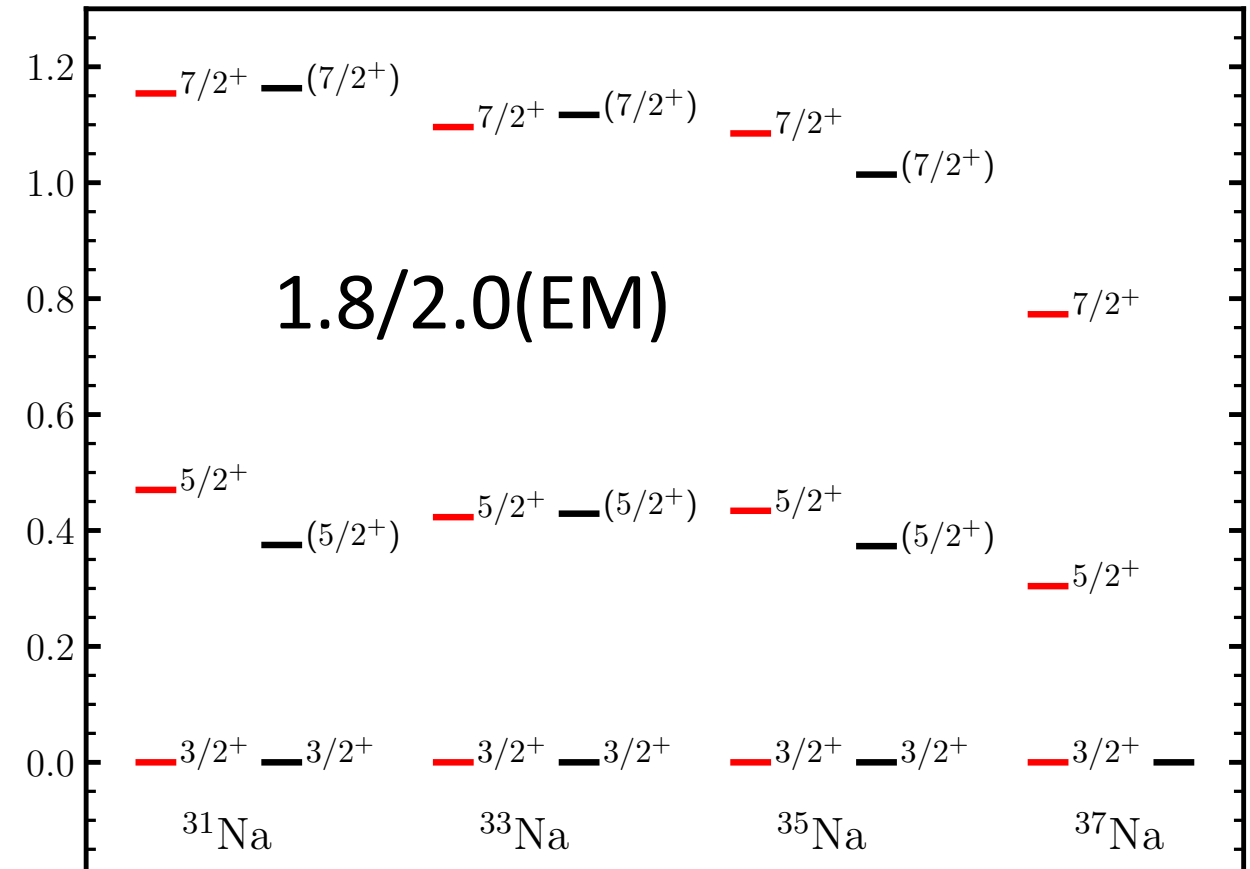
Protons are paired

Neutron occupy ($j = d5/2, j_z=1/2, 3/2$ and $5/2$)



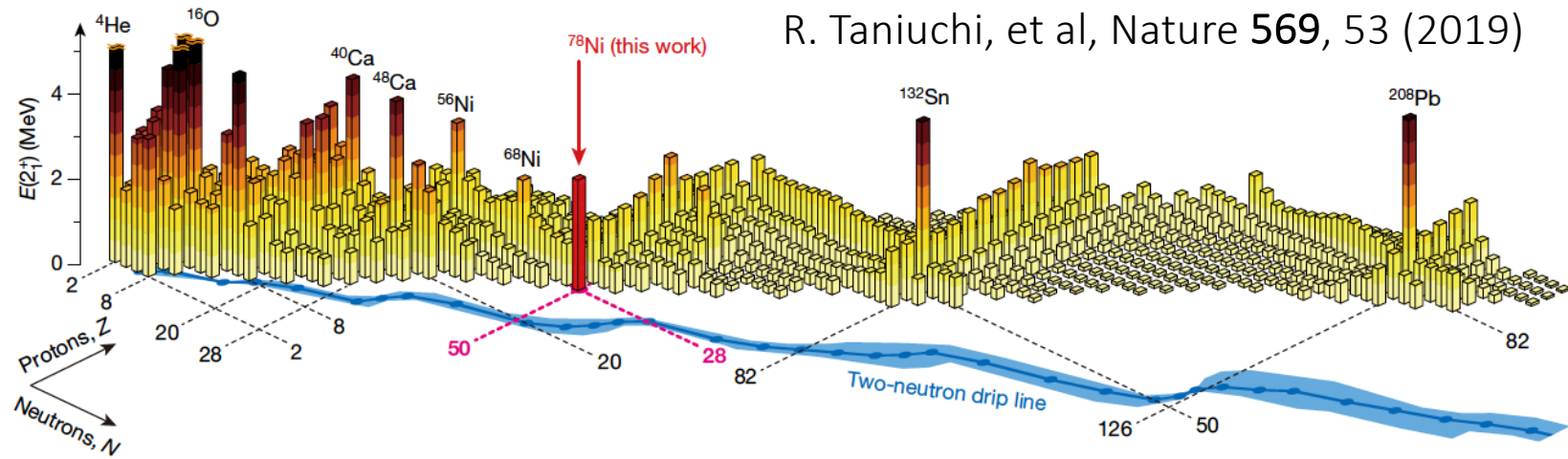
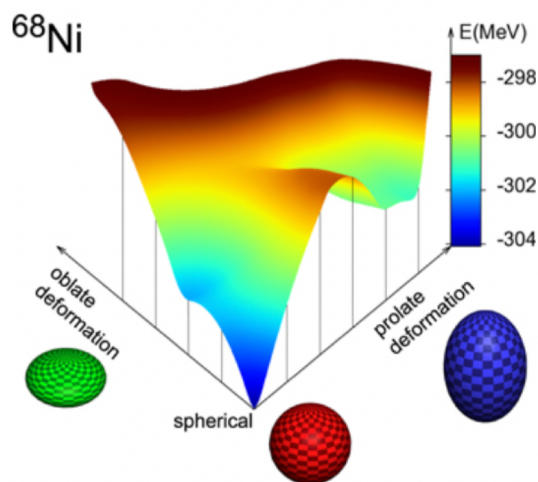
Proton occupy ($j = d5/2, j_z=3/2$)

Neutrons are paired.



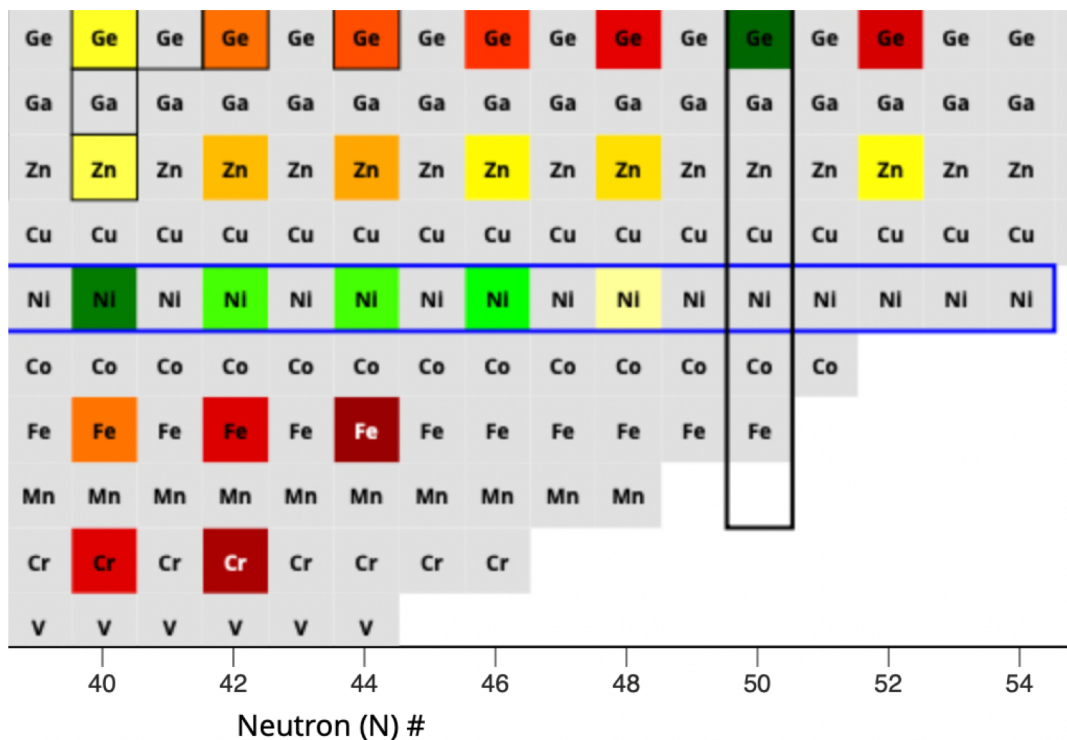
Zhonghao Sun et al., in preparation (2024)

Onset of deformation around ^{78}Ni

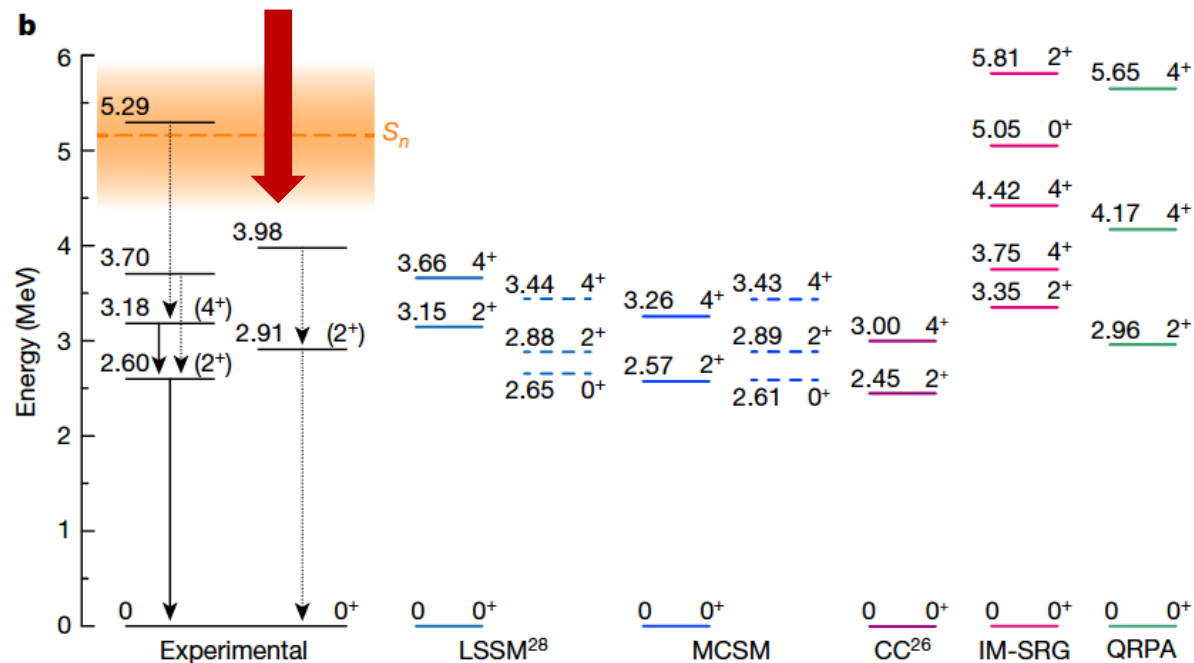


R. Taniuchi, et al, Nature 569, 53 (2019)

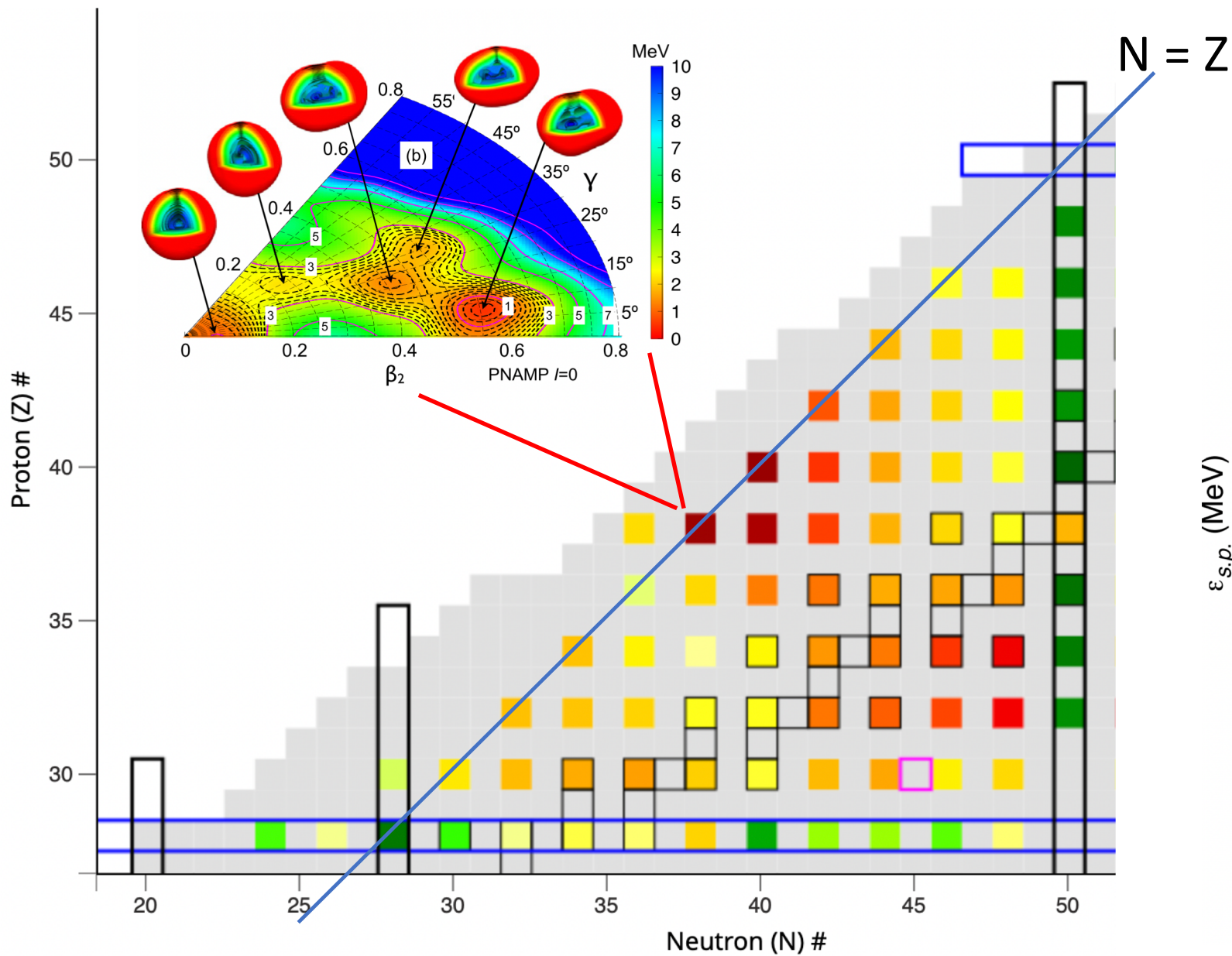
T Otsuka and Y Tsunoda *J. Phys. G* **43** 024009 (2016)



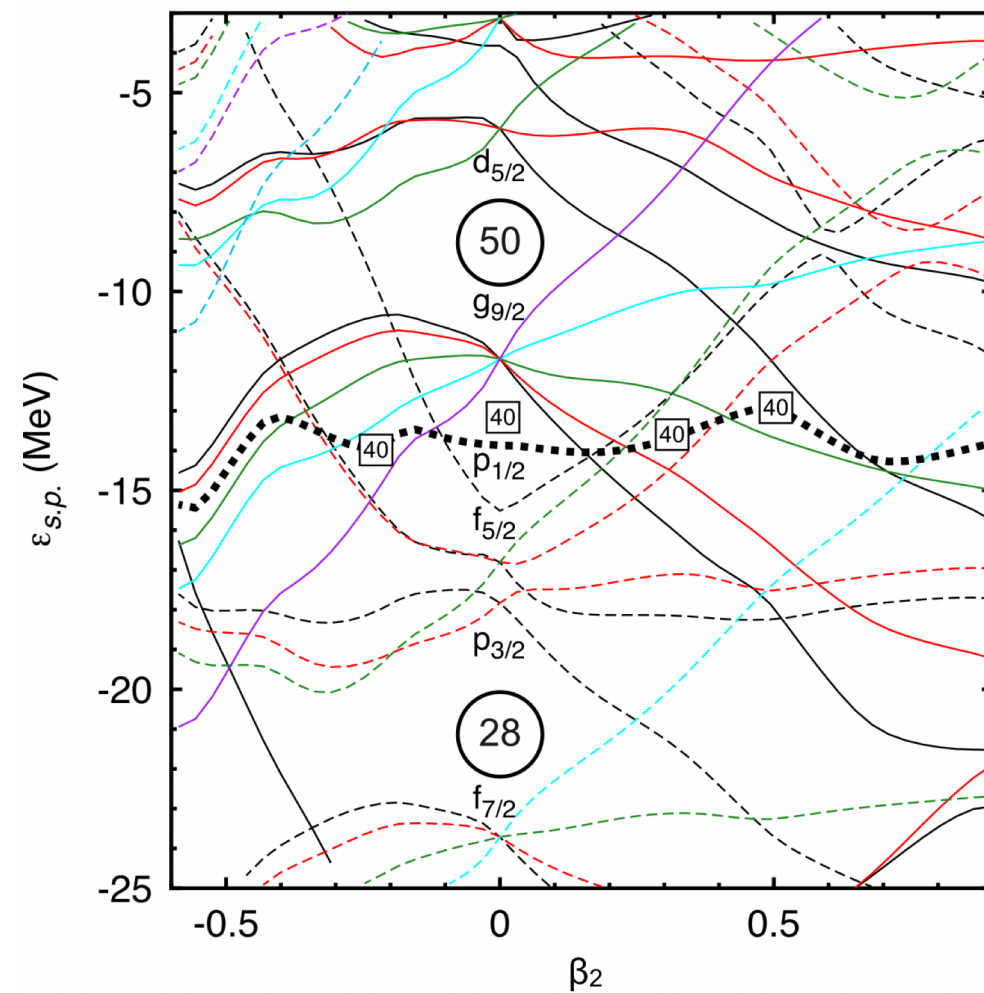
Deformed band?
Where is the band head?



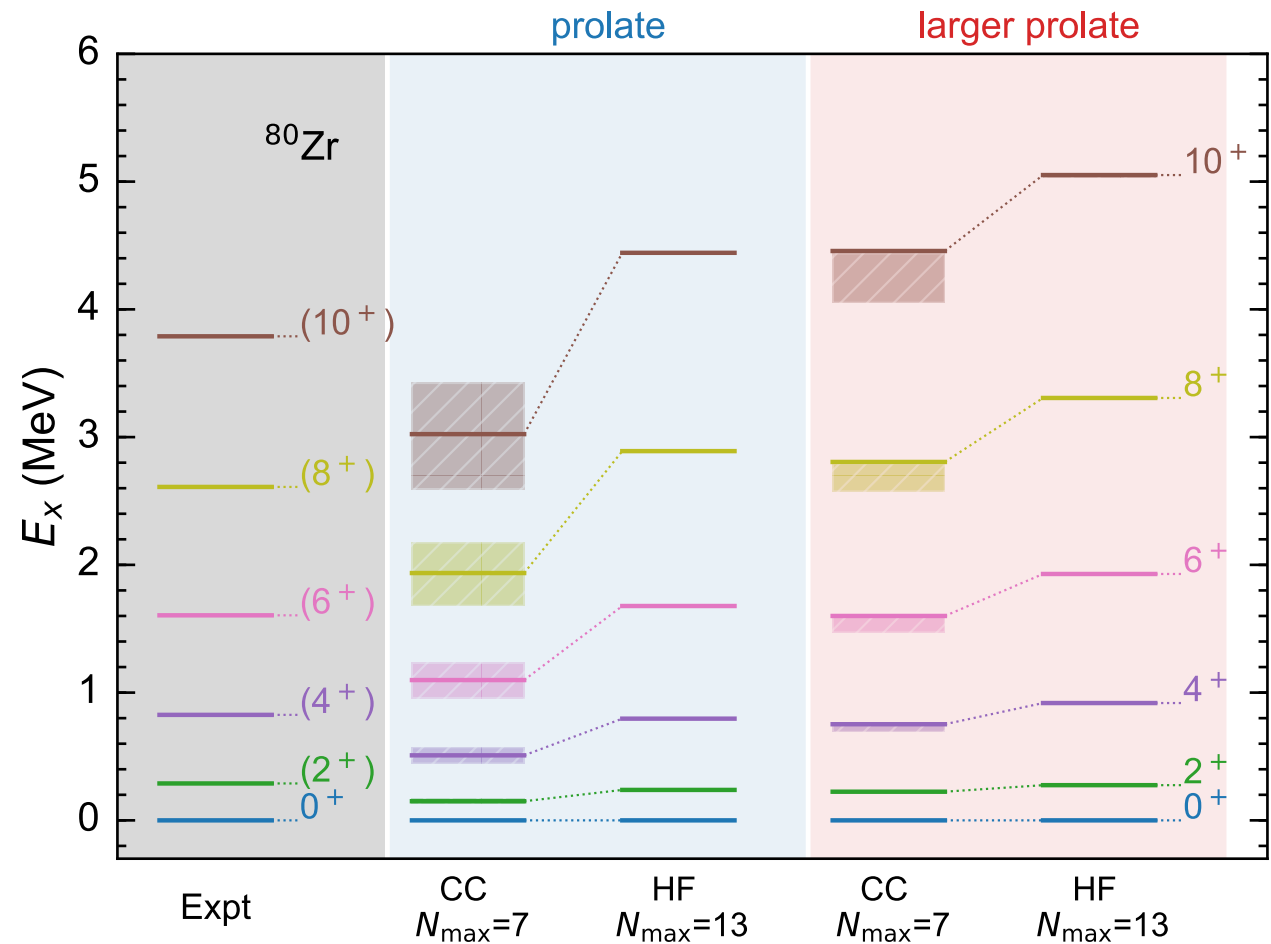
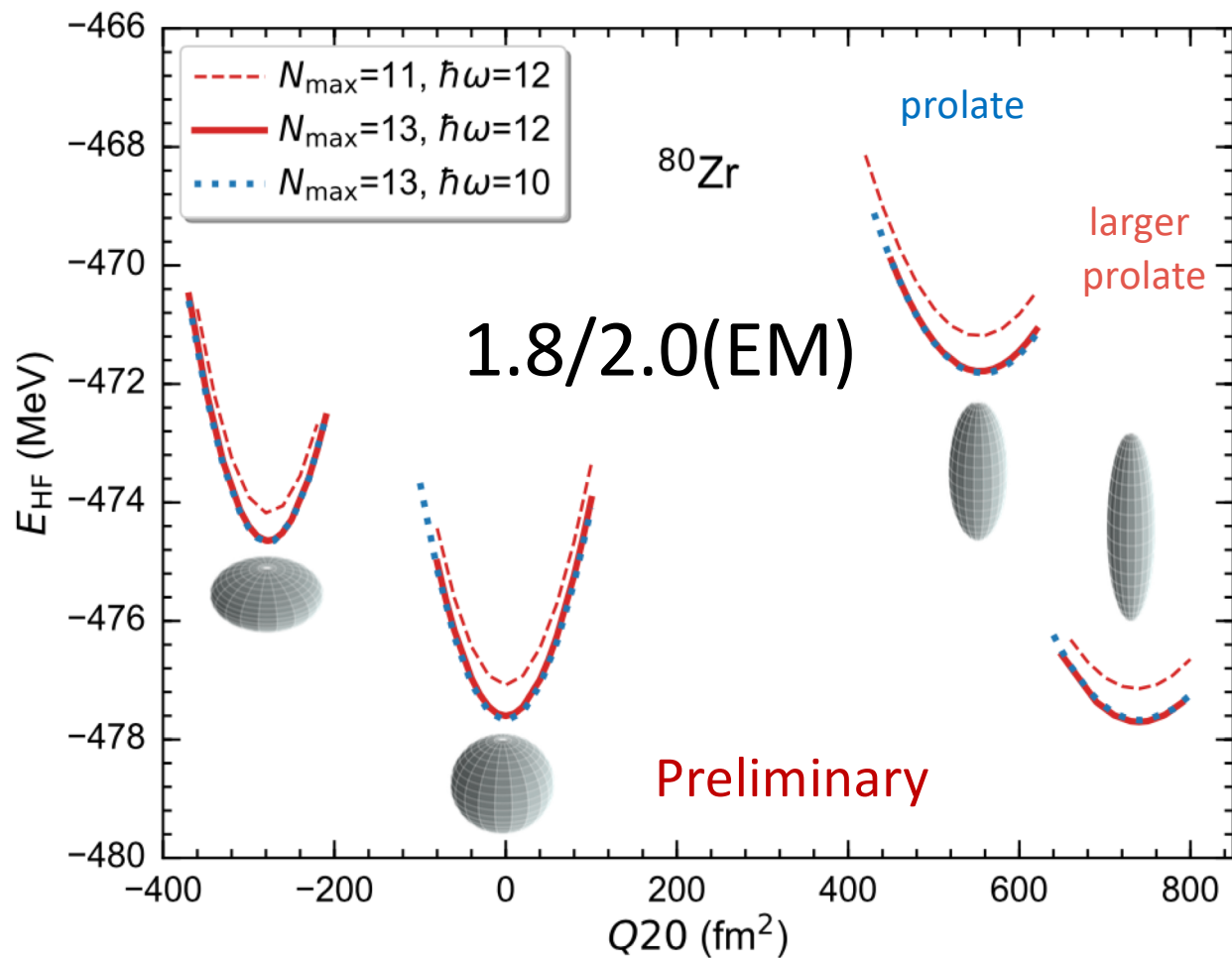
Coupled-cluster computations of strongly deformed nuclei around ^{80}Zr



Tomás R. Rodríguez, J. Luis Egido,
Phys. Lett. B 705 255 (2011)

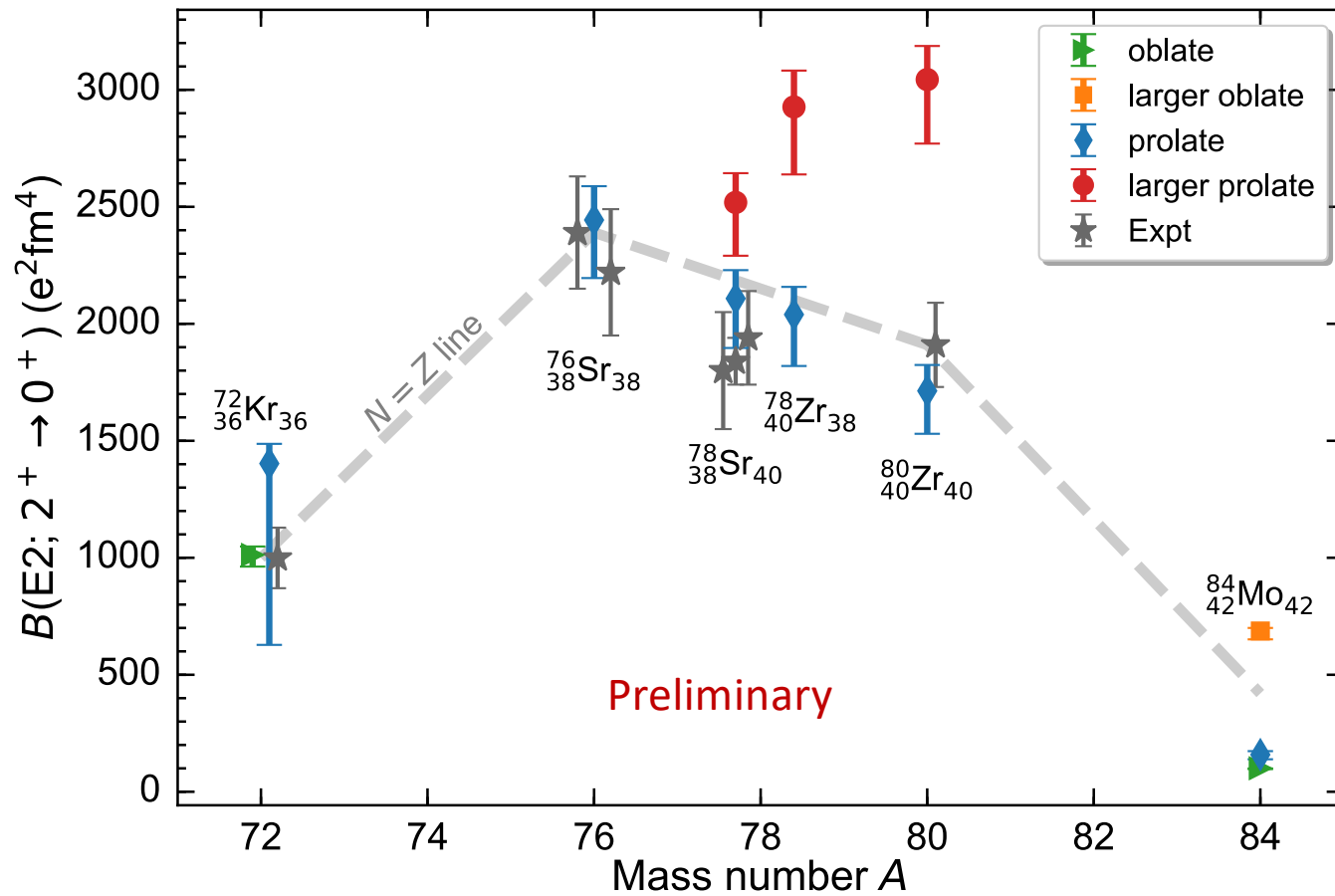


Coupled-cluster computations of strongly deformed nuclei around ^{80}Zr



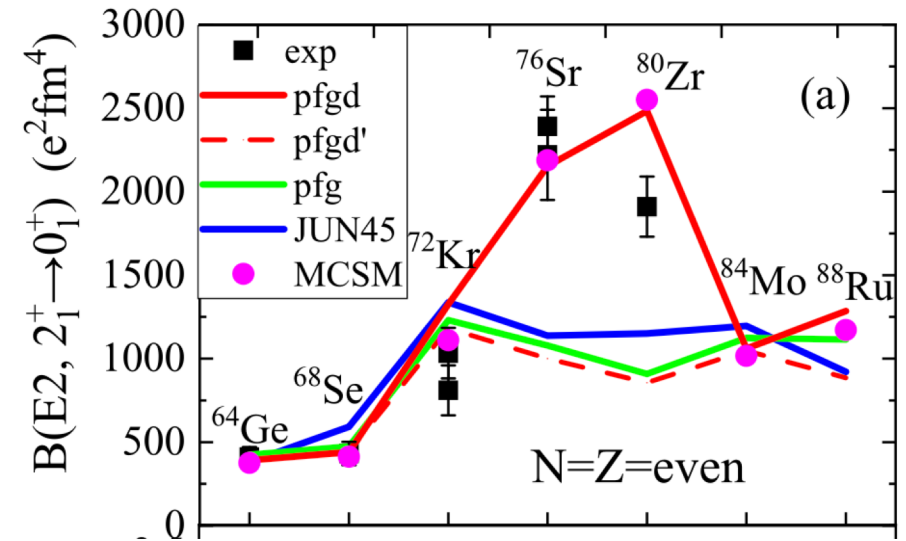
Baishan Hu, Zhonghao Sun, G. Hagen, T. Papenbrock. in preparation (2024)

Coupled-cluster computations of strongly deformed nuclei around ^{80}Zr

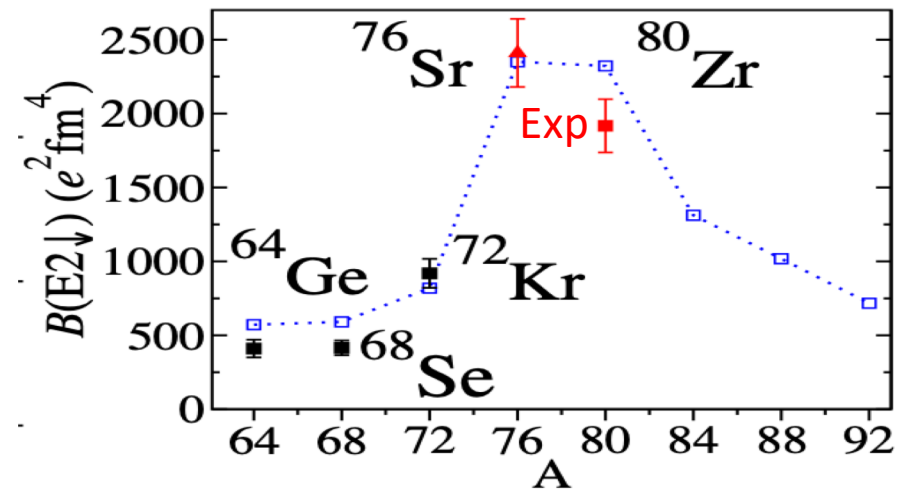


Baishan Hu, Zhonghao Sun, G. Hagen, T. Papenbrock.
in preparation (2024)

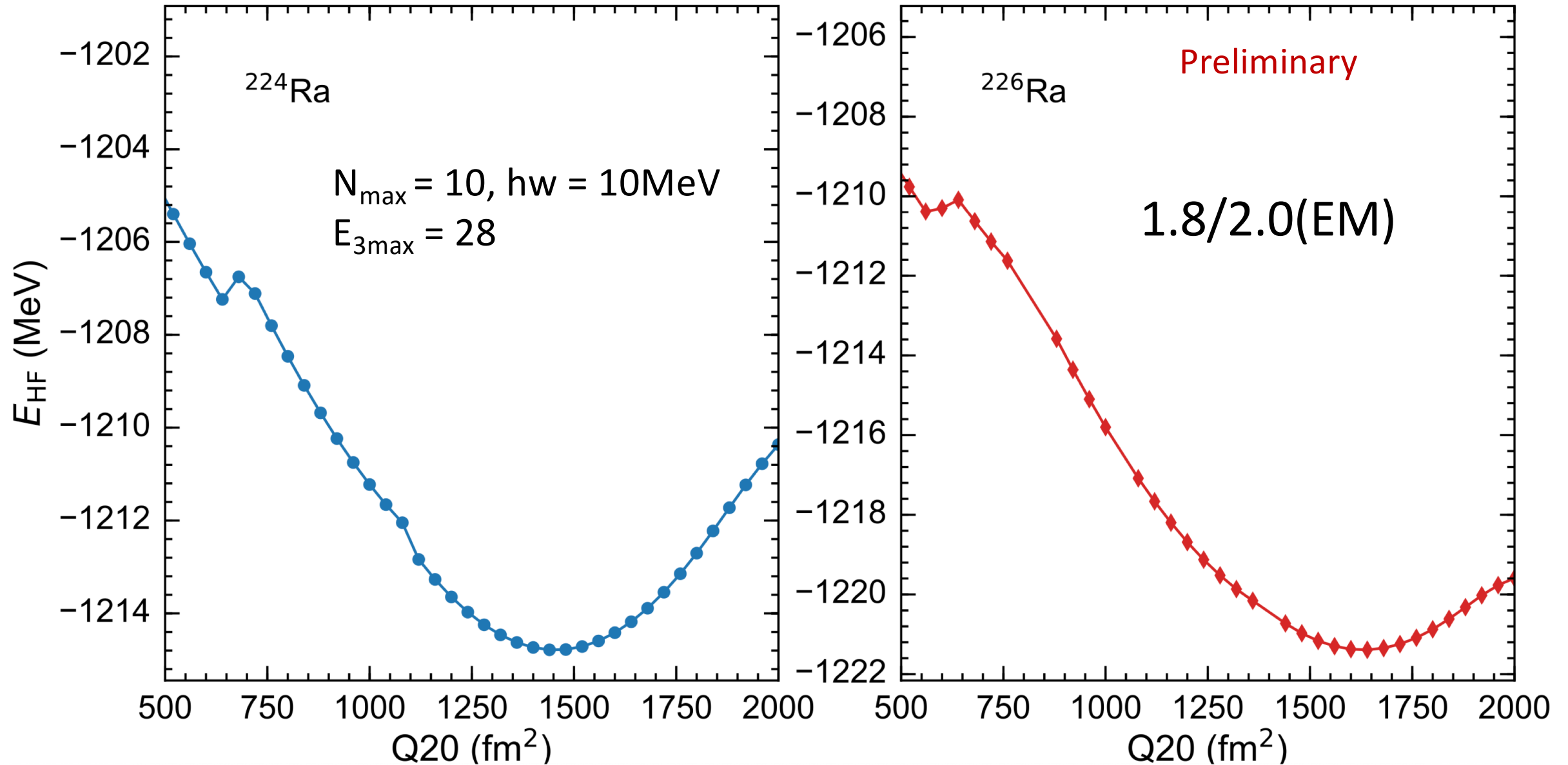
Shell model K. Kaneko, et al, Phys Lett B **817**, 136286 (2021)



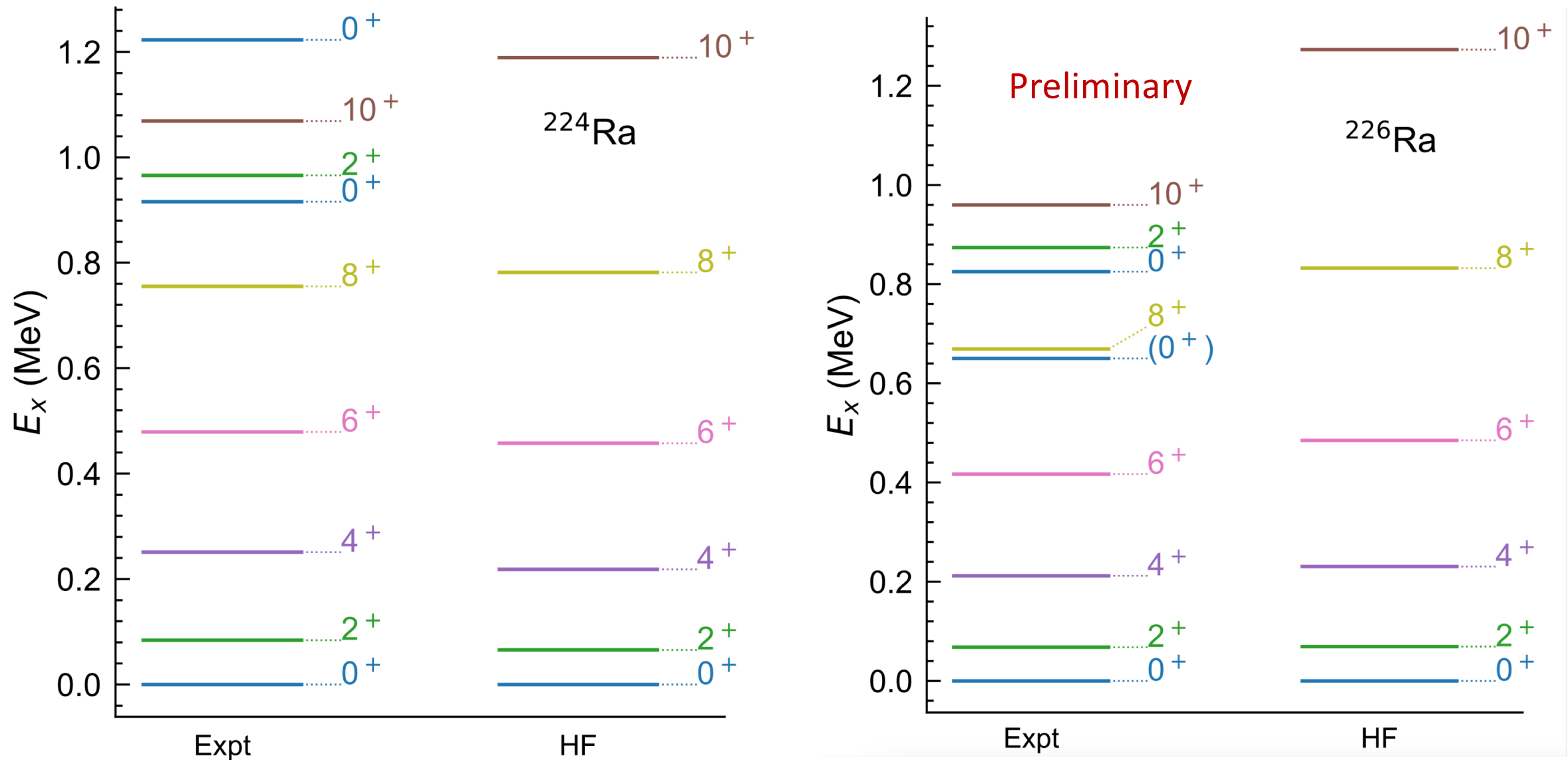
Mean field R.D.O. Llewellyn, et al, Phys Rev Lett **124**, 152501 (2020)



Ab-initio description of Schiff moments in heavy deformed nuclei?

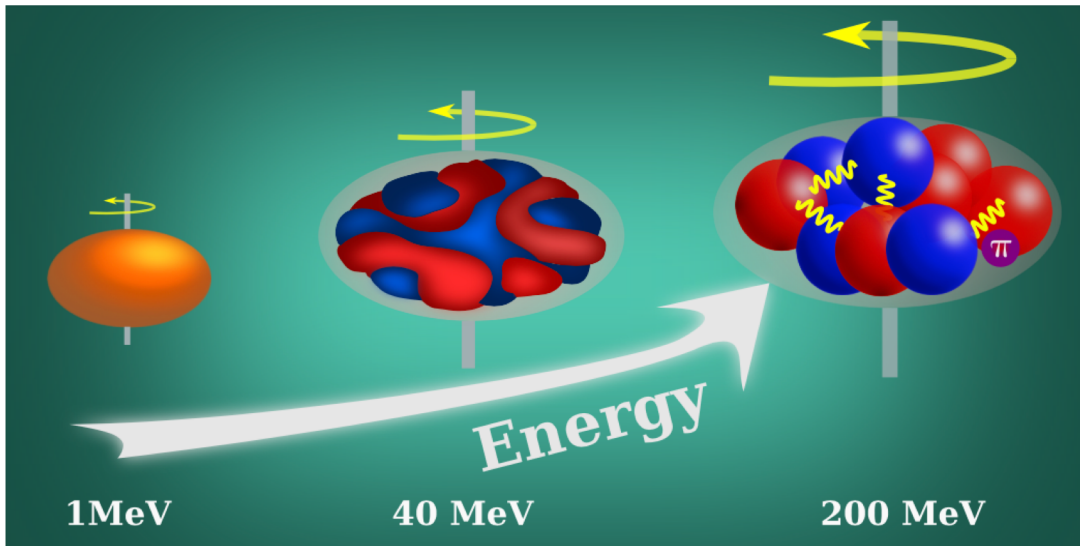


Ab-initio description of Schiff moments in heavy deformed nuclei?

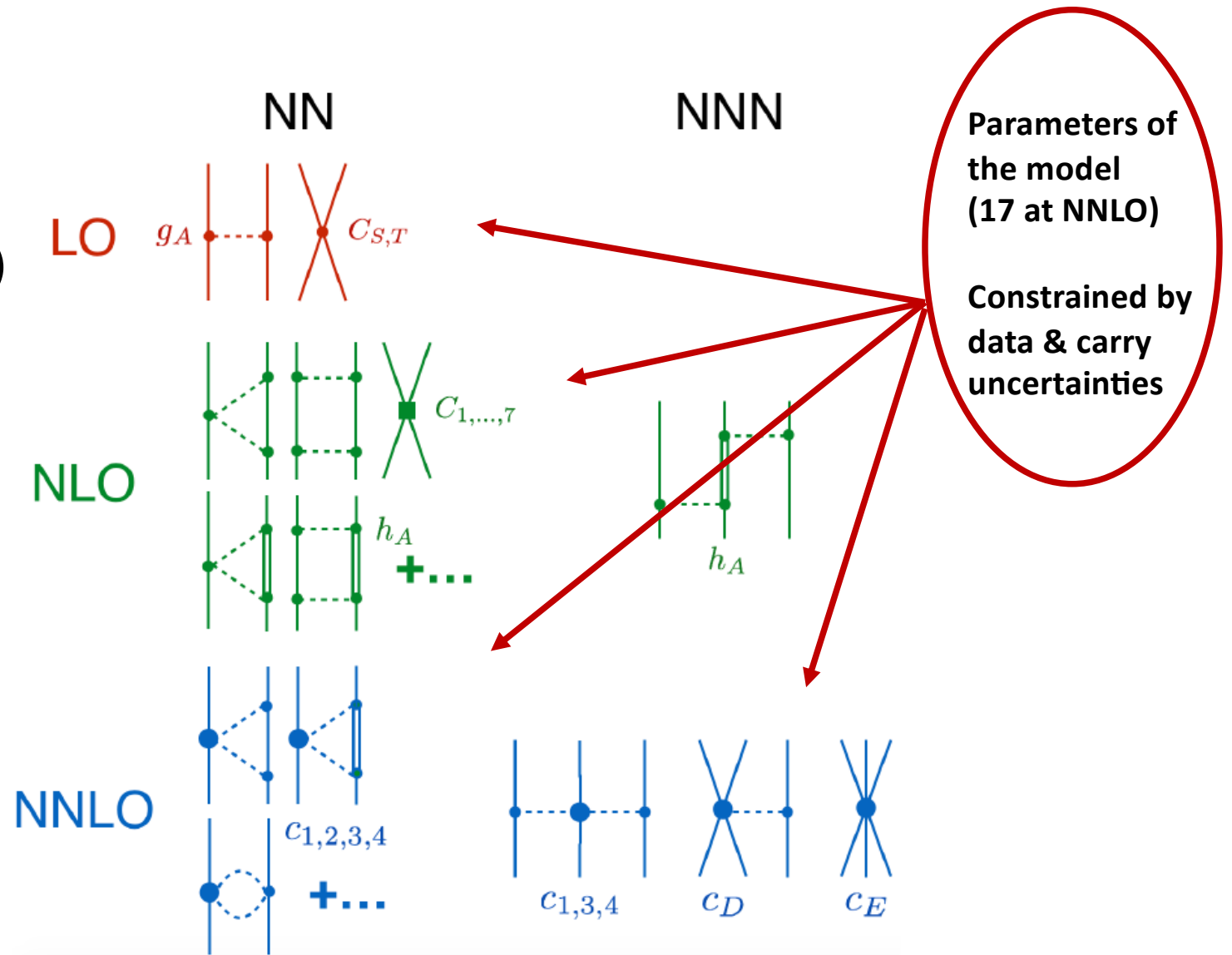


What drives deformation in nuclei?

- 50's: surface vibrations of a liquid drop (Bohr/Mottelson)
- 60's: competition between pairing and quadrupole interactions from HFB calculations in two shells (Baranger/Kumar)
- 70's: isoscalar neutron-proton interactions dominate over isovector pairing from shell model (Federman/Pittel, Dufour/Zuker)



Nuclear deformation viewed at different resolution scales



Global sensitivity analysis

Sensitivity analysis addresses the question ‘How much does each model parameter contribute to the uncertainty in the prediction?’

Global methods deal with the uncertainties of the outputs due to input variations over the whole domain.

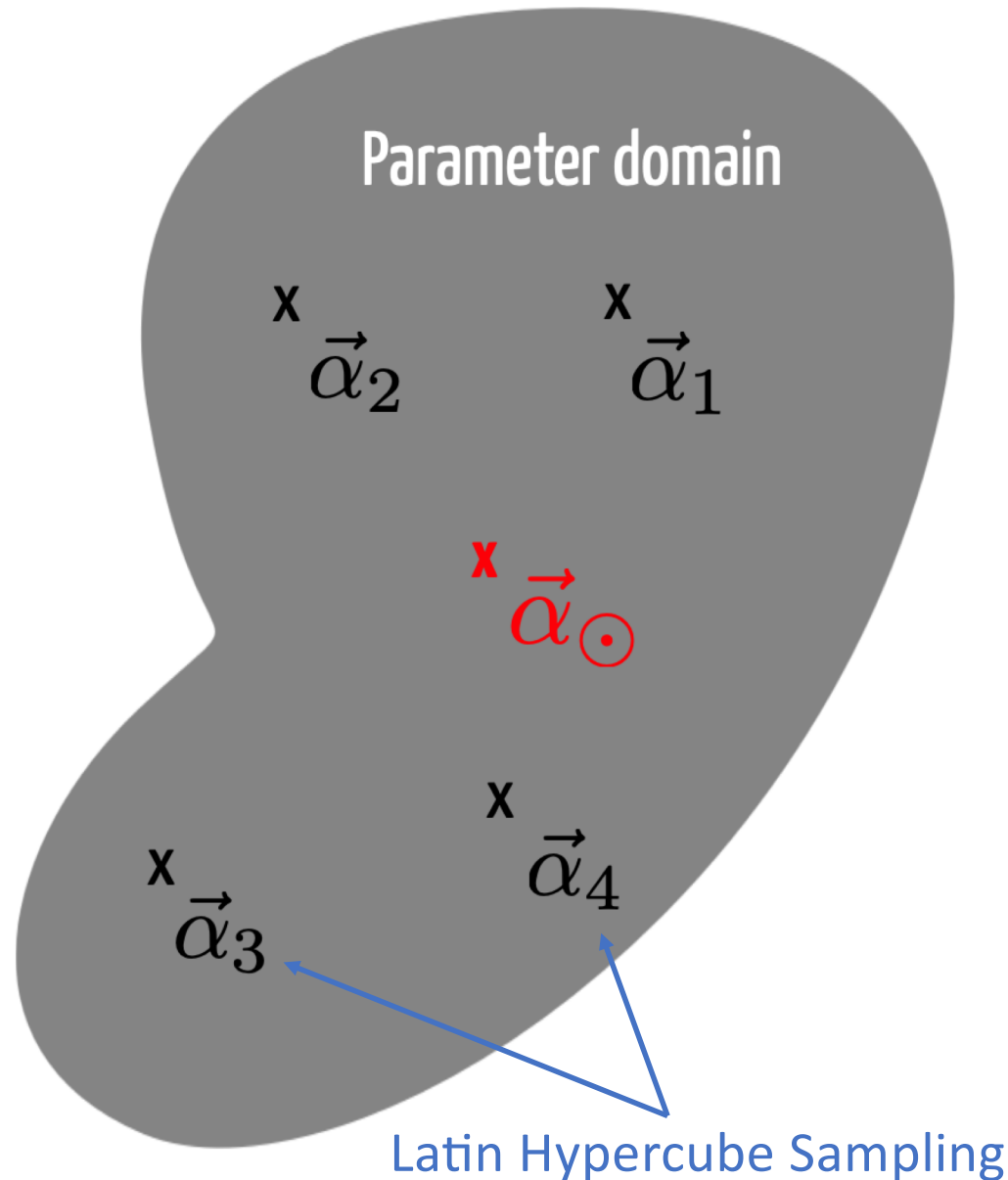
Computational bottleneck

A global sensitivity analyses of properties of atomic nuclei typically would require more than one million model evaluations



Emulating ab-initio coupled-cluster calculations

Andreas Ekström, Gaute Hagen PRL **123**, 252501 (2019)



- Eigenvector continuation method [Frame D. et al., Phys. Rev. Lett. 121, 032501 (2018), S. König et al Phys. Lett. B 810 (2020) 135814]

- Write the Hamiltonian in a linearized form

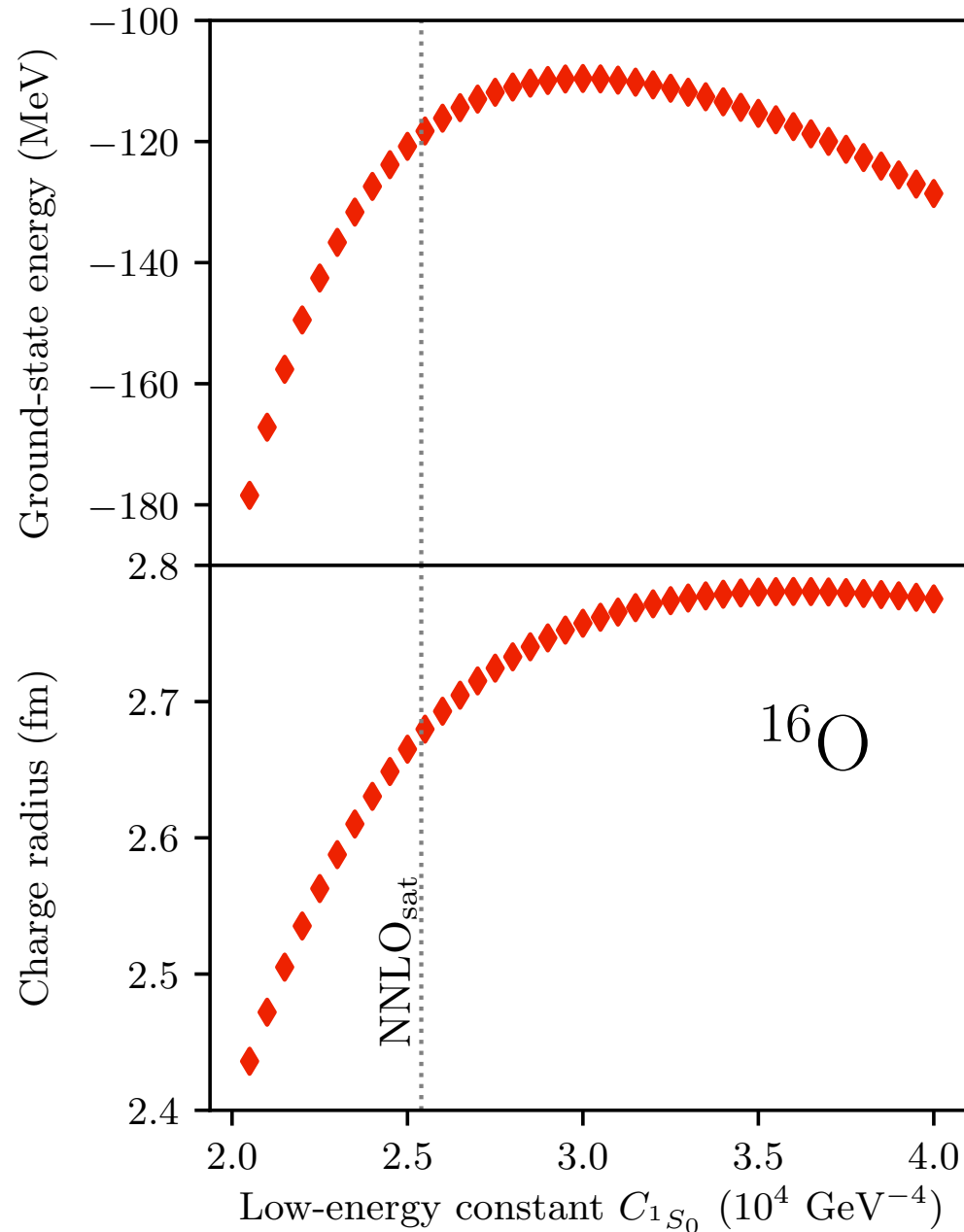
$$H(\vec{\alpha}) = h_0 + \sum_{i=1}^{N_{\text{LECS}}=17} \alpha_i h_i$$

- Select “training points” (snap-shots) where we solve the exact problem
- Project a target Hamiltonian onto subspace of training vectors and diagonalize the generalized eigenvalue problem

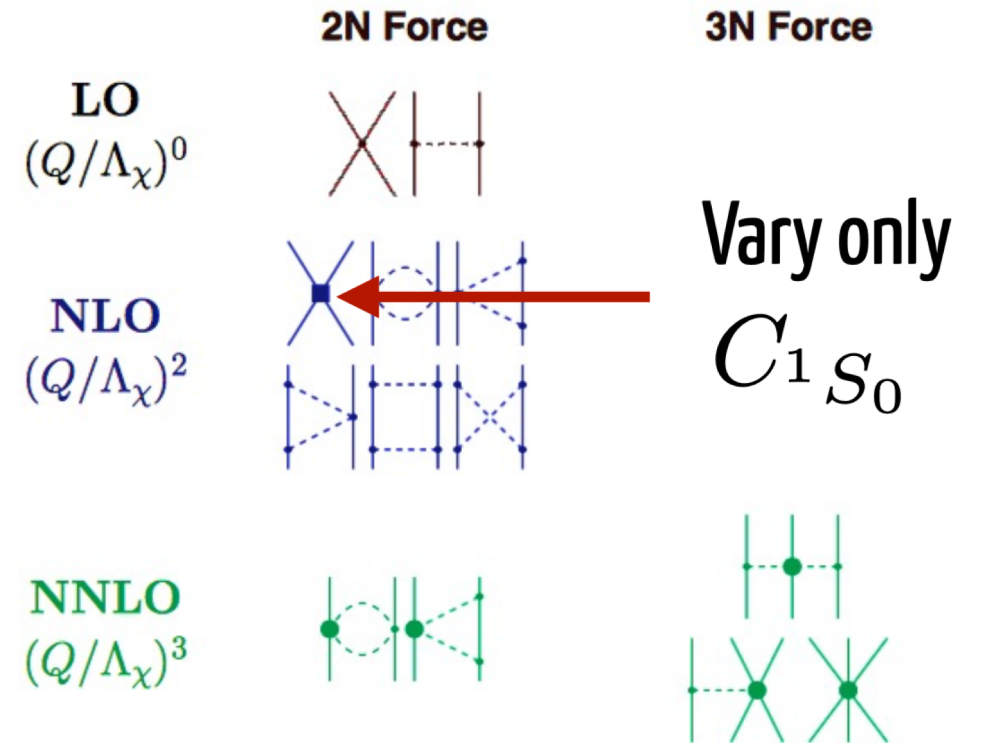
$$\mathbf{H}(\vec{\alpha}_\odot) \vec{c} = E(\vec{\alpha}_\odot) \mathbf{N} \vec{c},$$

Emulating ab-initio coupled-cluster calculations

Andreas Ekström, Gaute Hagen PRL **123**, 252501 (2019)

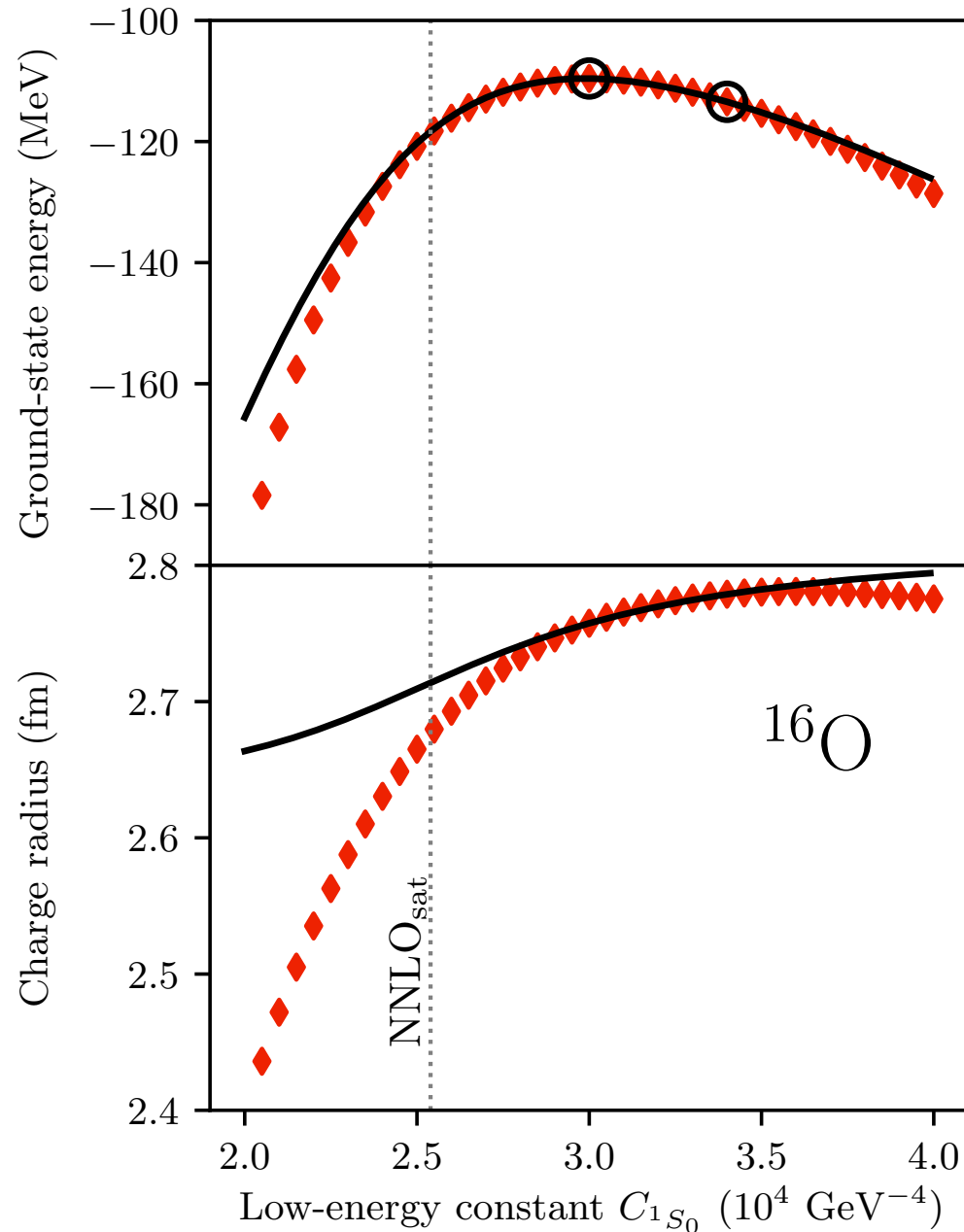


Exact coupled cluster calculations at the singles and doubles level

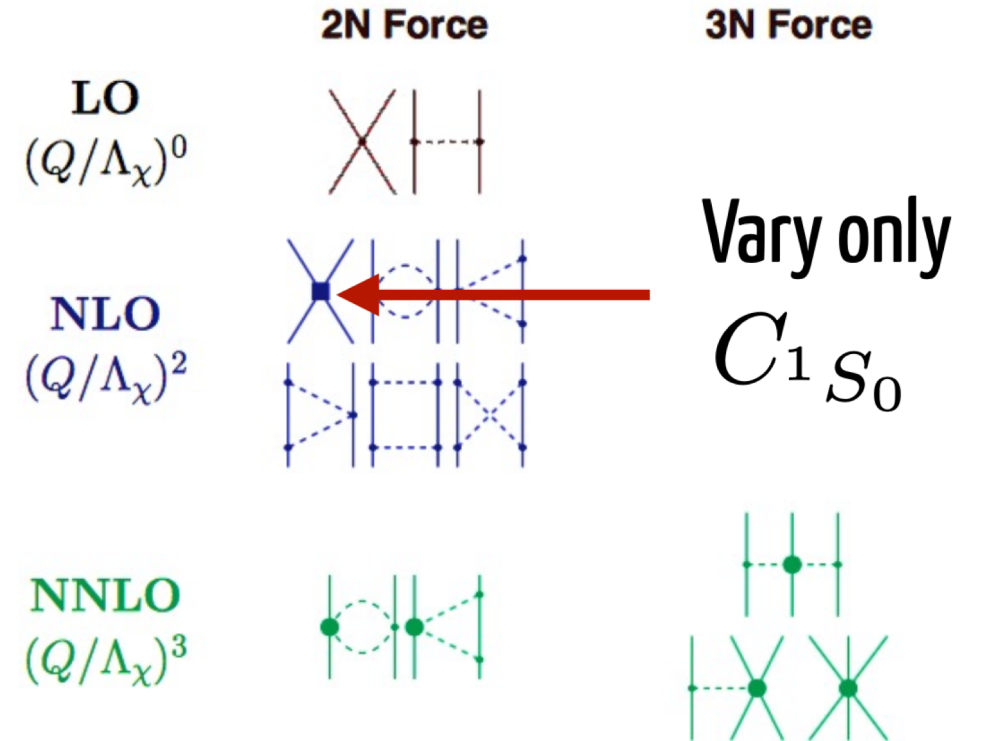


Emulating ab-initio coupled-cluster calculations

Andreas Ekström, Gaute Hagen PRL **123**, 252501 (2019)

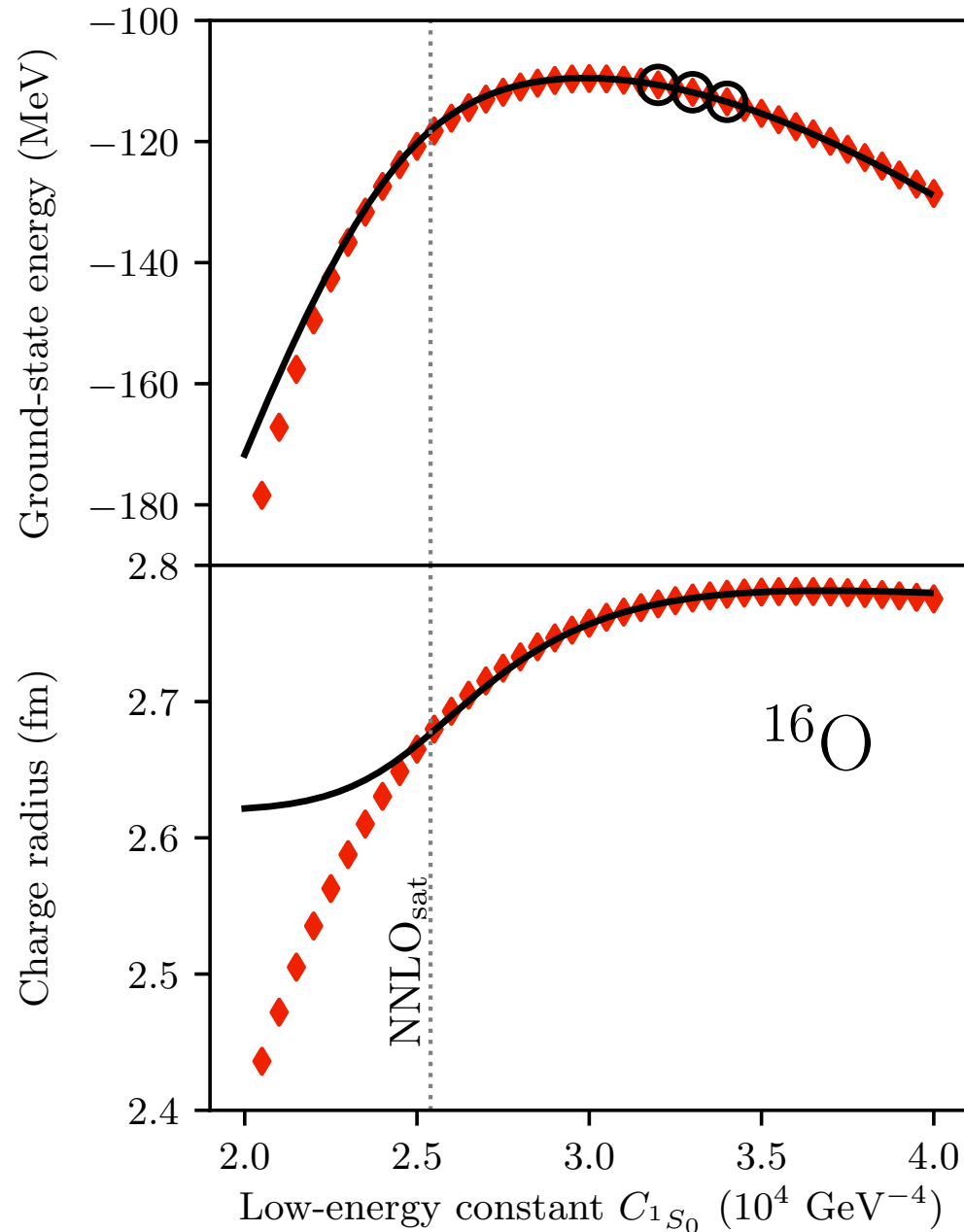


Exact coupled cluster calculations at the singles and doubles level

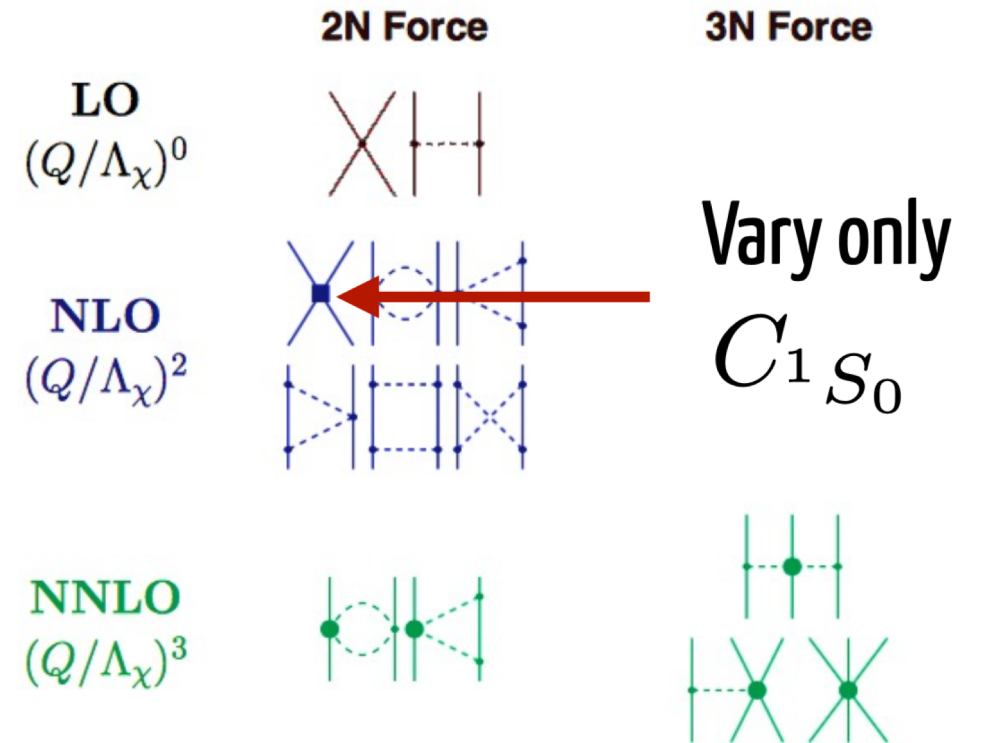


Emulating ab-initio coupled-cluster calculations

Andreas Ekström, Gaute Hagen PRL **123**, 252501 (2019)

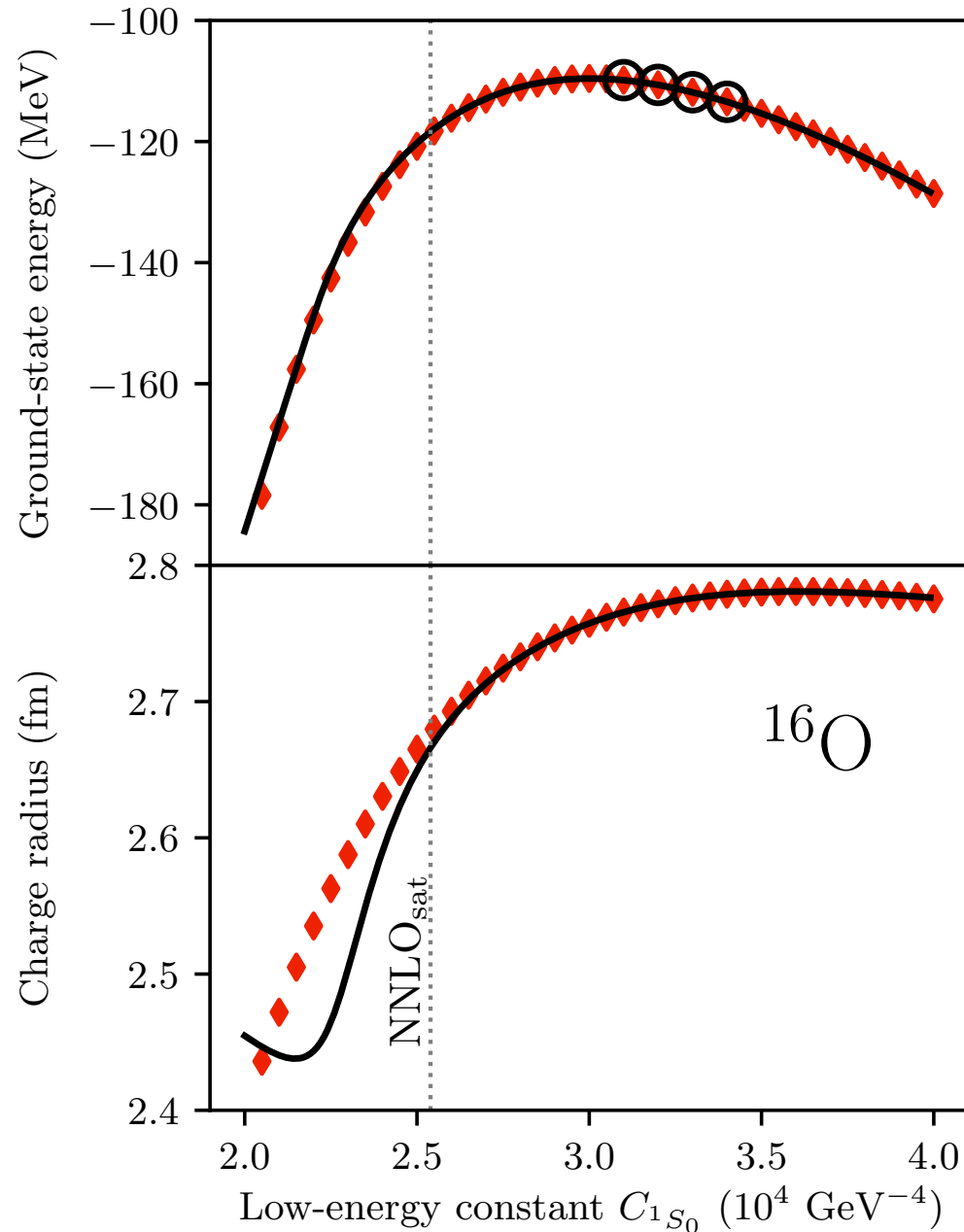


Exact coupled cluster calculations at the singles and doubles level

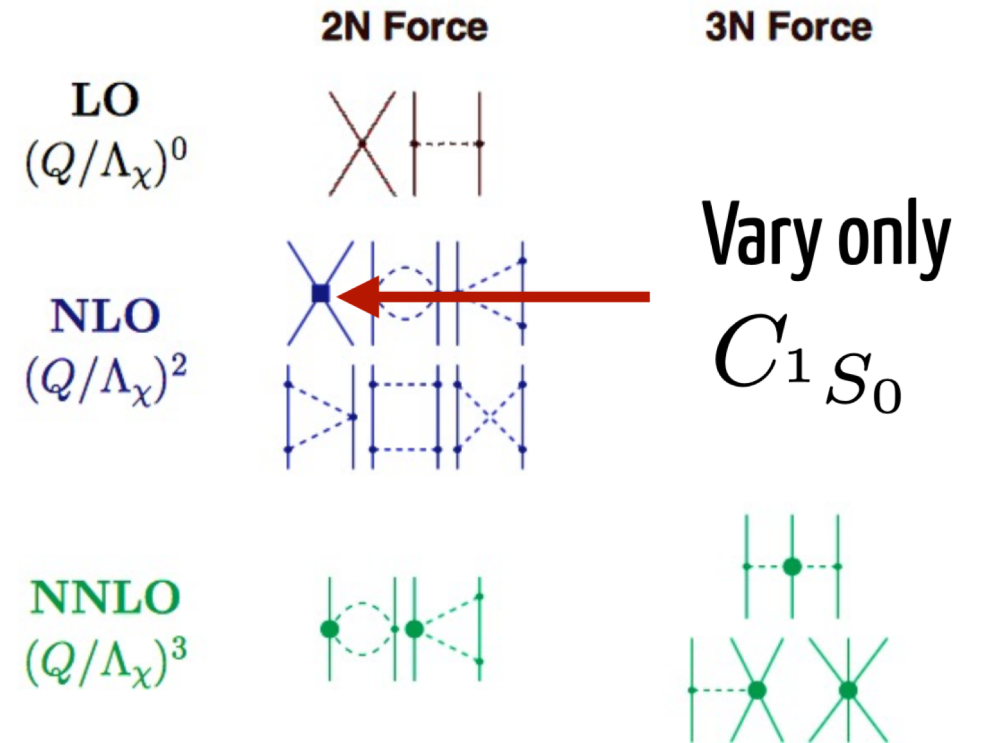


Emulating ab-initio coupled-cluster calculations

Andreas Ekström, Gaute Hagen PRL **123**, 252501 (2019)

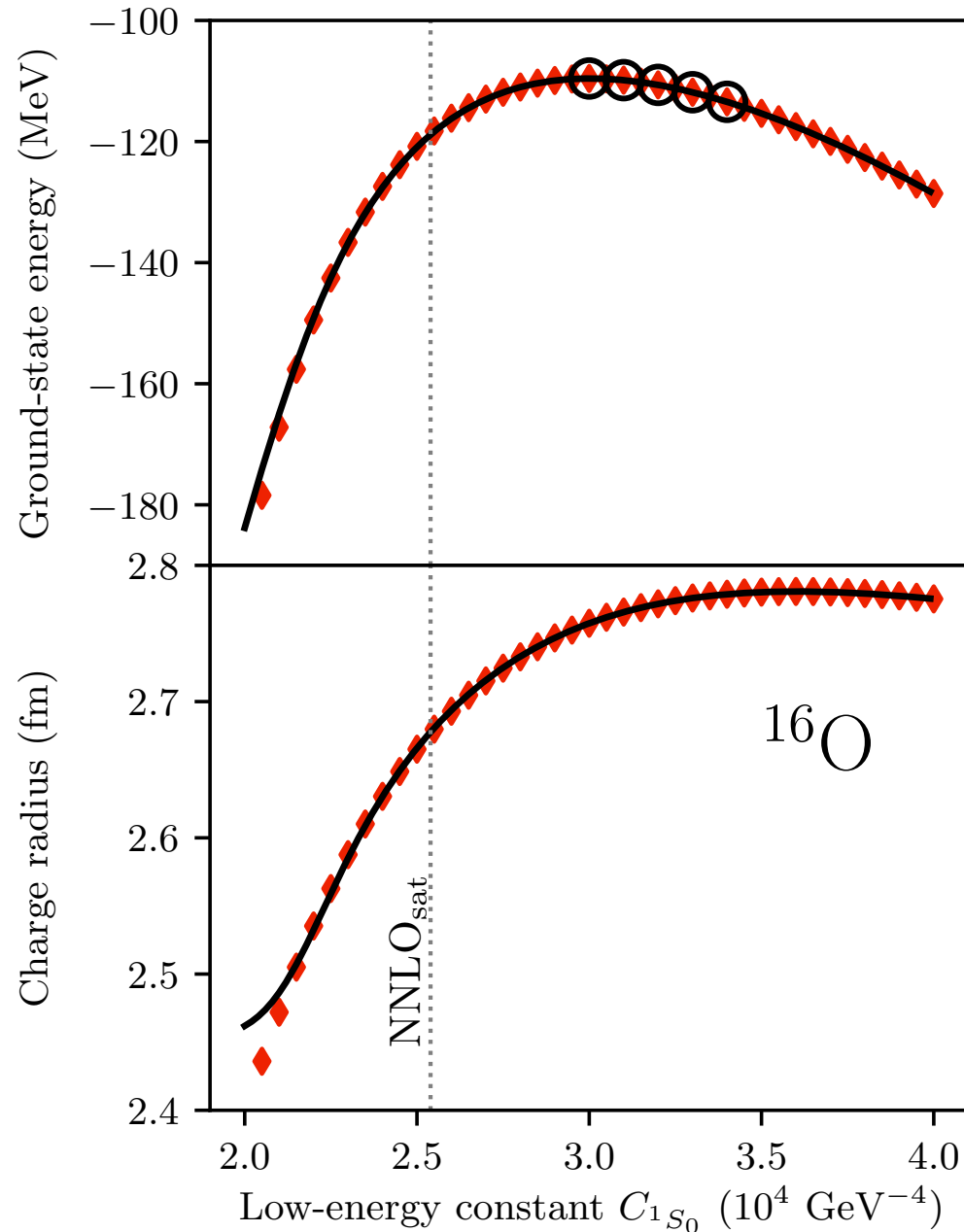


Exact coupled cluster calculations at the singles and doubles level

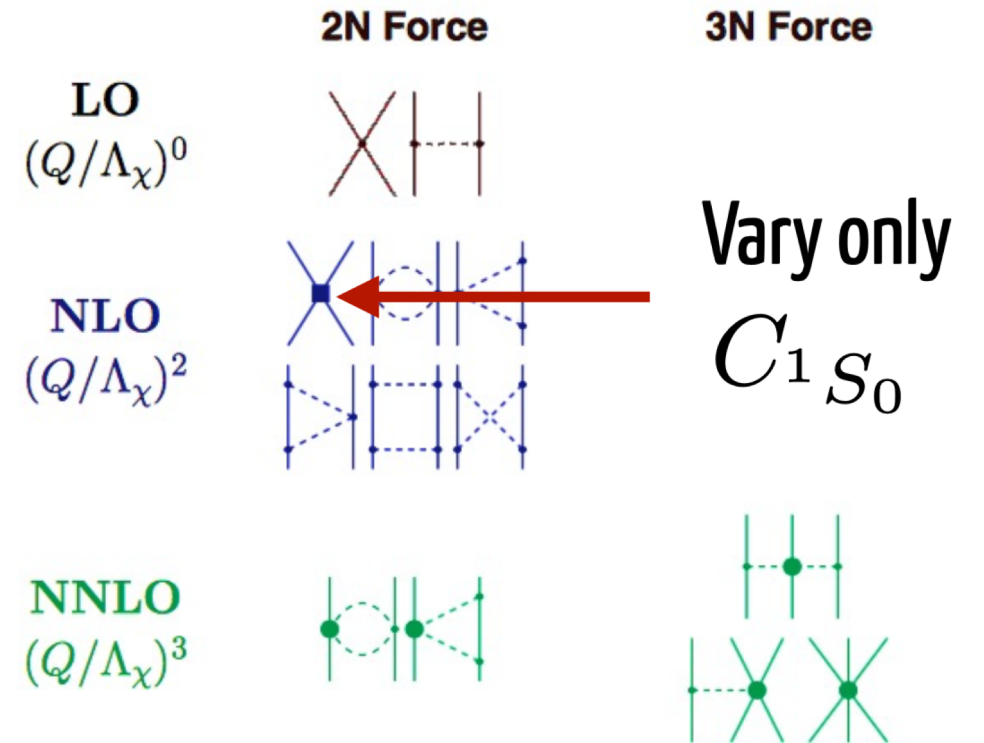


Emulating ab-initio coupled-cluster calculations

Andreas Ekström, Gaute Hagen PRL **123**, 252501 (2019)



Exact coupled cluster calculations at the singles and doubles level



Reduced order model for projected Hartree-Fock

Deformation is long-wave length physics and accurately described at projected Hartree-Fock level

Goal: Construct accurate emulator of projected Hartree-Fock

$$|\phi_{\odot}\rangle = \sum_i^{n_t} c_i |\phi_i\rangle$$

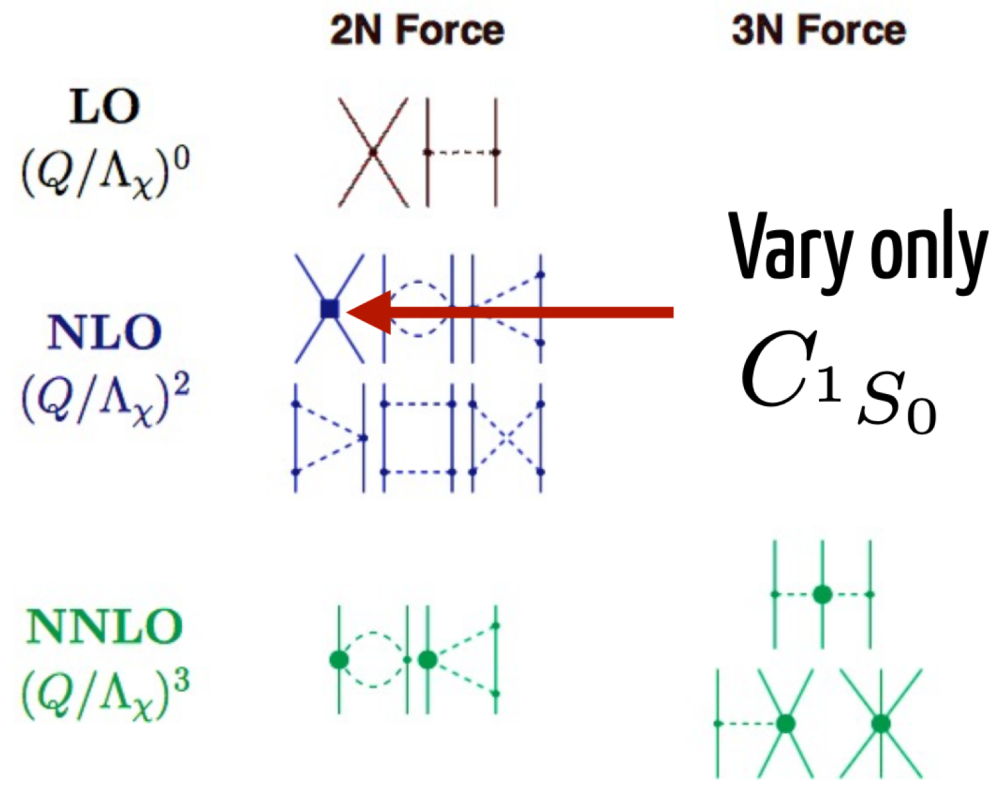
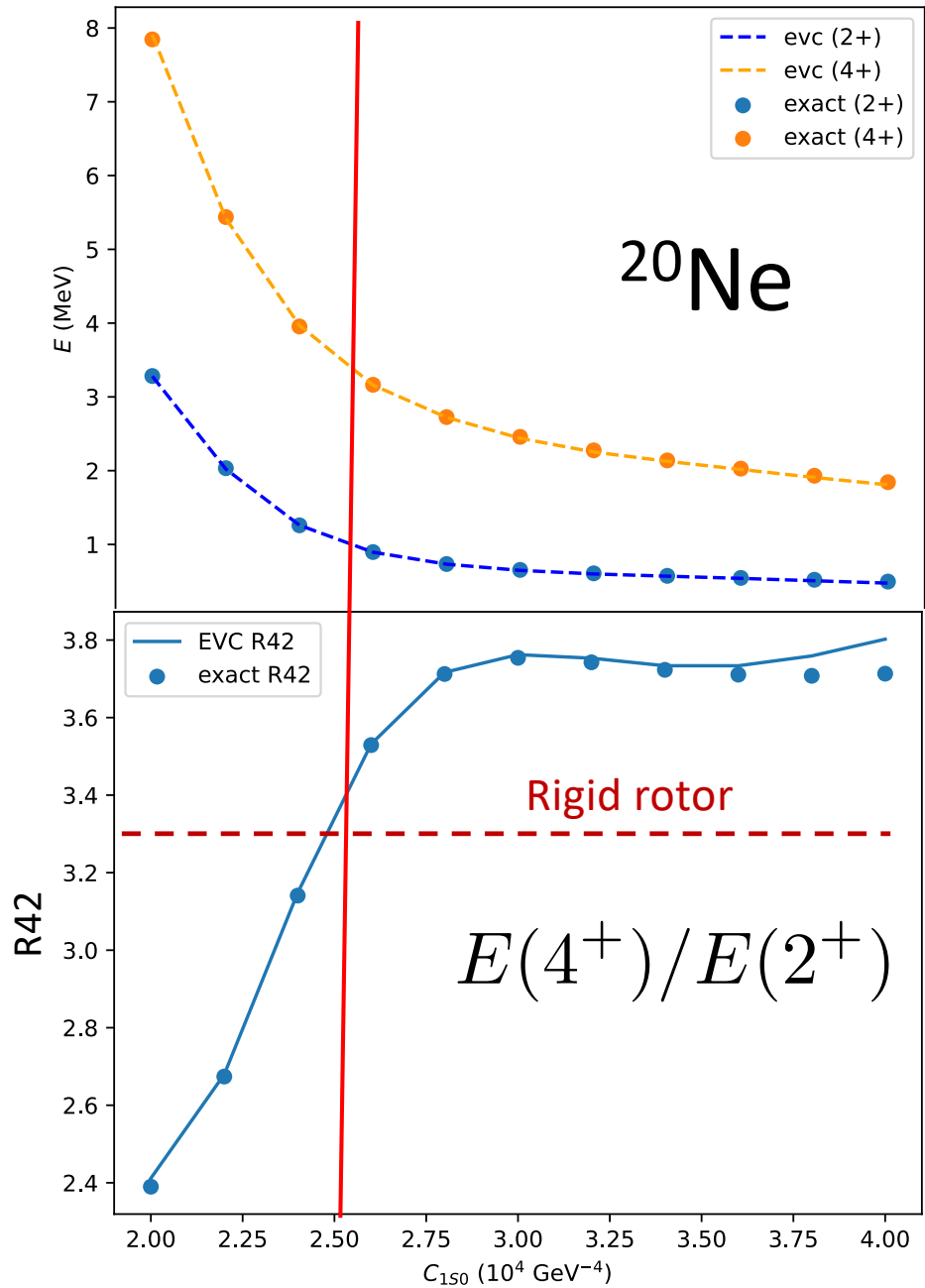
$$\sum_{ij} \langle \phi_i | H_{\text{HF}}(\vec{\alpha}_{\odot}) | \phi_j \rangle c_j = E_{\odot} \sum_{ij} \langle \phi_i | \phi_j \rangle c_j$$

Using Thouless theorem we can evaluate the norm and Hamiltonian kernels between non-orthogonal Hartree-Fock states

The target rotational states:

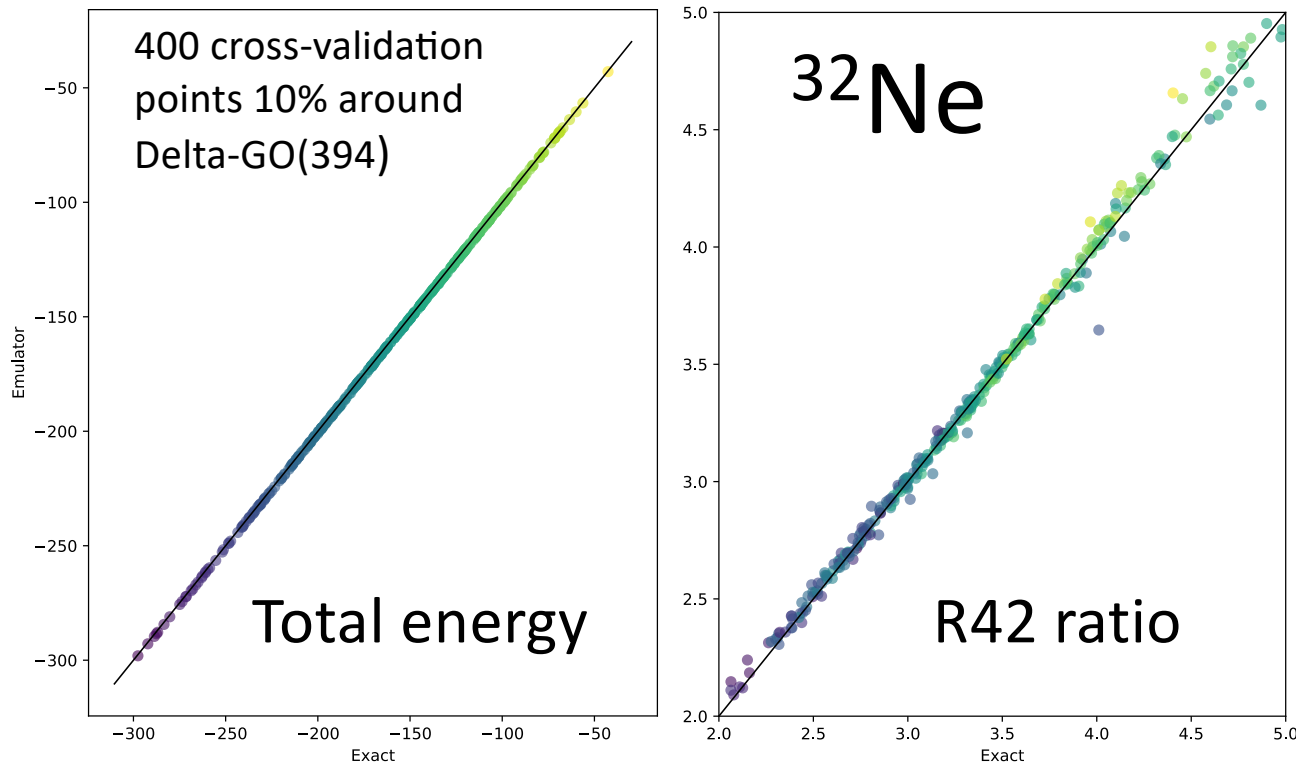
$$E_{\odot}^{(J)} = \frac{\langle \phi_{\odot} | P_J H(\vec{\alpha}_{\odot}) | \phi_{\odot} \rangle}{\langle \phi_{\odot} | P_J | \phi_{\odot} \rangle}$$

Linking deformation to nuclear forces

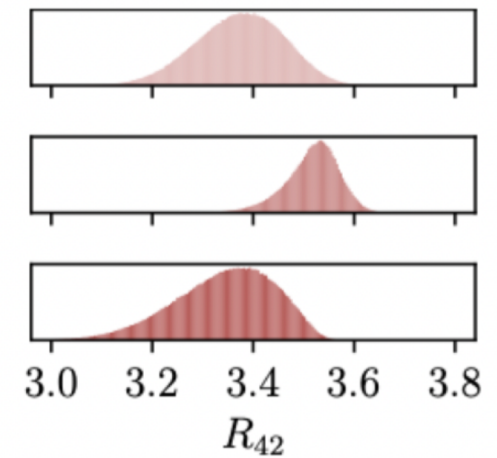
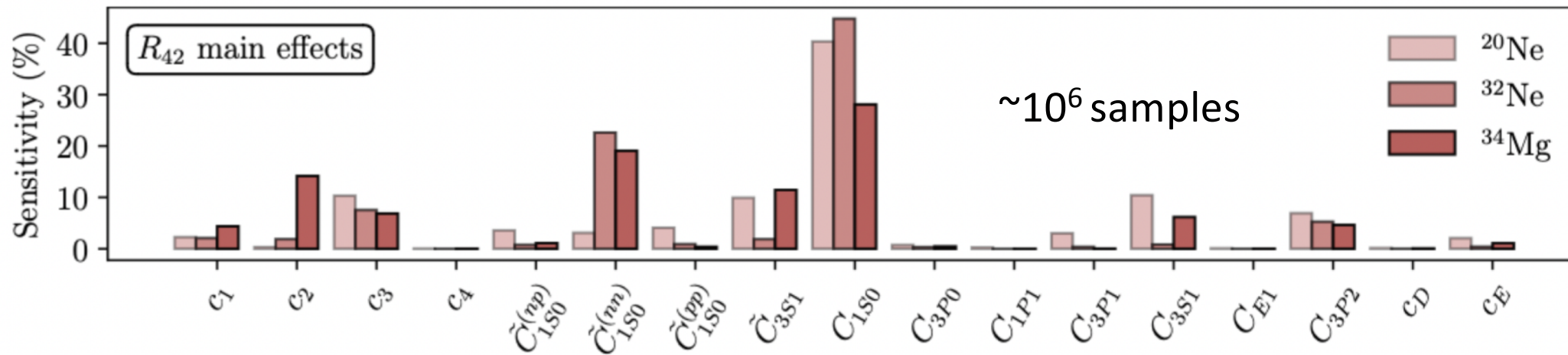


- Constructed accurate and efficient emulator of projected HF using 68 training vectors
- Training points obtained by using Latin Hypercube sampling within 20% of original low-energy constants

Linking deformation to nuclear forces



- Deformation is mainly driven by the pion-nucleon coupling LEC c_3 and short range contact C_{1S0}
- Adding short-range repulsion increase deformation presumably by reducing pairing
- Increasing the pion-nucleon coupling strength also increases deformation, presumably by adding attraction in higher partial waves



M1 transition in ^{48}Ca

- Large $B(M1: 0^+ \rightarrow 1^+)$ due to strong $\nu 1f_{7/2} \rightarrow \nu 1f_{5/2}$ excitation
- Darmstadt results are consistent with strong quenching factor (0.75) for the isovector strength
- Similarity of 1B operators in spin-flip M1 and GT transitions has been used as explanation for strong quenching. We test this by explicitly including 2B operators.

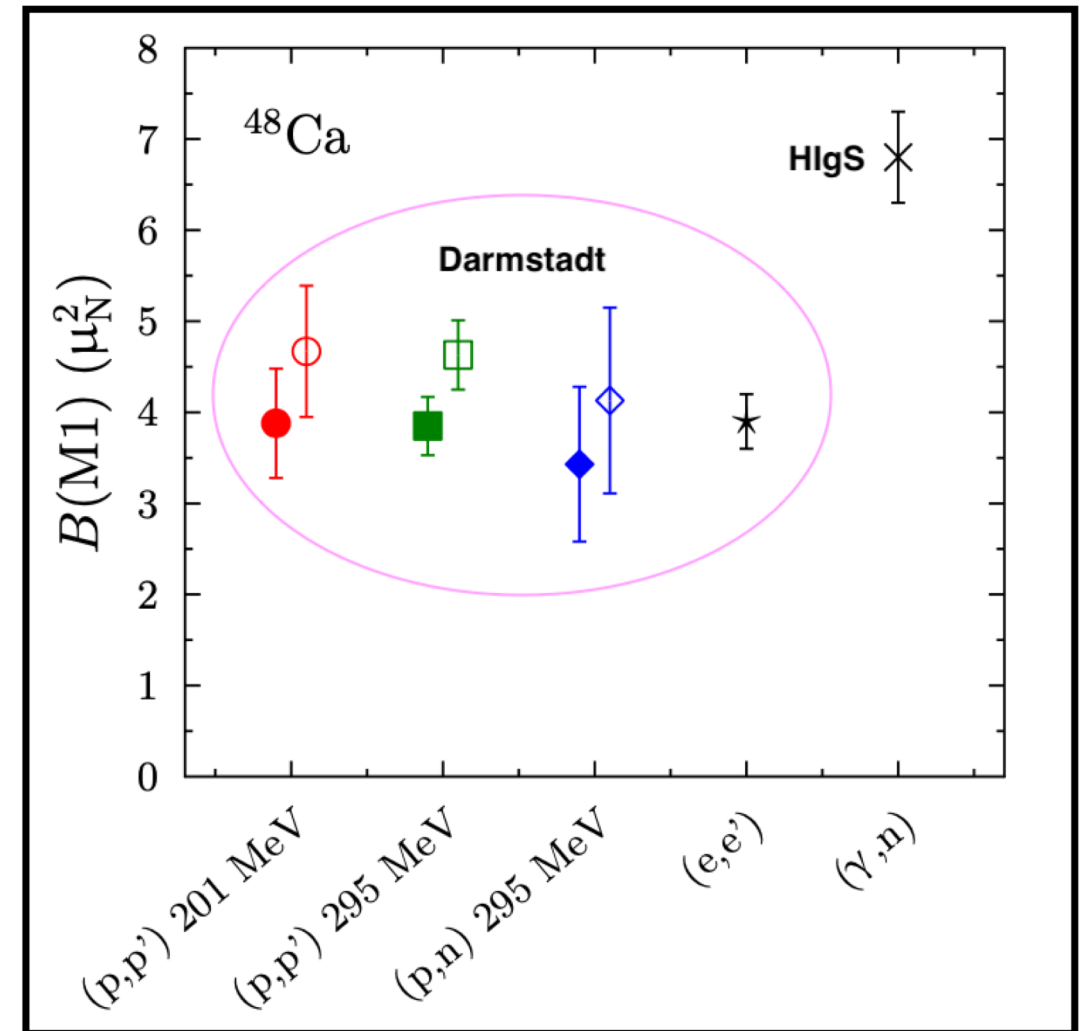


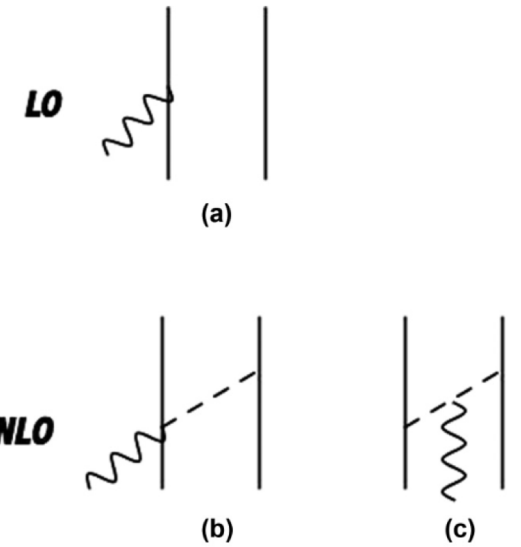
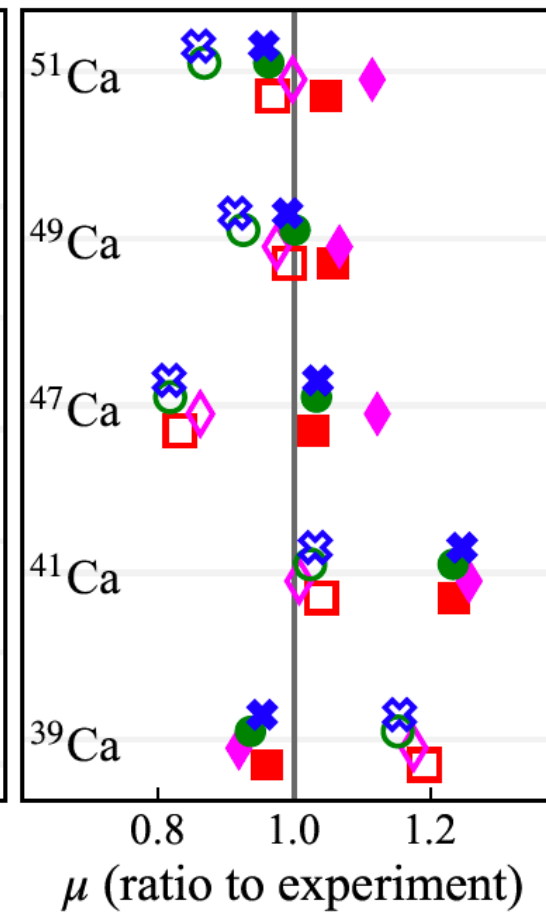
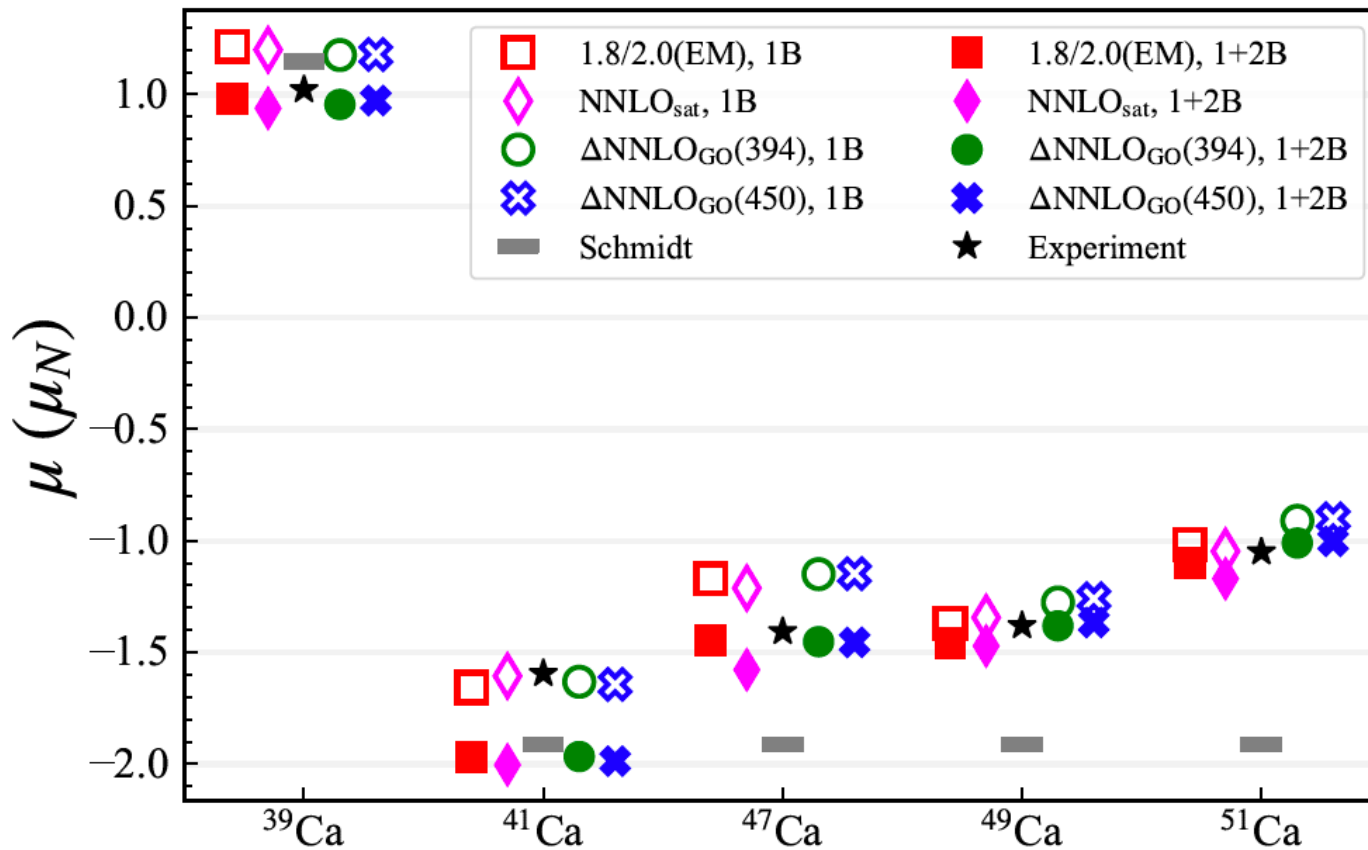
Figure adapted from PRC **93**, 041302(R) (2016)

M1 moments in calcium

$$\mu_{\text{NLO}}(k) = -\frac{i}{2} \nabla_q \times \mathbf{J}_{1\pi}(q, k)|_{q=0} + \frac{i}{2} e (\boldsymbol{\tau}_1 \times \boldsymbol{\tau}_2)_z \mathbf{R} \times \nabla_k V_{1\pi}(k)$$

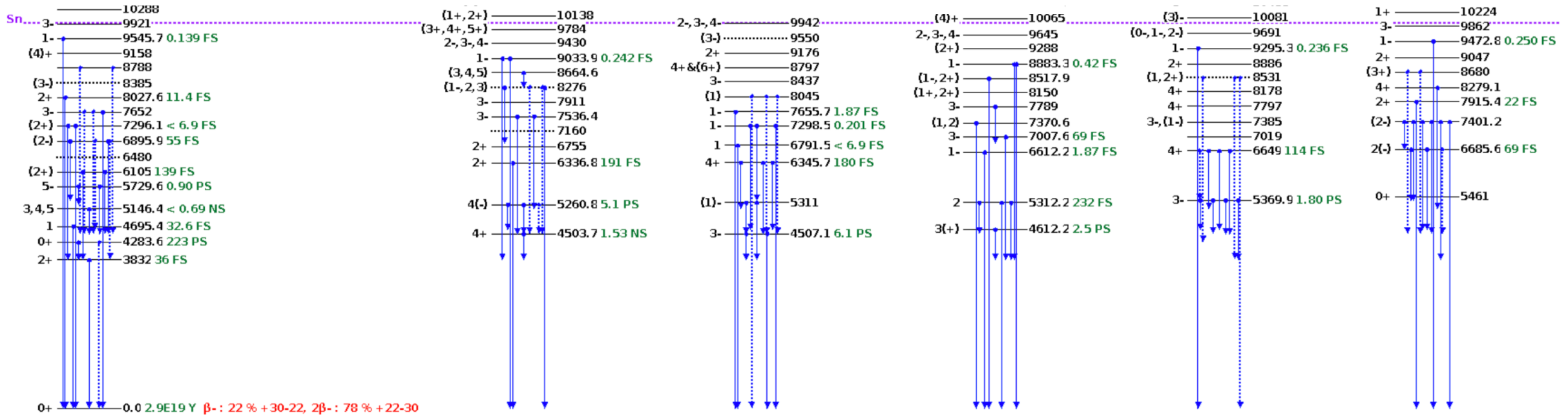
“Intrinsic”

“Sachs”



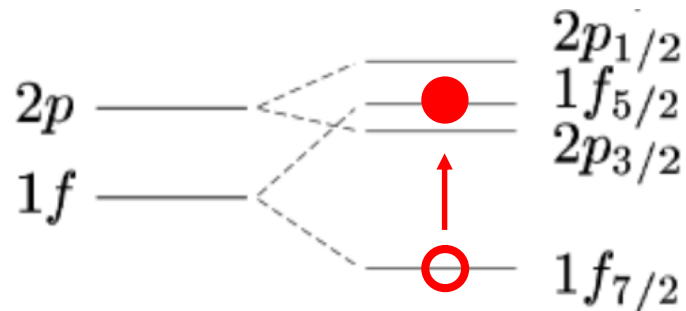
Sachs term give dominant contribution

The resonant 1^+ state in ^{48}Ca at 10.224 MeV

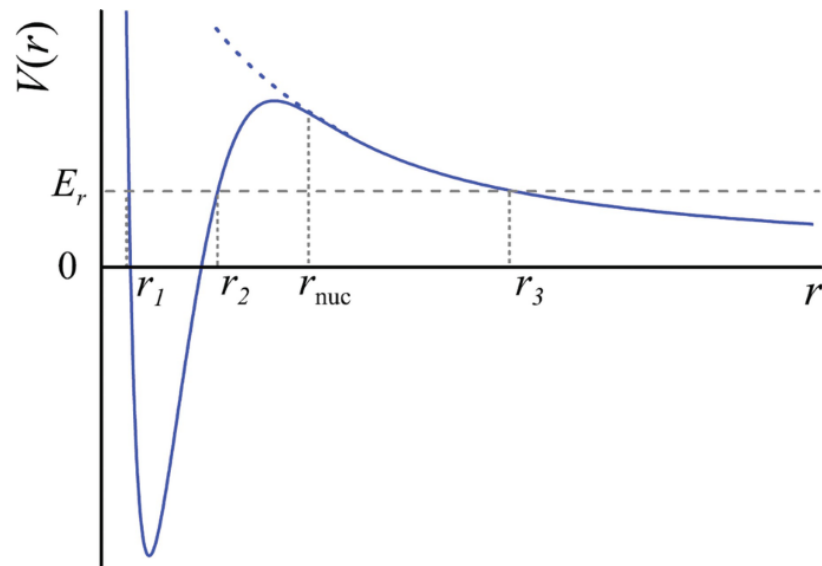


Scattering / reactions that probe the 1^+ state: (e, e') , (p, p') , (p, n) , or (γ, n)

Simple picture of the 1^+ state: neutron $1p-1h$ excitation; extreme single-particle model: $B(M1) = 12 \mu_N^2$



The resonant 1^+ state in ^{48}Ca at 10.224 MeV

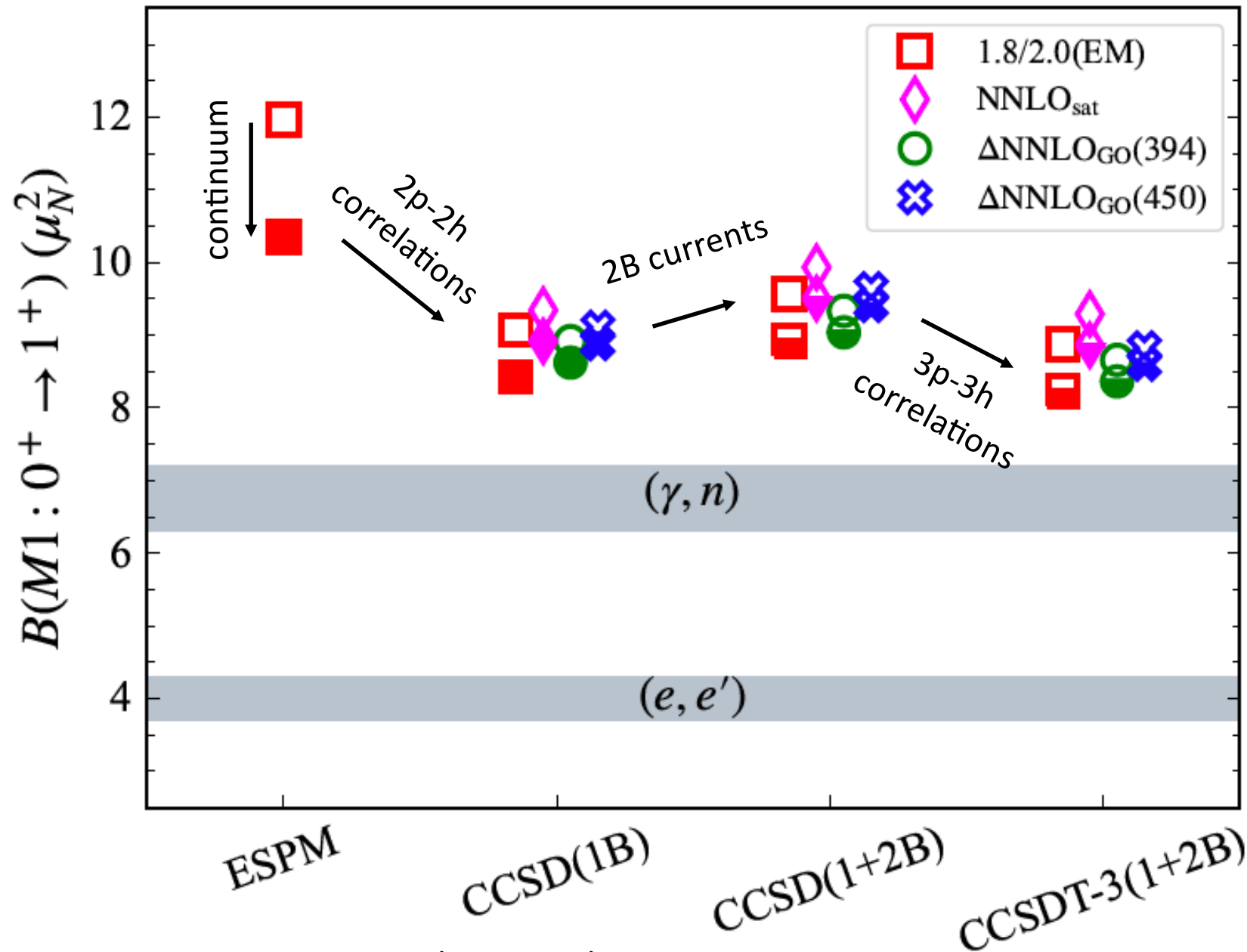


The $l = 3$ orbital angular-momentum barrier permits a neutron resonant state

Interaction	S_n (MeV)	ΔE (MeV)	Γ (keV)	$1p-1h$
$\Delta\text{NNLO}_{\text{GO}}(394)$	9.74	-0.44	0	91%
$\Delta\text{NNLO}_{\text{GO}}(450)$	9.38	-1.26	0	91%
NNLO_{sat}	9.34	-0.23	0	91%
1.8/2.0(EM)	10.00	0.55	4	92%
Experiment	9.95	0.28	≤ 17	

Bijaya Acharya et al., arXiv:2311.11438

The magnetic dipole transition in ^{48}Ca

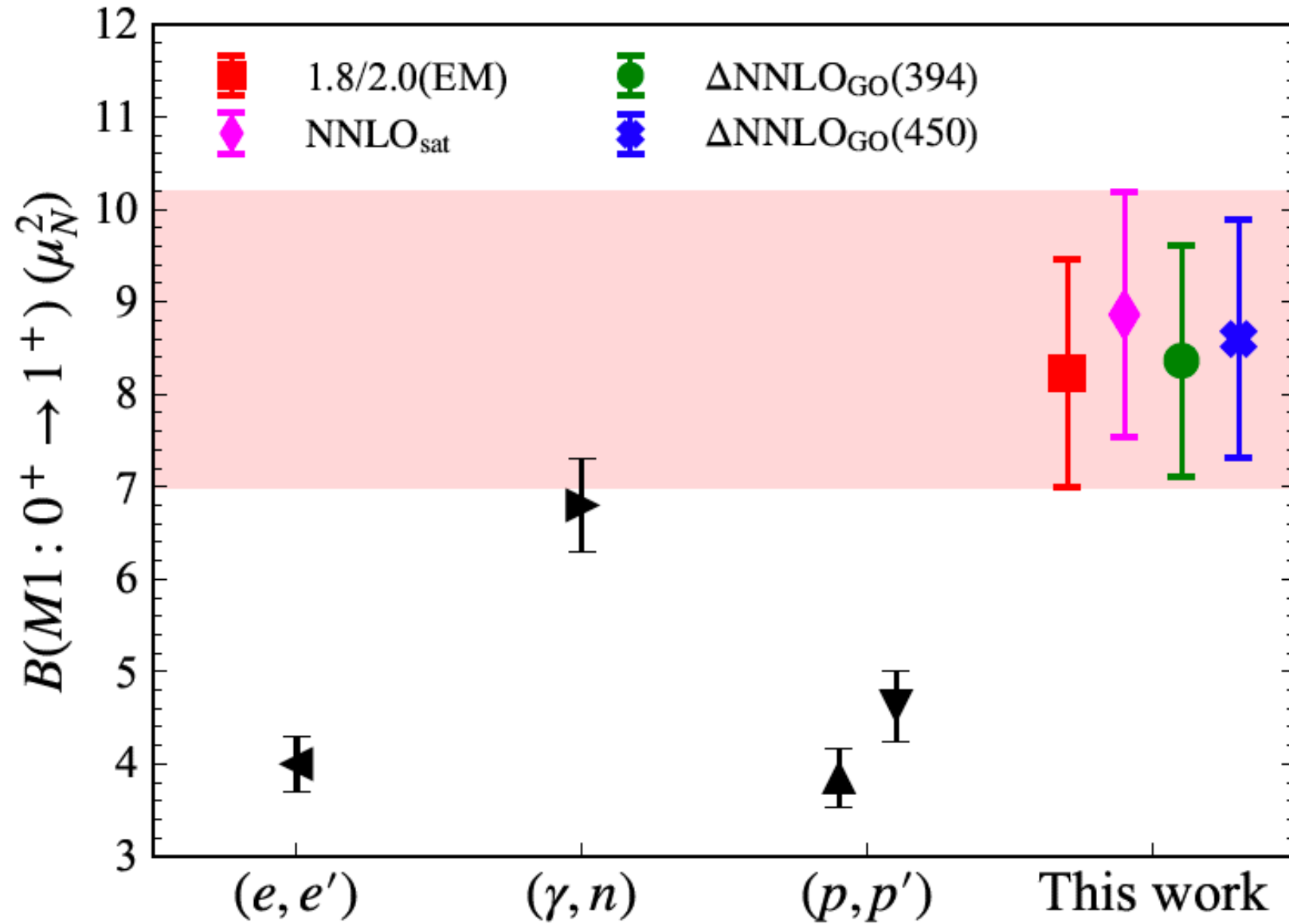


Two-body currents do not quench M1 transitions in light nuclei

$(J_i^\pi \rightarrow J_f^\pi)$	M1 and Γ	IA	MEC	Total	Expt.
${}^6\text{Li}(0^+ \rightarrow 1^+)$	M1	3.63(1)	0.38	4.01(1)	8.19(17)
	$\Gamma(\text{eV})$	6.90(2)		8.41(3)	
${}^7\text{Li}(\frac{1}{2}^- \rightarrow \frac{3}{2}^-)$	M1	2.66(1)	0.47(1)	3.13(2)	6.30(31)
	$\Gamma(10^{-3} \text{ eV})$	4.47(5)		6.19(8)	
${}^7\text{Be}(\frac{1}{2}^- \rightarrow \frac{3}{2}^-)$	M1	2.31(2)	0.41(1)	2.72(2)	3.43(45)
	$\Gamma(10^{-3} \text{ eV})$	2.44(4)		3.39(6)	
${}^8\text{Li}(1^+ \rightarrow 2^+)$	M1	3.47(4)	0.74(2)	4.21(5)	5.5(1.8)
	$\Gamma(10^{-2} \text{ eV})$	4.4(1)		6.5(2)	
${}^8\text{B}(1^+ \rightarrow 2^+)$	M1	3.17(5)	0.67(2)	3.84(6)	2.52(11)
	$\Gamma(10^{-2} \text{ eV})$	1.8(1)		2.6(1)	
${}^8\text{Li}(3^+ \rightarrow 2^+)$	M1	0.98(6)	0.20(5)	1.17(8)	7.0(3.0)
	$\Gamma(10^{-2} \text{ eV})$	1.8(2)		2.6(3)	
${}^8\text{B}(3^+ \rightarrow 2^+)$	M1	1.31(6)	0.23(5)	1.56(8)	10(5)
	$\Gamma(10^{-2} \text{ eV})$	3.5(3)		4.9(5)	
${}^9\text{Li}(\frac{1}{2}^- \rightarrow \frac{3}{2}^-)$	M1	2.28(3)	0.36(4)	2.64(5)	n.a.
	$\Gamma(10^{-1} \text{ eV})$	5.9(2)		7.9(3)	
${}^9\text{Be}(\frac{5}{2}^- \rightarrow \frac{3}{2}^-)$	M1	1.42(3)	0.20(2)	1.62(4)	8.9(1.0)
	$\Gamma(10^{-2} \text{ eV})$	5.6(3)		7.2(4)	

Pastore, Pieper, Schiavilla, Wiringa, Phys Rev C 87, 035503 (2013)

Magnetic dipole transition in ^{48}Ca



Summary

- Neutron-rich neon isotopes are strongly deformed: ^{34}Ne as rotational as ^{32}Ne and ^{34}Mg
- Electromagnetic transitions follow experimental trends
- Signatures of shape co-existence along $N = 20$ towards ^{28}O
- Nuclei around ^{80}Zr are strongly deformed with rich prolate and oblate structure
- Predict low-lying rotational states in ^{78}Ni consistent with data and shell-model predictions
- Towards Schiff moment calculations in ^{225}Ra

Summary

- The discrepancy between (e, e') and (γ, n) experiments regarding $B(M1)$ in ^{48}Ca is puzzling
- Our ab initio computations based on chiral effective field theory, including treatment of the state as a resonance, yield $7\mu_N^2 < B(M1) < 10\mu_N^2$
 - Two-body currents do not yield a quenching
- Resolution of this situation will impact ab initio computations and/or theory of neutrino-nucleus reactions relevant for supernova signals and dynamics

Thank you for your attention!